Inexpensive CO_2 Thickening Agents for Improved Mobility Control of CO_2 Floods

Final Report

Start Date: October 1, 2001
End Date: September 30, 2004

Dr. Robert M. Enick
Dr. Eric J. Beckman
Chemical and Petroleum Engineering
University of Pittsburgh

Dr. Andrew Hamilton
Chemistry
Yale University

Date Issued: October 2004

DOE-FC26-01BC15315

Dr. Robert M. Enick and Dr. Eric J. Beckman
Department of Chemical and Petroleum Engineering
University of Pittsburgh
1249 Benedum Engineering Hall
Pittsburgh, PA 15261

Dr. Andrew Hamilton
Chemistry Department
Yale University
2250 Prospect Ave.
PO Box 208107
New Haven, CT
06520-8107

Disclaimer

Abstract

The objective of this research was the design, synthesis and evaluation of inexpensive, non-fluorous carbon dioxide thickening agents. We followed the same strategy employed in the design of fluorinated CO_2 polymeric thickeners. First, a highly CO_2-philic, hydrocarbon-based monomer was to be identified. Polymers or oligomers of this monomer were then synthesized. The second step was to be completed only when a CO_2-soluble polymer that was soluble in CO2 at pressures comparable to the MMP was identified. In the second step, viscosity-enhancing associating groups were to be incorporated into the polymer to make it a viable thickener that exhibited high CO_2 solubility at EOR MMP conditions.

This final report documents the CO_2 solubility of a series of commercial and novel polymers composed of carbon, hydrogen, oxygen and, in some cases, nitrogen.

In the first section of the report, we demonstrate that poly(vinyl acetate), PVAc, is the most CO_2 soluble, inexpensive, commodity polymer that has yet been identified. The pressure required to dissolve PVAc in CO_2 was 6000 – 9000 psia; thousands of psi greater than the range of MMP values. Therefore PVAc was not soluble enough in CO_2 to serve as the "base polymer" from which CO_2 thickeners would be developed. The next objective of this investigation was to determine if any polymer (composed of C, H, O, N and/or S) could exhibit CO_2 solubility greater than that of PVAc.

The second section is a report on the comparison of CO_2-philicity of oxygenated hydrocarbon side groups on a PDMS polymer. These side-functionalized PDMS polymers are not candidates for a CO_2 thickener because they contain silicon, nonetheless the PDMS backbone provides a highly CO_2-soluble molecular framework onto which the side chains composed of C, H, O and N can be grafted. The side groups that interacted most favorably with CO_2 caused the functionalized PDMS molecule to have the greatest miscibility with CO_2. These results provided a useful tool for comparing the CO_2-philicity of various side chains, and the most promising side groups were incorporated into a polymer containing neither silicon nor fluorine. Both ethers and acetates appeared particularly promising. To date, these polymers have not been more CO_2-soluble than PVAc.

The third section is a report on a novel class of highly CO_2 soluble compounds known as sugar acetates. Low molecular weight sugar acetates are remarkably CO_2 soluble. Although we were successful in designing CO_2 soluble hydrogen bonding compounds, they were not capable of thickening the CO2. High molecular weight sugar acetate polymers, cellulose triacetate and per-acetlyated xanthan gum, were insoluble in CO2.

The fourth section is a report on a novel type of phase behavior that was discovered while studying the sugar acetates. Highly CO_2-philic solids, including small molecules and polymers, can exhibit melting point depression in dense CO_2, i.e. these solids melt instantly in dense CO_2. This phenomenon is symptomatic of a favorable thermodynamic interaction of the compound with CO_2, and serves as an indicator that the compound may be a potential CO_2-thickener.

The fifth section presents a new tool that our research group began to use in an attempt to have a more direct and quantitative method of identifying promising new CO_2-philes. This paper shows how quantitiative *ab initio* calculations can used to qualitatively explain why some polymers are more CO_2 soluble than others. In particular, this paper demonstrates why poly(tetrafluoroethylene-co-vinyl acetate) copolymers are more CO_2 soluble than PVAc. The objective of this section is *not* to promote the use of the fluorinated polymer as a CO_2 thickener. Rather, the purpose is to demonstrate that we have a computational tool than can help us to design CO_2-soluble polymers – especially ones that are composed solely of C, H, O, N and S.

The sixth section focuses on the CO2 solubility of nitrogen-containing polymers. Although the presence of nitrogen-containing groups would appear to generate strong Lewis acid : Lewis base interactions – and hence high solubility – with CO_2, the intramolecular interactions between nitrogen –containing polymer groups with other nitrogen-containing groups – rather than CO2 - is so strong that the CO_2 solubility of these polymers was disappointingly low.

The seventh section contains a tabular listing of all of the polymers studied during this project during the first two years, along with a summary of their solubility in CO_2 and a listing of candidates being considered for the third year of the project. Unfortunately, none of these novel polymers were more CO_2 soluble than PVAc. Some did dissolve in CO_2, but required greater pressures to attain dissolution than PVAc oligomers and polymers of a comparable chain length, while most were completely insoluble in CO_2 at 298 K and pressures up to 70 MPa.

In that we did not identify a high molecular weight polymer that was soluble in CO_2 at pressures corresponding to the MMP, we did not functionalize any of the polymer candidates to make them thickeners because this functionalization with CO_2 phobic associating groups makes the polymer even less CO_2 soluble.

Table of Contents

Executive Summary	6
Section 1. A Comparison of Highly Carbon Dioxide-Soluble Homopolymers	7
Section 2. Design, Synthesis, and Optimization of Non-Fluorous, CO_2-Philic Polymers: A Systematic Approach	24
Section 3 High CO_2 Solubility of Per-acetylated Compounds	106
Section 4. Novel Phase Behavior of CO_2-Philic Solids	110
Section 5. Use of Molecular Modeling to Design CO_2 Soluble Polymers	124
Section 6. CO_2 Solubility of Aminated Polymers	155
Section 7. Summary of Polymers Evaluated During This Study	175

Executive Summary

Poly(vinyl acetate), PVAc, is the most CO_2 soluble, inexpensive, commodity polymer that has yet been identified. The pressure required to dissolve PVAc in CO_2 was 6000 – 9000 psia; thousands of psi greater than the range of MMP values. Therefore PVAc was not soluble enough in CO_2 to serve as the "base polymer" from which CO_2 thickeners would be developed. The next objective of this investigation was to determine if any polymer (composed of C, H, O, N and/or S) could exhibit CO_2 solubility greater than that of PVAc. A comparison of the CO_2-philicity of oxygenated hydrocarbon groups was made by incorporating them as side groups for a PDMS polymer. These side-functionalized PDMS polymers are not candidates for a CO_2 thickener because they contain silicon, nonetheless the PDMS backbone provides a highly CO_2-soluble molecular framework onto which the side chains composed of C, H, O and N can be grafted. The side groups that interacted most favorably with CO_2 caused the functionalized PDMS molecule to have the greatest miscibility with CO_2. These results provided a useful tool for comparing the CO_2-philicity of various side chains, and the most promising side groups were incorporated into a polymer containing neither silicon nor fluorine. Both ethers and acetates appeared particularly promising. Although it was found that small compounds known as sugar acetates, especially low molecular weight sugar acetates, are remarkably CO_2 soluble, high molecular weight sugar acetate polymers, including cellulose triacetate and per-acetlyated xanthan gum, were insoluble in CO2. Although the presence of nitrogen-containing groups would appear to generate strong Lewis acid : Lewis base interactions – and hence high solubility – with CO_2, the intramolecular interactions between nitrogen –containing polymer groups with other nitrogen-containing groups – rather than CO2 - is so strong that the CO_2 solubility of these polymers was disappointingly low. After evaluating numerous polymers, we initiated a more direct and quantitative method of identifying promising new CO_2-philes. *ab initio* calculations can used to qualitatively explain why some polymers are more CO_2 soluble than others. As this contract came to a close, molecular modeling was used to design several novel polymers that appear (based on molecular modeling) to have the possibility of being more CO2 soluble than PVAc. These polymers include poly(3-acetoxy oxetane), poly(vinyl methoxy methyl ether), and an acetylated polyester.

In that we did not identify a high molecular weight polymer that was soluble in CO_2 at pressures corresponding to the MMP, we did not functionalize any of the polymer candidates to make them thickeners because this functionalization with CO_2 phobic associating groups makes the polymer even less CO_2 soluble.

Section 1. A Comparison of Highly Carbon Dioxide-Soluble Homopolymers

Xu, J.; MacPhearson, H.; Kilic, S.; Mesiano, A.; Bane, S.; Karnikas, C.; Beckman, E.; Enick, R.
Department ofChemical and Petroleum Engineering
1249 Benedum Engineering Hall
University of Pittsburgh
Pittsburgh, PA 15261
(412) 624-9630

Shen, Z.; McHugh, M.A.

Abstract

Poly(vinyl acetate) is remarkably miscible with CO_2 over a broad range of molecular weight. The pressure required to dissolve ~5 wt % PVAc is bounded by pressures of 13.6 and 67.5 MPa at 10 and 6800 repeat units, respectively. The cloud-point pressures needed to dissolve 5 wt% poly(methyl acrylate) (PMA) at 298 K are dramatically greater than those needed to dissolve PVAc, even though a PMA repeat group has the same number of carbon, hydrogen, and oxygen atoms as in PVAc. This large difference in dissolution pressures is attributed to the lack of accessibility of the carbon dioxide to the carbonyl group in PMA, although experimental data presented for PDMS copolymers with readily accessible side groups suggest that an acetate group is slightly more CO_2-philic than an acrylate group. PVAc is more CO_2 soluble than other hydrocarbon homopolymers that have been previously shown to dissolve at high concentration in dense CO_2, including poly(propylene oxide) (PPO) and poly(lactide) (PLA). PVAc is significantly less miscible with CO_2 than silicone polymers and poly(fluoroacrylates), however. Therefore PVAc may serve as a non-fluorous CO_2-philic constituent of polymers, dispersants, surfactants and chelating agents, but significantly higher pressures will be required for dissolution than analogous fluorocarbon- or silicone-based compounds.

Introduction

The identification of highly CO_2-soluble polymers composed of only carbon, hydrogen, and oxygen could facilitate the design of safe, inexpensive, environmentally benign "CO_2-philes". These compounds could enhance the performance and economics of CO_2-based technologies that require the dissolution of amphiphiles, such as surfactants, chelating agents, thickeners, and dispersants and homopolymers or copolymers for foam, fiber and film applications. An extensive review of polymer solubility in dense carbon dioxide was previously conducted in an attempt to identify a thickener that would reduce the mobility of supercritical CO_2 flowing through porous media (Heller, et al. 1985). Although no viscosity-enhancing polymer was identified, hydrocarbon-based polymers that exhibited slight solubility in CO_2 (0.1 – 1.0 wt%) were water-insoluble, atactic, amorphous, and had solubility parameters less than 8 $(cal/cm^3)^{0.5}$. For reference, the solubility parameter of CO_2 is calculated to be in the range of 5.5 – 6.0 $(cal/cm^3)^{0.5}$ at reservoir conditions.

Subsequent solubility studies were more successful in identifying polymers capable of dissolving at much higher concentrations in CO_2. In one particular study, cloud-point data at a concentration of 5 wt% polymer, which is expected to be the maximum of a pressure-concentration isotherm, were reported for a series of polyacrylates along with PVAc (Rindfleisch, et al. 1996). Despite their identical composition, PVAc (Mw = 125000) was much more soluble in CO_2 at 298 K than poly(methyl acrylate) (Mw = 31000) (PMA) even though the PMA had a much lower molecular weight. The PVAc (Mw = 125000) cloud-point pressures increased with temperature over the 295 – 423 K range while the PMA (Mw = 31000) cloud-point pressures increased slightly between 295 – 313 K and then decreased over the 313 – 458 K temperature range, yet the PVAc two-phase locus remained lower than that of PMA by approximately 150 – 100 MPa. It should be noted that the pressure required to dissolve PVAc increased from 60 MPa at 295 K to 100 MPa at 423 K, which is high relative to most proposed CO_2-based technologies. The glass transition temperature of PVAc (Mw = 125000) is 21 K higher than that of PMA, indicative of the stronger polar interactions between acetate groups relative to methyl acrylate groups tethered to alternating carbons of the polymer backbone. PVAc was therefore considered to be more polar than PMA, facilitating the formation of a weak complex between CO_2 and vinyl acetate especially at low to moderate temperatures. McHugh and coworkers

concluded that a slight degree of polarity is required to establish CO_2 solubility, and the solubility-enhancing weak complex between CO_2 and a carbonyl group in the polymer was more readily formed in the CO_2 – PVAc system (Rindfleisch, et al. 1996).

A review of CO_2 solubility studies with amorphous polyether and polyacrylate homopolymers revealed that CO_2 solubility increased as the surface tension of the polymer decreased (O'Neill et al. 1998). The lower surface tension is correlated with a lower polymer cohesive energy density which is now closer to the value expected for CO_2. Low molecular weight poly(propylene oxide) (PPO) exhibited substantial solubility in dense CO_2. For example, 10 wt% PPO, with a molecular weight of 400, dissolved in CO_2 at 303 K and 8.3 MPa. PPO was significantly more soluble than poly(ethylene oxide) (PEO) each at the same molecular weight. This difference in solubility was attributed to the weaker segment-segment interactions of PPO and the weaker self-association of PPO relative to PEO.

Poly(lactide) (PLA) has been previously shown to dissolve at high concentrations in neat CO_2 (Conway et al. 2001). The pressure required to attain a single-phase exceeded that needed for PVAc, however. For example, at 308 K the cloud-point pressures of PVAc (Mw = 125000) and PLA (Mw = 128500) at 5 wt% in carbon dioxide were 70 MPa and 140 MPa, respectively. Copolymers of lactide and glycolide were even more difficult to dissolve, indicating that polymers rich in the glycolide functionality are even less CO_2-philic that PLA.

PMA, PVAc, and PLA contain the carbonyl group in the repeat unit. The CO_2-solubility of these polymers is undoubtedly attributable to favorable interactions between the oxygen of the carbonyl group and the carbon of CO_2. Results from ab initio calculations (Nelson and Borkman, 1998), Fourier transform IR spectroscopy (Kazarian, et al. 1996), and the design of ether-carbonate copolymers (Sarbu, et al. 2000) all suggest that the electron-donating carbonyl group promotes Lewis acid-base interactions that enhance CO_2-philicity of a polymer, if the carbonyl is accessible to the CO_2. Further studies have also support this conjecture. For example, the cloud-point locus of polydimethylsiloxane can be reduced via the incorporation of pendant acetate groups (Fink, et al. 1999). Small sugar molecules, such as 1,2,3,4,6-pentaacetyl α-D-glucose, 1,2,3,4,6-pentaacetyl β-D-glucose and 1,2,3,4,6-pentaacetyl β-D-galactose, have been functionalized with acetate groups to dramatically enhance CO_2-solubility (Raveendran and Wallen, 2002). The enhancement in CO_2 solubility was attributed to a two-point interaction of the methyl acetate with CO_2, including the Lewis acid-Lewis base interaction and a weak cooperative hydrogen bond between a proton on the methyl group and an oxygen of the CO_2 (Raveendran and Wallen, 2002). Subsequently, sorbitol, β-cyclodextrin and small hydrogen-bonding compounds were acetylated to promote CO_2 solubility (Hamilton, et al. 2002). Interestingly, cellulose triacetate remains insoluble in CO_2, however, at temperatures up to 373 K and pressures of 70 MPa. It is also noted that the carbonyl-CO_2 interaction contributes to the high solubility of CO_2 in a polymer-rich phase. For example, both PVAc (Sato, et al. 2001) and PMA (Liau and McHugh 1985; Wissinger and Paulitis, 1987) exhibit very high sorption of CO_2.

The objective of this work was to identify the most CO_2-soluble homopolymer composed solely of hydrogen, carbon and oxygen, and to identify the polymer characteristics that promote CO_2-philicity. Solubility was determined over a wide range of molecular weights, and comparisons were conducted on an equivalent number of repeat units basis. The solubility of PVAc, PMA, poly(vinyl formate) (PVF), and PPO in CO_2 was determined and compared with previously published data for PLA (Conway et al. 2001). The repeat unit of each of these non-fluorous homopolymers is presented in Figure 1. Finally, the conditions needed to dissolve the most CO_2 soluble hydrocarbon-based homopolymer were compared to those needed to dissolve several expensive CO_2 soluble polymers, poly(fluoroacrylate) (PFA) and poly(dimethyl siloxane) (PDMS).

Experimental

Materials

Poly(propylene oxide), poly(vinyl acetate) (M_w > 10000), and poly(methyl acrylate) (M_w > 10000) were obtained from Aldrich Chemical Company. Poly(vinyl formate), poly(vinyl acetate) (M_w = 1700), and poly(methyl acrylate) (M_w = 1390) were synthesized by Scientific Polymer Products. Low molecular weight poly(vinyl acetate) (4000 < M_w < 10000) and poly(methyl acrylate) (M_w = 2848) were synthesized at the University of Pittsburgh using vinyl acetate or methyl acrylate, methyl 2-bromopropionate, CuBr, 2-2' bipryidine, CCl_4, $Fe(CH_3CO_2)_2$, and N,N,N'N',N"-pentamethyldiethylenetriamine, and tetrahydrofuran obtained from Aldrich Chemical Company. The shortest PVAc oligomer (M_w = 980) was synthesized at the University of Pittsburgh using vinyl acetate,

isopropanol, and di-tert-butylperoxide obtained from Aldrich Chemical Company. Methyl isobutyrate and dimethyl 2,4-dimethylglutarate, the monomer and dimer models of PMA, were obtained from Aldrich. Isopropyl acetate, which served as the model monomer of PVAc, was obtained from Aldrich.

Acetate- and acrylate-functionalized silicone copolymers were synthesized from methylhydrosiloxane (16.5 mole%)- dimethylsiloxane (83.5 mole%) copolymer and platinum-vinyl tetramethyldisiloxane complex in xylene (low color) as received from Gelest. Anhydrous toluene, allyl acetate and methyl-3-butenoate were obtained from Aldrich.

Polymer Synthesis

Atom Transfer Radical Polymerization (ATRP) was employed to synthesize low molecular weight poly(vinyl acetate) ($4000 < Mw < 10000$) and poly(methyl acrylate) ($Mw = 2848$) following the general procedures described in literature (Xia, et al. 1999). In a typical experiment, the vinyl acetate monomer was combined with the carbon tetrachloride initiator, iron (II) acetate catalyst, and N,N,N',N',N" pentamethyldiethylenetriamine (PMETA) ligand in a molar ratio of M:I:C:L was R:1:1:2, where R was varied to alter the polymer chain length. For example, when $R = 30$ the resulting Mn of PVAc was 2063. The mixture was exposed to a freeze-thaw-pump cycle three times and then degassed for 10 minutes with nitrogen. The flask was placed in an oil bath maintained at 333 K for 12 hours. The contents of the flask were poured through an alumina packed-column and subsequently washed twice with 100 ml of tetrahydrofuran (THF). Most of the THF was then removed using a rotovap and hexane was subsequently employed as an anti-solvent to precipitate the poly(vinyl acetate). The polymer was dried overnight in a vacuum oven. The PVAc yield was 40%.

The lowest molecular weight PVAc ($M_w = 980$) was synthesized following a recently described polymerization procedure (Zimmermann, 2002).

Propyl acetate- and methyl butyrate-grafted methylhydrosiloxane-dimethylsiloxane copolymers were synthesized according to the procedure described earlier (Fink et al. 1999).

Molecular Weight Determination

The molecular weight of each polymer synthesized in our laboratories (or not reported by the manufacturer) was determined using a Waters 150CV gel permeation chromatograph equipped with a refractive index detector. THF was used as the mobile phase at a flow rate of 1.0 ml/min and 308 K. Three columns in series were installed in the instrument to achieve sufficient separation for the molecular weight range of 500-30,000 Da. The first two columns, PL-gel Mixed-E columns from Polymer Laboratories, had mixed porosity. The third column, a Waters Ultrastyragel column, had a uniform pore size of 500 Å. A calibration curve, which plotted the log of the molecular weight versus the retention time, was constructed using 11 polystyrene standards in the molecular weight range of 580-66,000 Da.

Phase Behavior Procedures

Low pressure (<50 MPa) data were determined at the University of Pittsburgh. A known amount of the polymer and six stainless steel mixing balls were introduced to the sample volume to within ± 0.001 gr of a high pressure, windowed, variable-volume view cell (DB Robinson & Assoc. 3.18 cm ID, ~100 cm^3 working volume). After the sample volume was purged with carbon dioxide at 0.2 MPa, the volume of the cell was minimized. High pressure liquid carbon dioxide (295 K, 13.78 MPa) was then introduced to the sample volume as the silicone oil overburden fluid was withdrawn at the equivalent flow rate using a dual-proportioning positive displacement pump (Ruska, Inc.). This technique facilitated the isothermal, isobaric additional of a known volume of CO_2 to within ± 0.001 cm^3 into the sample volume. The mass of CO_2 was determined from the displaced volume, temperature and pressure using an equation of state for carbon dioxide (Span and Wagner, 1996). The polymer-CO_2 mixture was then compressed and mixed via rocking until a single, transparent phase was attained. Cloud-points were determined by slowly expanding the sample volume until it was no longer possible to see through the solution. Cloud-points are reproduced two to three times to within approximately ± 0.5 MPa, as measured with a Heise pressure gauge accurate

to within ± 0.07 MPa for data to 70 MPa, at each temperature held to within ± 0.2 K, as measured with a type K thermocouple.

Cloud-point pressures greater than 50 MPa were determined at Virginia Commonwealth University. The apparatus and techniques used to obtain CO_2-polymer cloud-point are described elsewhere (Meilchen, et al. 1991; Mertdogan et al. 1996). The main component of the apparatus was a high-pressure, variable-volume cell (Nitronic 50, 7.0 cm OD x 1.6 cm ID, ~30 cm^3 working volume). The cell was first loaded with a measured amount of polymer to within ± 0.002 grams. The cell was then flushed very slowly with gaseous CO_2, at pressures less than three bar, to remove entrapped air. CO_2 was then transferred into the cell gravimetrically to within ± 0.02 grams using a high-pressure bomb. The mixture in the cell was viewed with a borescope (Olympus Corporation, model F100-024-000-55) placed against a sapphire window secured at one end of the cell. A stir bar activated by a magnet located below the cell mixed the contents of the cell. The cloud point pressure was defined as the point at which the solution becomes so opaque that it is no longer possible to see the stir bar in solution. These cloud points have been compared in our laboratories to those obtained using a laser light set-up where the phase transition is the condition of 90 % drop off in light transmitted through the solution. Both methods gave identical results within the reproducibility of the data. Cloud-points are reproduced two to three times to within approximately ± 4.0 bar, as measured with two Heise pressure gauges accurate to within ± 0.07 MPa for data to 70 MPa and to within ± 0.35 MPa for data from 70 MPa to 300 MPa, at each temperature held to within ± 0.3 K, as measured with a type K thermocouple.

Results and Discussion

Poly(vinyl acetate) Isopropyl acetate served as the model of the PVAc monomer. The CO_2-isopropyl acetate binary exhibits Type I phase behavior and the vapor pressure of CO_2 is the maximum pressure bounding the two-phase region. For longer oligomers of PVAc, Figure 2 shows that the two-phase loci of PVAc-CO_2 mixtures exhibits a relatively flat profile over the 1-15 wt % region at 298 K with the cloud-point maximum occurring near 5 wt% concentration. The cloud-point pressure increases with PVAc chain length. Table 1 presents the cloud-point pressure data at the 5 wt % concentration of these loci and other PVAc samples. Even the highest molecular weight PVAc (M_w = 585000) is soluble in CO_2 at 298 K at a pressure of 67.6 MPa. The strength of the CO_2-acetate interactions is apparently great enough to overcome repeat group-repeat group interactions, and entropic effects associated with polymer conformation do not have a dramatic effect on the cloud-point pressure with increasing polymer molecular weight. The temperature-dependence of the miscibility pressure is illustrated in Figure 3 for several high molecular weight PVAc samples (M_w = 125000 and 585000). The cloud-point pressure over the entire range of temperature and higher pressures are required for the dissolution of higher molecular weights.

Poly(vinyl formate) PVF was insoluble in CO_2 at temperatures up to 484 K and pressures up to 240 MPa. This result is consistent with the previous observations (Rindfleisch, et al. 1996), which concluded that very polar or hydrogen bonded polymers do not dissolve in carbon dioxide. The formate will interact with itself more strongly than an acetate, even though the formate proton is not highly acidic. Nonetheless, this interaction is much stronger than a CO_2-formate interaction, causing PVF to be CO_2-insoluble.

Poly(propylene oxide) Figure 2 shows that low molecular weight PPO (M_w = 2079) was soluble in CO_2 at 298 K, especially at low concentration. The result at 1 wt% is in very good agreement with previously reported solubility results at low concentrations (O'Neill, et al. 1998; Drohmann and Beckman, 2002). The cloud-point pressure is strongly related to the polymer concentration at 298 K, increasing from 22 MPa to 55 MPa as the PPO concentration increased from 1 wt% to 6 wt %. PPO (M_w = 3500) could not be dissolved at temperatures at 298 K, but cloud point pressure data was obtained at higher temperatures, Figure 4. Although the UCST behavior of the CO_2-PPO (M_w = 3500) system prevented miscibility from being attained at temperatures in the 298 - 322 K range, the cloud point pressure decreased with temperature over the 322.6 – 343.1 K temperature range.

Low molecular weight PPO oligomers may be promising non-fluorous, CO_2-philic tails in the design of CO_2-soluble surfactants, dispersants and chelating agents because these amphiphiles are typically used in dilute concentration. High molecular weight PVAc is more CO_2 soluble than PPO, even though the surface tension of PVAc, 36.5 mN/m, is greater than that of PPO, 31.5 mN/m. Polymers with lower surface tensions typically exhibit greater CO_2

solubility, however (O'Neill, et al. 1998). The relatively high solubility of PVAc in CO_2 may therefore be attributed to the acetate – CO_2 interaction of the PVAc – CO_2 system being more favorable than the ether – CO_2 interaction associated with the PPO – CO_2 system.

Poly(methyl acrylate) The monomer and dimer results (n = 1 and 2) for PMA at 298 K were obtained by measuring the maximum dew point pressure needed to dissolve methyl isobutyrate and dimethyl 2,4-dimethylglutarate, respectively. These binaries exhibit Type I phase behavior, therefore the vapor pressure of CO_2 is the maximum pressure bounding the two-phase region. The PMA oligomer (Mw = 1390) dissolves in CO_2 at 298K and 34.6 MPa. A higher molecular weight PMA (Mw = 2848) dissolves in CO_2 at 298K at a much higher pressure, (see Table 1 and Figure 2) and also remains CO_2-soluble at slightly higher pressures in the 298 – 323 K temperature range as shown in Figure 5. The cloud-point loci exhibit a maximum value at about 5 wt% PMA at each temperature. The maximum in cloud-point pressure near 5 wt% which characterizes the PMA-CO_2 and PVAc-CO_2 mixtures has been previously observed for other polymer-solvent mixtures (Rindfleisch, et al. 1996; Meilchen, et al. 1991; Mertdogan et al. 1996; Allen and Baker, 1965; Irani and Cozewith 1986; Lee. et al. 1994). PMA is also characterized by a steep increase in cloud-point pressure with increasing polymer chain length (see Table 1). Despite their identical composition, PMA was much less soluble in CO_2 than PVAc. Figure 6 illustrates that the cloud-point pressure of PMA increases dramatically with molecular weight relative to PVAc. Note that the PMA carbonyl group is closer to the polymer backbone, while the PVAc carbonyl group can rotate more freely due to the ether linkage between the polymer backbone and the acetate. Therefore the PVAc carbonyl group is more accessible to interact with CO_2. Further, the carbonyl functionality of PVAc is adjacent to a methyl group. Ab initio calculations suggest that a weak but cooperative bond between the hydrogen of the acetate methyl group and the oxygen of the CO_2, along with the stronger Lewis acid-Lewis base interaction of the carbonyl's oxygen and the carbon of CO_2 account for the effectiveness of acetylation in enhancing CO_2-philicity (Raveendran and Wallen, 2002).

Two graft copolymers were synthesized in order to assess the influence of carbonyl accessibility and the CO_2-philicity of the acetate and acrylate groups on polymer solubility in CO_2. A 25-repeat unit silicone polymer was functionalized by adding five pendant acetate or acrylate groups separated from the polymer backbone by a linear propyl spacer as depicted in Figure 7. Phase behavior results in Figure 8 illustrate that the propyl acetate (analog to the PVAc side chain)-functionalized copolymer is slightly more CO_2 soluble than the methyl butyrate (analog to the PMA side chain)-functionalized PDMS. This indicates that the acetate functionality is more CO_2-philic than the methyl acrylate functionality. The difference between the cloud-point curves shown in Figure 8 is modest, however, relative to the substantial differences between PVAc and PMA solubility illustrated in Figure 6. The difference between the methyl acrylate-CO_2 and acetate-CO_2 interactions alone is unlikely to account for the low solubility of PMA relative to PVAc. Therefore steric effects, which prevent the carbonyl of PMA from being easily accessed by the CO_2, are also responsible for the low solubility of PMA relative to PVAc.

Poly(lactide) The solubility of PLA in CO_2, Figure 6, has been determined previously (Conway et al. 2001). PVAc is also more soluble in CO_2 than PLA despite the similarity of their compositions. PVAc is an amorphous polymer with a pendant acetate on each repeat unit, however, resulting in an entropic advantage for dissolution due to an increased concentration of side groups. Further, PLA is a high melting point, crystalline polyester that is likely to exhibit enhanced polymer-polymer interactions that inhibit dissolution in dense CO_2.

Poly(fluoroacrylate) Although PVAc is a promising non-fluorous, CO_2-soluble homopolymer, it is far less CO_2-philic than fluoroacrylate polymers. DeSimone pioneered the incorporation of fluoroacrylate into a homopolymer or copolymer to attain CO_2-solubility (DeSimone, et al. 1992). Figure 6 illustrates that the cloud-point pressures of PFA (Blasig, et al. 2002; Mawson et al. 1995; Hsiao, et al. 1995) are significantly lower than those of PVAc. This difference in solubility in dense CO_2 at relatively low pressures has been exploited in PVAc-PFA copolymers, which have been used to facilitate the emulsion polymerization of vinyl acetate in CO_2 (Canelas, et al. 1998) because PVAc is CO_2-phobic relative to PFA at low pressure.

Poly(dimethyl siloxane) The solubility of PDMS in CO_2 has been previously reported at ~298K (O'Neill et al. 1998; Bayraktar and Kiran, 2000). Silicone homopolymers are also more CO_2 soluble than PVAc as seen in Figure 6, although PDMS is not as CO_2-soluble as PFA.

Conclusions

PVAc is the most CO_2-soluble vinyl homopolymer composed solely of carbon, hydrogen, and oxygen identified to date, as reflected by the relatively low pressure required to attain dissolution of 5 wt% polymer at 298 K. PVAc exhibits remarkable CO_2 solubility over a wide range of concentration (1-15 wt%) and molecular weight (11-6800 repeat units based on Mw) at 298 K and pressures ranging from 13.6-67.6 MPa. The highest molecular weight PVAc investigated (Mw = 585000) exhibited an increase in cloud-point pressure from 68 to 130 MPa as temperature increased from 298 K to 430 K. The CO_2-philic nature of this amorphous, low-melting point polymer was attributed to the accessibility of the acetate group for favorable interactions with the CO_2 solvent. Other carbonyl-rich polymers with similar or identical composition were significantly less soluble or insoluble in CO_2 due to their crystallinity, lack of side chains or less accessible acetate groups. PVAc may serve as a non-fluorous, CO_2-philic tail of polymeric or amphiphilic compounds designed to exhibit CO_2 solubility. Copolymers containing vinyl acetate may even exhibit lower solubility than the PVAc homopolymer (Sarbu, et al. 2000). Despite the high degree of CO_2 miscibility attained with PVAc relative to other hydrocarbon homopolymers, PFA and PDMS are CO_2-soluble at markedly lower pressure.

Acknowledgements

The University of Pittsburgh would like to acknowledge the support of the US DOE NPTO as administered by the US DOE NETL for support of this work through Contract DOE-FC26-01BC15315. The NSF also supported this research through grant CHE-0131477. Mary Ann Wittig and John Newcome of Bayer Corporation evaluated the molecular weight distribution of the highest molecular weight PVAc sample by gel permeation chromatography.

References

Allen, G.; Baker, C.H.;Polymer 1965, 6, 81. Should be: Allen, G.; Baker, C.H.; Lower critical-solution phenomena in polymer-solvent systems; Polymer 1965, 6, 181-191.

Bayraktar, Z.; Kiran, E.; Miscibility, Phase Separation, and Volumetric Properties in Solutions of Poly(dimethylsiloxane) in Supercritical Carbon Dioxide; Journal of Applied Polymer Science 2000, 75, 1397-1403 -- remove the parens around the year 2000 and add a comma after 2000.

Blasig, A.; Shi, C.; Enick, R.; Thies, M.; Effect of Concentration and Degree of Saturation on RESS of a CO_2-Soluble Fluoropolymer; Industrial and Engineering Chemistry Research (in press)

Canelas, D.; Betts, D.; DeSimone, J.; Yates. M.; Johnston, K.; Poly(vinyl acetate) and Poly(vinyl acetate-co-ethylene) Latexes via Dispersion Polymerization in Carbon Dioxide; Macromolecules 1998, 31, 6794-6805

Conway, S.E.; Byun, H.-S.; McHugh, M.A.; Wang, J.D.; Mandel, F.S.; Poly(lactide-co-glycolide) Solution Behavior in Supercritical CO_2, CHF_3, and $CHClF_2$; Journal of Applied Polymer Science 2001, 80, 1155-1161

DeSimone, J.; Guan, Z.; Elsbernd, C.; Science 1992, 257, 945.

Drohmann, C.; Beckman, E.; Phase Behavior of Polymers Containing Ether Groups in Carbon Dioxide; Journal of Supercritical Fluids (2002) 22 103-110 -- remove the parens around the year 2002 and add a comma after 2002, 22,.

Fink, R.; Hancu, D.; Valentine, R.; Beckman, E.; Toward the Development of "CO_2-philic" Hydrocarbons. 1. Use of Side-Chain Functionalization to Lower the Miscibility Pressure of Polydimethylsiloxanes in CO_2; J. Phys. Chem. B 1999, 103, 6441-6444

Heller, J.P.; Dandge, D.K.; Card, R.J.; Donaruma, L.G.; Direct Thickeners for Mobility Control of CO_2 Floods, SPEJ 1985 679-686.

Hsiao, Y.; Maury, E.; DeSimone, J.; Mawson, S.; Johnston, K.; Dispersion Polymerization of Methyl Methacrylate Stabilized with Poly(1,1-dihydroperfluorooctyl acrylate) in Supercritical Carbon Dioxide, Macromolecules 1995, 28, 8159-8166.

Irani, C.A.; Cozewith, C.J.; Lower critical solution temperature behavior of ethylene propylene copolymers in multicomponent solvents; J. Appl. Polym. Sci. 1986, 31, 1879

Kazarian, S.; Vincent, M.; Bright, F.; Liotta, C.; Eckert, C.; Specific Intermolecular Interaction of Carbon Dioxide with Polymers; JACS 1996, 118, 1729-1736

Lee, S.H.; LoStracco, M.A.; Hasch, B.M.; McHugh, M.A.; Solubility of poly(ethylene-co-acrylic acid) in low molecular weight hydrocarbons and dimethyl ether. Effect of copolymer concentration, solvent quality, and copolymer molecular weight; J. Phys. Chem. 1994, 98, 4055.

Liau, I.; McHugh, M.A.; High Pressure Solid Polymer-Supercritical Fluid Phase Behavior; in Supercritical Fluid Technology, ed. Penninger, J. M. L.; Radosz, M.; McHugh, M.A.; Krukonis, V.J.; (1985) 415, New York, Elsevier

Mawson , S.; Johnston, K.; Combes, J.; DeSImone, J.; Formation of Poly(1,1,2,2-tetrahydroperfluorodecyl acrylate) Submicron Fibers and Particles from Supercritical Carbon Dioxide Solutions; Macromolecules 1995, 28, 3182-3191.

Meilchen, M.A.; Hasch, B.M.; McHugh, M.A.; Effect of copolymer composition on the phase behavior ofmixtures of poly(ethylene-co-methyl acrylate) with propane and chlorodifluoromethane; Macromolecules 1991, 24, 4874

Mertdogan, C.A.; Byun, H.-S.; McHugh, M.A.; Tuminello, W.H.; Solubility of poly(tetrafluoroethylene-co-19 mol % hexafluoropropylene) in supercritical CO_2 and halogenated supercritical solvents; Macromolecules 1996, 29, 6548

Nelson, M.; Borkman, R.; Ab Initio Calculations on CO_2 Binding to Carbonyl Groups; J. Phys. Chem. A 1998 102, 7860-7863.

O'Neill, M.; Cao, Q.; Fang, M.; Johnston, K.; Wilkinson, S.; Smith, C.; Kerschner, J.; Jureller, S.; Solubility of Homopolymers and Copolymers in Carbon Dioxide; Ind. Eng. Chem. Res. 1998, 37, 3067-3079

Poltluri, V.; Xu, J.; Enick, R.; Beckman, E.; Hamilton, A.; Per-acetylated Sugar Derivatives Show High Solubility in Liquid and Supercritical CO_2; Organic Letters 2002, 4:14, 2333-2335.

Raveendran, P.; Wallen, S.; Sugar Acetates as Novel, Renewable CO_2-philes; JACS Communications, 2002 124 (25) 7274-7275.

Rindfleisch, F.; DiNoia, T. P.; McHugh, M. A.; Solubility of Polymers and Copolymers in Supercritical CO_2; J. Phys. Chem. 1996, 100, 15581-15587

Sarbu, T.; Styranec, T.; Beckman; E.; Non-fluorous Polymers with Very High Solubility in Supercritical CO_2 Down to Low Pressures; Nature 405, May 11 2000, 165-168

Sato, Y.; Takikawa, T.; Takishima, S.; Masuoka, H.; Solubilities and Diffusion Coefficients of Carbon Dioxide in Poly(Vinyl Acetate) and Polystyrene; Journal of Supercritical Fluids 19, 2001, 187-198

Span, R,; Wagner, W.; A New Equation of State for Carbon Dioxide Covering the Fluid Region from the Triple-Point Temperature to 1100 K at Pressures up to 800 MPa; J. Phys. Chem. Ref. Data 1996 25(6) 1509-1596

Wissinger, R.; Paulitis, M.; Swelling and Sorption in Polymer CO_2 Mixtures at Elevated Pressures; J. Polym. Sci.: Part B: Polym. Phys. (1987) 25:2497

Xia, J.; Paik, H.-J.; Matyjaszewski, K.; Polymerization of Vinyl Acetate Promoted by Iron Complexes; Macromolecules 1999, 32, 8310-8314

Zimmermann, J.; Sunder, A.; Mulhaupt, R.; Preparation of Partially Hydrolized Oligo(vinylacetate) as Polyol for Poluurethane Formation; Journal of Polymer Science: Part A: Polymer Chemistry 2002, 40, 2085-2092

Table 1. PMA, PVAc, PPO, PVF Molecular Weight and CO_2 Solubility

Polymer	Mn	Mw	PDI	#RU (Mn)	#RU (Mw)	Pcp, 5wt% 298 K
PMA	780	1390	1.78	9.1	16	34.6
PMA	2079	2848	1.37	24	33	89.1
PMA	10600	30700	2.90	123	357	225.0*
PVAc	782	980	1.25	9.1	11	13.6
PVAc	850	1700	2.00	9.9	20	20.8
PVAc	2063	4147	2.01	24	48	37.4
PVAc	3092	4638	1.5	36	54	37.6
PVAc	5680	8377	1.47	66	97	42.0
PVAc	7697	12469	1.62	89	145	43.6
PVAc		12800			149	45.7
PVAc	12991	17018	1.31	151	198	45.7
PVAc	52700	124800	2.37	612	1451	60.2*
PVAc		167000			1941	62.5
PVAc	61600	182000	2.95	716	2116	63.7
PVAc	193000	585000	3.02	2244	6802	67.6
PPO	1642	2029	1.24	28	35	43.6
PPO		3500			60	insoluble
PVF	1068	2327	2.18	15	27	insoluble

* - Rindfleisch, et al. 1996

Figure 1. Structure of Non-Fluorous Polymeric Repeat Units

Polymer Name	**Repeat Unit Structure**
PVF poly(vinyl formate)	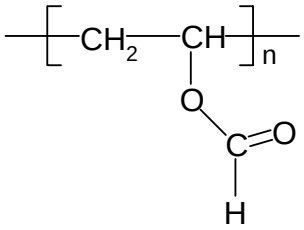
PMA poly(methyl acrylate)	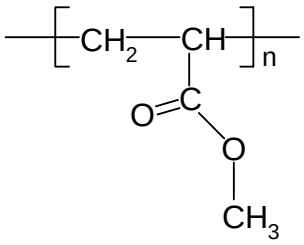
PVAc poly(vinyl acetate)	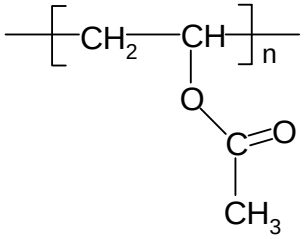
PLA poly(lactide)	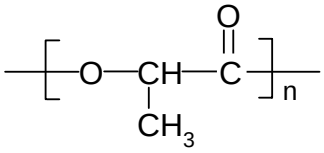
PPO poly(propylene oxide)	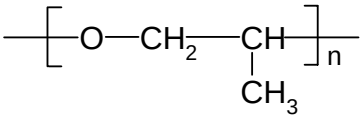

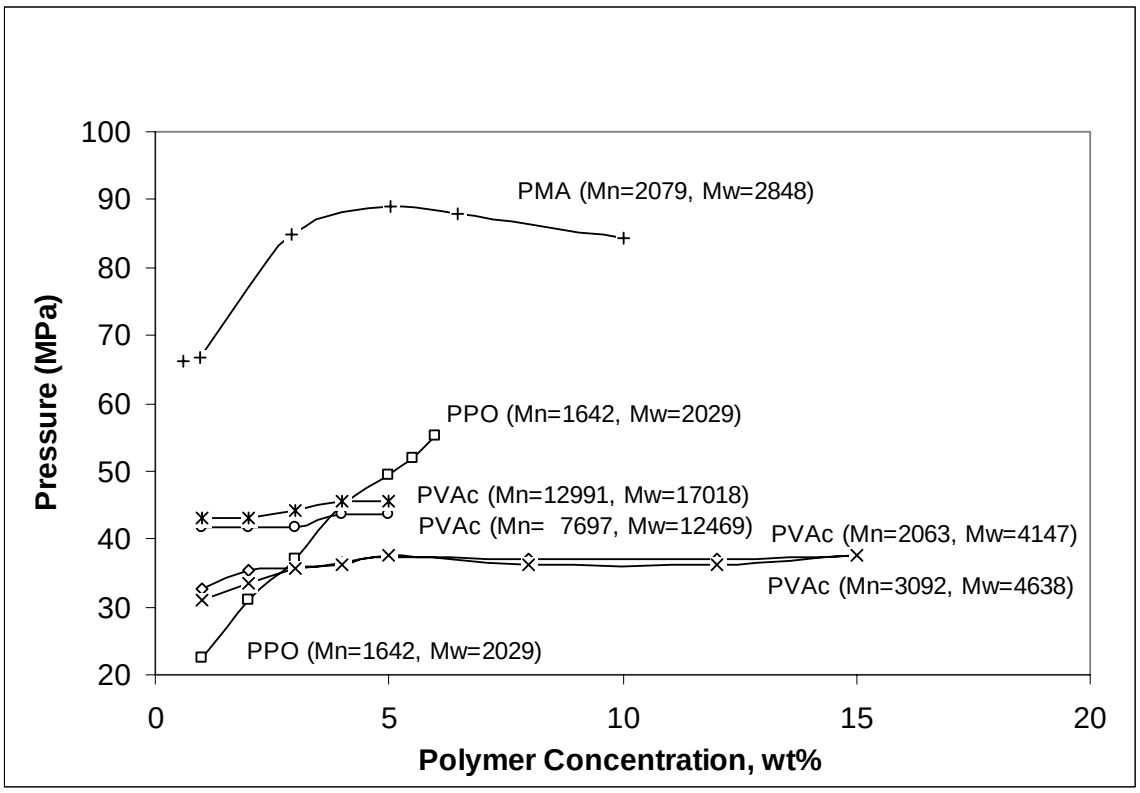

Figure 2. Pressure-Composition Diagrams at 298 K for Mixtures of Carbon Dioxide and Polymer, Including PPO, PMA, and PVAc

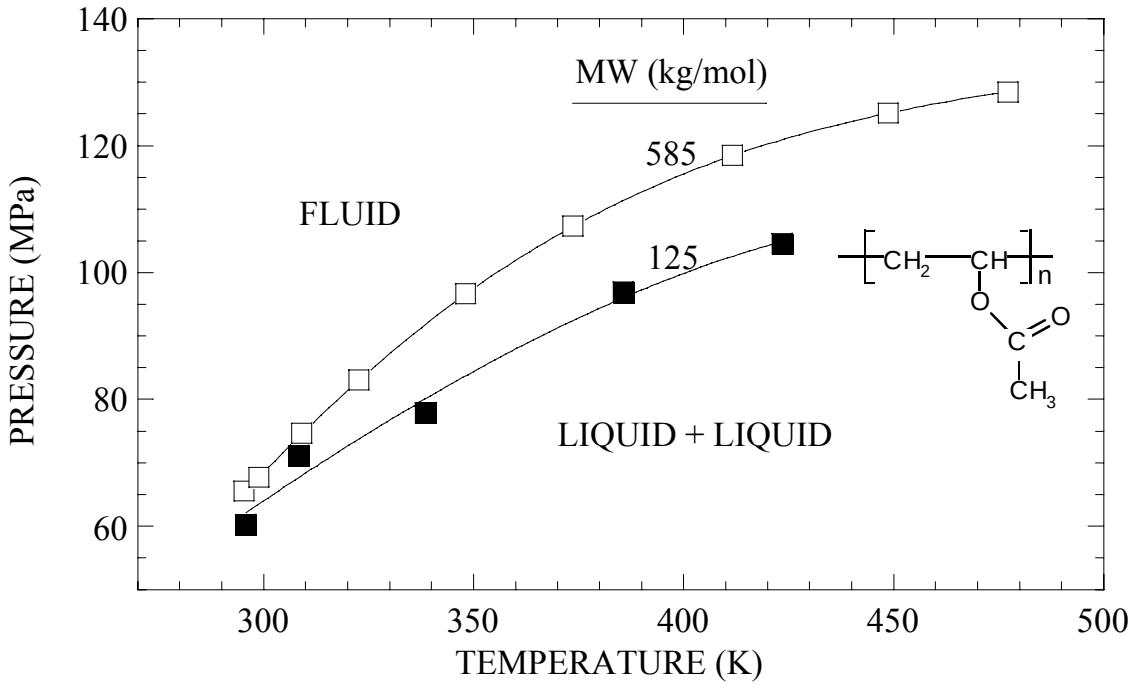

Figure 3. Pressure – Temperature Diagram for the Carbon Dioxide (95 wt%) – PVAc (5 wt%) System as a Function of PVAc Molecular Weight. PVAc 125000 Data from Rindfleisch et al. 1996.

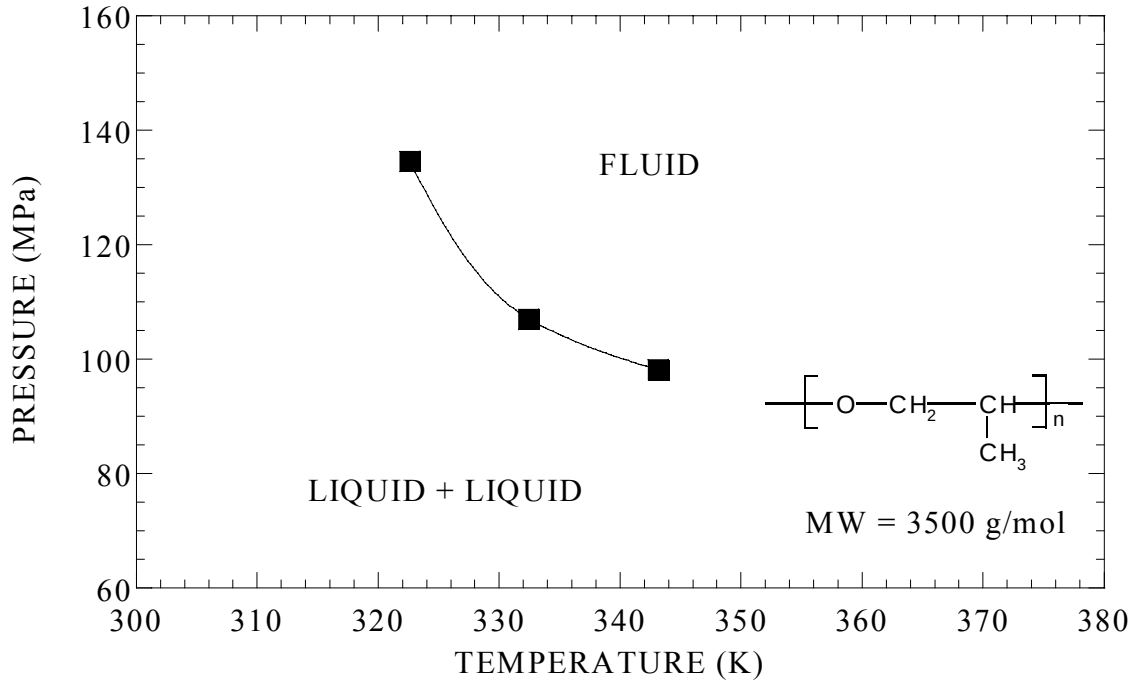

Figure 4. . Pressure – Temperature Diagram for the Carbon Dioxide (95 wt%) – PPO (5 wt%) System, M_w = 3500

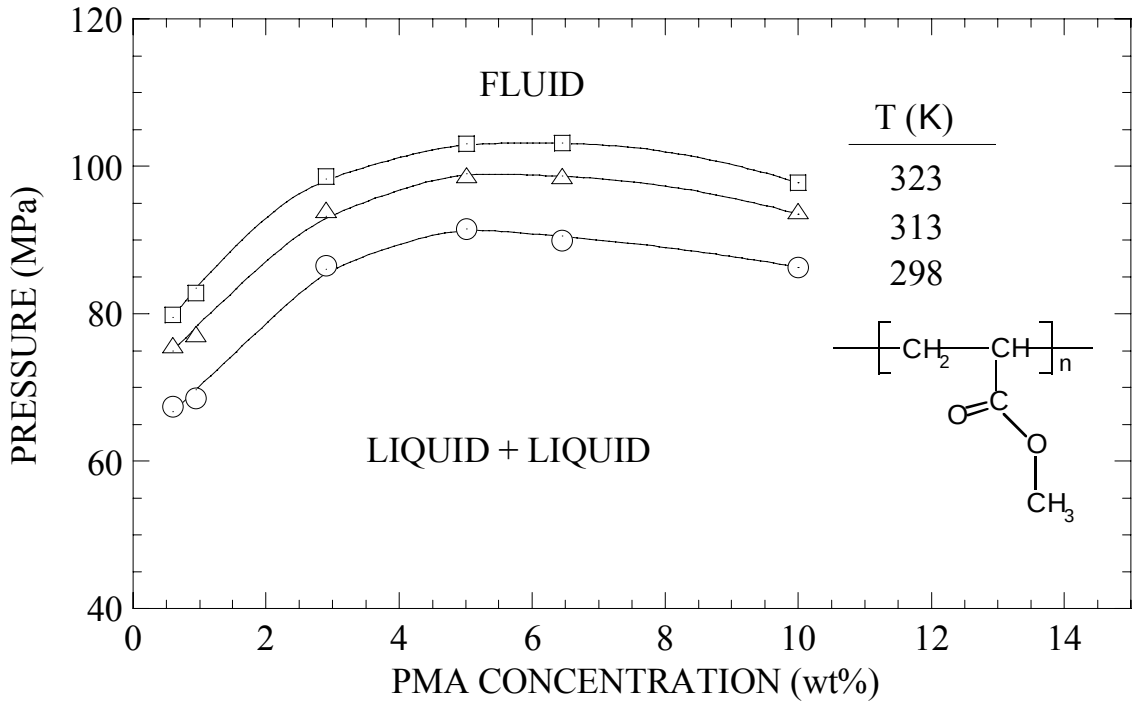

Figure 5. Pressure-Composition Isotherms for the CO_2 – PMA (Mw = 2848) System.

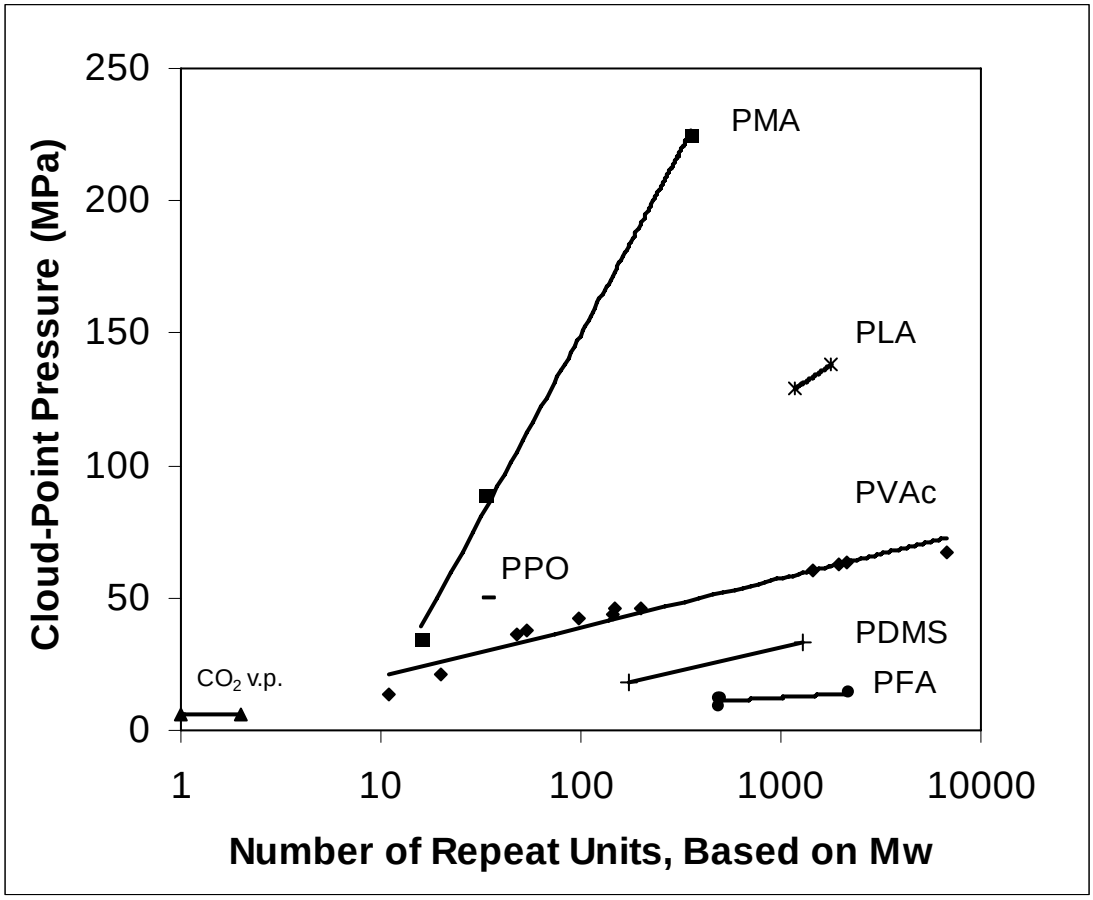

Figure 6. Cloud-Point Pressure at 5 wt% Polymer Concentration and 298 K for Mixtures of CO_2 with PMA, PPO, PLA, PVAc, PDMS, and PFA as a Function of Repeat Units Based on Mw.

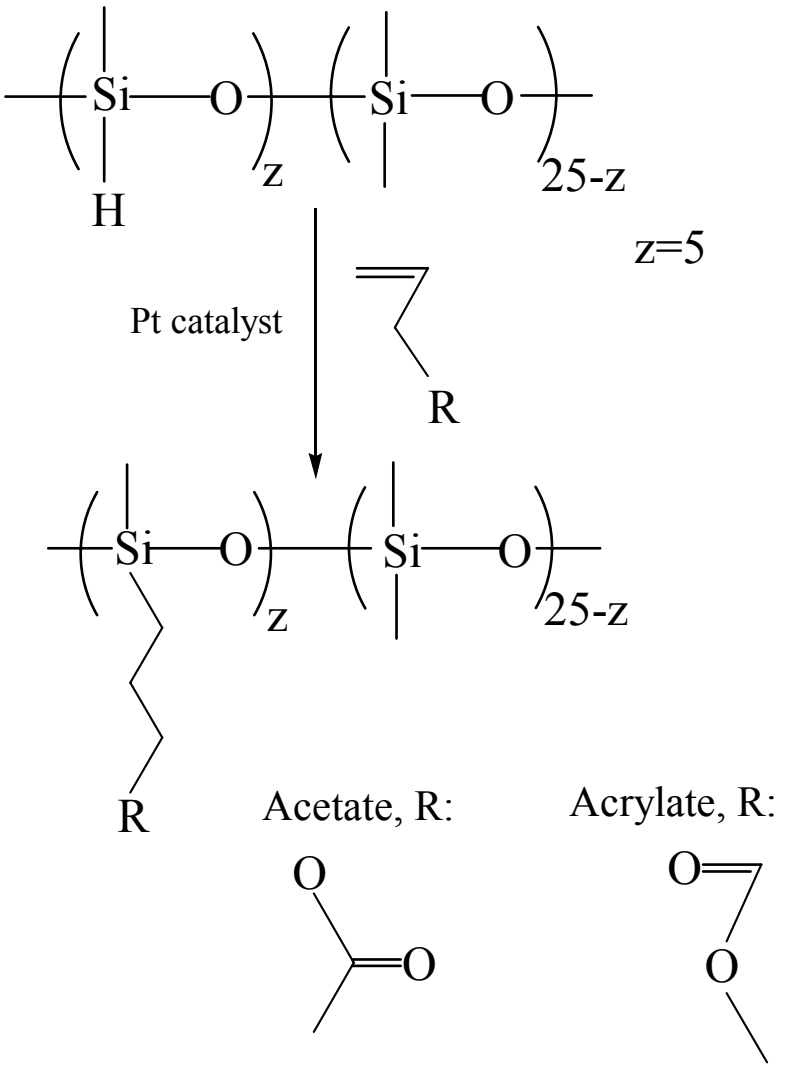

Figure 7. Structures of the Random Copolymers of PDMS Side-Functionalized with Propyl Acetate and Methyl Butyrate Groups to Establish Effect of Accessible Acetate and Acrylate Groups, Respectively

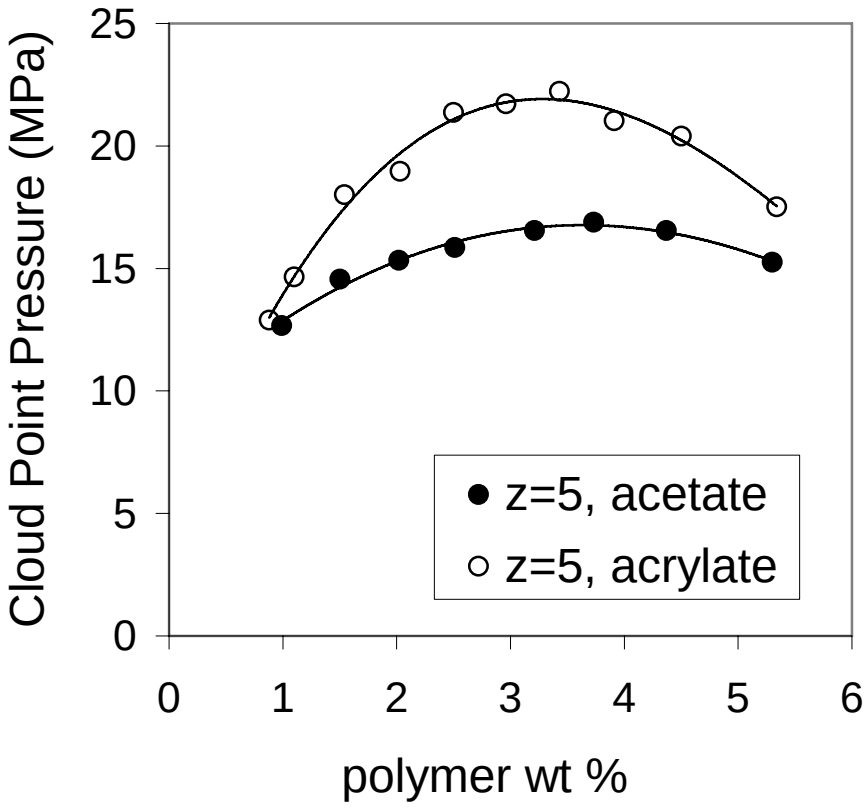

Figure 8. Cloud Point Curves of Siloxane Random Copolymers with Pendant Propyl Acetate and Methyl Butyrate Groups to Establish Effect of Accessible Acetate and Acrylate Groups, Respectively, z = 25, 298 K.

Section 2. Design, Synthesis, and Optimization of Non-fluorous, CO_2-Soluble Polymers, A Systematic Approach

Research done during the last 15 years has proven that one can use CO_2 as a solvent in many processes. There have been compounds from surfactants to chelating agents that were shown to be soluble in CO_2 to low pressures. By attaching CO_2-philic groups to polymer chains, previously insoluble polymers have exhibited miscibility with CO_2, allowing for applications such as emulsion polymerization, dispersion polymerization, dissolution of proteins, extraction of heavy metals, and other processes. Unfortunately, the most successful CO_2-philes, the fluorinated polymers, have a very unfavorable economic drawback that makes their commercial use impractical. As a result, this work seeks to determine the characteristics that could be built into a carbon based polymer to allow for the polymer to be miscible with CO_2 down to low pressures.

Several design elements were considered in this work: the cohesive energy density, the free volume, and the Lewis acid/base interactions with CO_2 acting as a Lewis acid. Lowering the cohesive energy density and increasing the free volume limited undesirable polymer-polymer interactions, while the addition of Lewis base groups to the polymer in the backbone and as grafted side chains increased the favorable polymer-CO_2 interactions. Several side chains containing Lewis base groups were first grafted onto silicon-backbone polymers. The effects of the grafting and degree of substitution were determined, and the best performing side chains were then grafted onto a polyether backbone to investigate their interactions with the carbon/oxygen backbone.

This work made clear the importance of adding optimal amounts of a Lewis base group to the polymer, whether in the backbone or as a grafted side chain. While attaining a low cohesive energy density and maintaining a low glass transition temperature are important, polymers with these features alone performed very poorly in CO_2. The addition of Lewis base groups in the backbone or as a side chain dramatically improved the solubility of the polymers and showed the importance of favorable polymer-CO_2 interactions. A key observation was that an ether functional group may provide the same Lewis acid/base interaction with CO_2 that is seen with the acetate group.

NOMENCLATURE

CO_2	Carbon Dioxide
$scCO_2$	Supercritical Carbon Dioxide
CED	Cohesive Energy Density
T_g	Glass Transition Temperature
T_c	Critical Temperature
P_c	Critical Pressure
CFC	Chlorofluorocarbon
PDMS	Poly(dimethyl siloxane)
PPO	Poly(propylene oxide)
PEO	Poly(ethylene oxide)
PECH	Poly(epichlorohydrin)
PP	Poly(propylene)
PEVE	Poly(ethyl vinyl ether)
PVAc	Poly(vinyl acetate)
PVME	Poly(vinyl methyl ether)
FEP_{19}	Poly(tetrafluoroethylene-co-19 mol % hexafluoropropylene)

TABLE OF CONTENTS

ABSTRACT....6

NOMENCLATURE....8

TABLE OF CONTENTS....9

LIST OF TABLES....11

LIST OF FIGURES....12

1.0 INTRODUCTION....15

2.0 BACKGROUND AND LITERATURE REVIEW....17

2.1 Overview of Supercritical/Liquid CO_2....17

2.2 Uses for CO_2-philic Polymers....18

2.3 Literature Review....19

3.0 RESEARCH OBJECTIVES....25

4.0 EXPERIMENTAL METHODOLOGY....27

4.1 Materials....27

4.2 Analysis....27

4.3 Synthesis of Grafted MethylHydrosiloxane-Dimethylsiloxane Copolymers....28

4.4 Partial Reduction of PECH to form PECH/PPO Copolymers....32

4.5 Synthesis of Acetate-functionalized Poly(propylene oxide)....35

4.6 Synthesis of Methyl-Ether Functionalized Poly(propylene oxide)....38

4.7 Capping of the Hydroxyl End Groups of Select PECH/PPO Polymers....40

4.8 Purification of Low Molecular Weight Poly(propylene)....43

4.9 Synthesis of Low Molecular Weight Poly(acetaldehyde)....44

4.10 Phase Behavior Determination....45

5.0 RESULTS AND DISCUSSION 47
5.1 The Effect of Grafted Side Chains on a PDMS Backbone 47
5.1.1 Phase Behavior of PDMS with Grafted Ketone 47
5.1.2 Phase Behavior of PDMS with Grafted Ethyl Ether 49
5.1.3 Phase Behavior of PDMS with Grafted Hydrocarbon Branching 51
5.1.4 Phase Behavior of PDMS with Grafted Acetate and Hexane 52
5.1.5 The Effect of Molecular Weight on the Phase Behavior of PDMS 53
5.1.6 Comparison of Grafted Lewis Base Chains on PDMS 55
5.2 The Effect of Grafted Side Chains on a Polyether Backbone 58
5.2.1 The Phase Behavior of PPO with Grafted Acetate 59
5.2.2 The Phase Behavior of PPO with Grafted Methyl Ether 59
5.3 The Effect of End Group Capping on PPO Polymers 62
5.4 The Effect of Molecular Weight on the Phase Behavior of PPO 64
5.5 Phase Behavior of Poly(propylene) 65
5.6 Phase Behavior of Poly(ethyl vinyl ether) 67
6.0 CONCLUSIONS 69
7.0 RECOMMENDED FUTURE WORK 71
8.0 APPENDIX A: FT-IR Spectrum 76
9.0 APPENDIX B: ^{1}H-NMR Spectra 77
10.0 REFERENCES CITED 84

LIST OF TABLES

Table #	Title	Page
1	Synthesis of Grafted MethylHydrosiloxane-Dimethylsiloxane Copolymers	29
2	Reduction of Poly(epichlorohydrin)	34
3	Synthesis of Acetate-Functional Poly(propylene oxide)	37
4	Synthesis of Methyl Ether Functional Poly(propylene oxide)	41
5	Polymers Capped with Acetate	42
6	Selected Physical Properties of Polymers	69

LIST OF FIGURES

Figure #	Title	Page
1	Sample Poly(fluoroacrylate)	20
2	Sample Poly(fluoroether)	20
3	Sample Poly(dimethylsiloxane)	20
4	Poly(vinyl acetate)	24
5	Proposed CO_2 Interaction with Acetate[56,57]	24
6	Silicon Backbone Reaction Scheme	30
7	Reduction of Poly(epichlorohydrin)	33
8	Synthesis of Acetate-Functional PPO	36
9	Synthesis of Methyl Ether Functional PPO	39
10	Capping of PECH/PPO Polymers with the Acetate Group	42
11	High Pressure Equipment for Phase Behavior Determination	46
12	Phase Behavior of Ketone Substituted PDMS	50
13	Phase Behavior of Ethyl Ether Substituted PDMS	50
14	Phase Behavior of Branching Group Substituted PDMS	52
15	Phase Behavior of 5-Substituted Hexane and Acetate Substituted PDMS	54
16	Molecular Weight Effects on PDMS Solubility in Carbon Dioxide	54
17	Acetate vs. Ketone (5-sub) Grafted PDMS	55

Figure #	Title	Page
18	Comparison of Acetate, Ketone, and Ether Groups Substituted on Two Repeat Units of PDMS	56
19	Comparison of the Optimal Substitution of Grafted Side Chains on PDMS	57
20	Phase Behavior of Acetate Substituted PPO	61
21	Hypothesized Steric Hindrance in 3 Repeat Units of Ether-Substituted PPO	61
22	The Effect of End Group Capping on Acetate-Substituted PPO	63
23	Molecular Weight Effects on PPO Solubility in Carbon Dioxide	63
24	Cloud Point Effects of Lewis Base Groups on a Polymer	66
25	Phase Behavior of Ether and Acetate Containing Polymers	67
26	Poly(vinyl acetate-co-isobutylene)	72
27	Poly(2-methyltrimethylene oxide)	72
28	Ethyl Methyl Ether Substituted PPO	72
29	Grafted Nitrogen Lewis Base Groups	74
30	Poly(2-methyl-2-butene oxide)	74
31	Poly(vinyl ether methyl ketone)	74
32	Poly(vinyl sulfonate)	75
A1	The Monitoring of the Silicon Reaction by FT-IR through the disappearance of the Si-H peak	76

Figure #	Title	Page
B1	^{1}H-NMR Spectrum for Silicon Polymer	77
B2	^{1}H-NMR Spectrum for Propyl Ethyl Ether Substituted PDMS	77
B3	^{1}H-NMR Spectrum for Butyl Methyl Ketone Substituted PDMS	78
B4	-NMR Spectrum for Butyl Tri-Methyl Silane Substituted PDMS	78
B5	^{1}H-NMR Spectrum for 5,5 Dimethyl Hexane Substituted PDMS	79
B6	^{1}H-NMR Spectrum for Hexane Substituted PDMS	79
B7	^{1}H-NMR Spectrum for Propyl Acetate Substituted PDMS	80
B8	^{1}H-NMR Spectrum for Partially Reduced PECH	80
B9	^{1}H-NMR Spectrum for Acetate Substituted PPO	81
B10	^{1}H-NMR Spectrum for Methyl Ether Substituted PPO	81
B11	^{1}H-NMR Spectrum for PPO with Acetate-Functional End Groups	82
B12	^{1}H-NMR Spectrum for PECH with Acetate-Functional End Groups	82
B13	^{1}H-NMR Spectrum for Poly(acetaldehyde)	83

1.0 INTRODUCTION

The possibility for the use of carbon dioxide as a process solvent has been investigated in industry and academia due to CO_2 being considered an environmentally benign, low-cost, and abundant material. Solubility parameter studies using equation of state data showed that CO_2 had the solvent power of short n-alkanes[1], and it was hoped that CO_2 could be used to replace an array of environmentally and financially unfriendly non-polar organic solvents. Although, CO_2 initially looked to be useful only for non-polar materials, it was thought that polar materials could be brought into solution by adding conventional alkyl-functional surfactants into the mixture. However, early attempts to put these surfactants to use were hindered due to the poor solubility of these amphiphiles in CO_2 . The fact that these amphiphiles showed adequate solubility in short alkanes such as ethane and propane and were quite insoluble in CO_2[2] revealed a gap between the theoretical models and experimental data for CO_2 solubility. Bridging that gap, Johnston and colleagues suggested polarizabilty/free volume as a better method of evaluated solvent power[3,4], and by this method CO_2 is correctly seen as a very poor solvent when compared to short n-alkanes. A number of groups began a search for CO_2-philic materials that would be soluble in CO_2 at significantly lower pressures than similarly sized alkyl-functional equivalents, and it was soon found that by fluorinating materials they could be made to dissolve in CO_2. Harrison et al. synthesized a hybrid alkyl/fluoroalkyl surfactant that dissolved in CO_2 and solubilized a significant amount of water[5]. Polymers were dissolved in CO_2 at moderate pressures when DeSimone and

coworkers produced homo- and copolymers of fluorinated acrylates[6]. Dispersion polymerization in CO_2 was supported by block polymers composed of fluorinated acrylate monomers[7], leading to the generation of monodisperse, micron-sized spheres. Other developments with fluoro-functional amphiphiles were to support emulsion polymerization[8], solubilize proteins[9,10], and extract heavy metals from soil and water[11].

While very successful as CO_2-philic polymers, fluorinated amphiphiles have two substantial barriers limiting practical application. First, they are very expensive approaching $1/gram, making them economically impractical unless the material can be recycled at almost 100% efficiency. Secondly, fluorine has a debated and suspect environmental record. Consequently, a more economical and environmentally friendly method of dissolving polymers in supercritical carbon dioxide would be beneficial on many levels. The development of a CO_2-philic polymer composed of carbon, hydrogen, and oxygen would greatly increase the practical use of CO_2 as a solvent.

2.0 BACKGROUND AND LITERATURE REVIEW

2.1 Overview of Supercritical/Liquid CO_2

A significant amount of time and effort has been put into the use of supercritical carbon dioxide ($scCO_2$) as a solvent due to the many advantages that it presents. Supercritical CO_2 is considered an environmentally benign solvent and is also low-cost, abundant, non-toxic, non-flammable, and easy to discard after use. Reaching the critical point of CO_2 is also relatively easily accomplished as its critical temperature (31.0 °C) is low, and only modest effort is required to achieve its critical pressure (73.8 atm)[12]. A glaring disadvantage of using $scCO_2$ as a solvent lies in the fact that CO_2 is a very feeble solvent[2]. This barrier to CO_2 application was overcome as an effort was made to create and optimize CO_2-philic substances, materials which will dissolve in or be miscible with CO_2 at relatively mild conditions ($T < 100$ °C, $P < 200$ atm).

Beyond environmental and cost benefits, $scCO_2$ exhibits other desirable properties that lend to its usefulness in application. Supercritical fluids exhibit properties of both liquids and gases. For example, gases can be quite miscible with a supercritical fluid while having only limited solubility in a liquid solvent[13], and the density of a supercritical fluid may be changed by simply altering temperature or pressure. The ability to easily change the density of CO_2 can be used in separations. Though not without complications in the repressurization process, the removal of $scCO_2$ from the products of a reaction can be accomplished by opening a valve and discharging the gas.

Again, the disadvantages to using CO_2 as a process solvent are its poor solvent power and the pressure requirements to achieve the supercritical state. It is worth noting that liquid CO_2 can sometimes be used in the place of $scCO_2$ in certain procedures. Near the critical point, liquid CO_2 has many of the same properties of the supercritical fluid and can be achieved at milder conditions. Overall, CO_2 has great potential to be a valuable process solvent as industry continues to realize its environmental and economic advantages.

2.2 Uses for CO_2-philic Polymers

The search for CO_2-philic polymers has a great deal of importance due to the many applications that these materials can serve. CO_2-philic monomers can be polymerized using liquid or supercritical CO_2 as a solvent, eliminating the need for organic solvents and allowing for easy removal of the solvent[14-20]. The synthesis of CO_2-phobic polymers in CO_2 can be supported by the use of CO_2-philic materials via a dispersion or emulsion polymerization[7,8,21-24]. CO_2-philic chelating agents can be used to extract heavy metals[11,25,26]. For example, metal contamination in water can be cleaned effectively since the CO_2 does not leave residual solvent-contamination like that of conventional organic solvents. CO_2-philic fluorinated and siloxane-functional oligomers have been applied in biotechnology as a means of bringing proteins into solution in CO_2[9,27]. The process of producing hydrogen peroxide was aided by using fluoroether oligomers to bring the necessary material into solution in CO_2[28,29]. Poly(vinylidene fluoride) and poly(4-vinylbiphenyl) were dissolved in $scCO_2$ and used to provide a protective film for fused silica plates and metal (Al, Mg) powders[30].

Poly(dimethylsiloxane) has been especially useful in sensing applications, in one case showing a quick, reversible response to hexane vapor[31]. This overview of the many uses of CO_2-philic polymers, illustrates the diversity and large scope of their potential application.

2.3 Literature Review

Many common polymers such as the poly(propylene) seen in this work are CO_2-phobic; like many hydrocarbon polymers[32] they are not miscible in CO_2 even at high pressures. Another example of this is poly(isobutylene)[33], which also requires extremely high pressures to exhibit miscibility with CO_2. Due to the usefulness of CO_2 as a solvent and the perceived benefit of using polymers that would be miscible with CO_2 at moderate to low pressures, a great deal of work was done in the early 1990's to discover methods of dissolving common polymers in CO_2. It was soon found that by adding fluorine groups to polymers, they could be made to be miscible with CO_2 down to low pressures. DeSimone et al. began to produce fluoropolymers (see **Figure 1**) using CO_2 as a solvent, replacing the expensive and environmentally suspect chloroflurocarbons (CFCs) that were previously the most used of the few solvents for these materials[6]. Hoefling et al showed that adding a fluorinated ether (see **Figure 2**) functional group to polymers or surfactants greatly reduced the pressures required to dissolve the materials in CO_2[34]. Other studies also demonstrated the benefits of adding fluorinated groups to create CO_2-philic surfactants[5,10]. Further studies were done using fluorinated compounds to decrease the miscibility pressures of polymers in $scCO_2$[32,35-39].

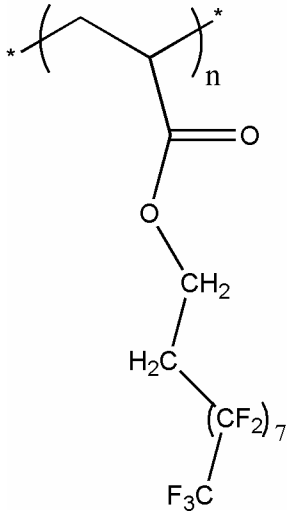

Figure 1: Sample Poly(Fluoroacrylate)

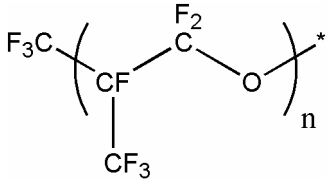

Figure 2: Sample Poly(Fluoroether)

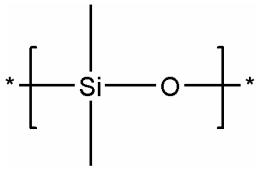

Figure 3: Poly(Dimethylsiloxane)

Given the success found in the solubility of fluorinated materials, can one assume that adding fluorinated groups in any fashion will always lower the miscibility pressures of a polymer? Poly(fluoroacrylates) have some of the lowest surface tensions and thus cohesive energy density values of all polymers[32], and this along with their low glass transition temperature (T_g) values are indications of low polymer self-interactions causing these materials to be among the most CO_2-philic of all polymers. There are three main interactions that govern the solubility of a polymer in CO_2: solvent-solvent interactions, solvent-solute interactions, and solute-solute interactions[40]. Ideally, the solvent-solute interactions should be high, while the other interactions are kept to a minimum, meaning that the polymer should have strong interactions with CO_2, while not interacting with itself. However, simply adding fluorinated groups to a polymer will not guarantee lower miscibility pressures in CO_2. Beckman and co-workers showed that there is an optimal amount of fluorinated groups necessary to achieve the lowest cloud point pressures[37]. Beckman also indicated that incorporating many short chains with the same fluoroether content given by fewer long chains resulted in lower miscibility pressures for the polymers. This was attributed to a more favorable entropy of mixing and increased free volume, giving the polymer a lower T_g[37].

McHugh et al. conducted work showing that a small amount of polarity plays a role in dissolving fluorinated polymers in CO_2. The works compared poly(vinylidene fluoride-co-22 mol % hexafluoropropylene) (Fluorel) and poly(tetrafluoroethylene-co-19 mol % hexafluoropropylene) (FEP_{19}). Fluorel stays in solution to temperatures down to approximately 100 °C and pressures of 750 bar while FEP_{19} falls out of solution below

185 °C regardless of the pressure. Despite the incorporation of fluorinated groups, FEP_{19} lacks the polar vinylidene group of Fluorel. McHugh observed that the dipole moment of vinylidene fluoride interacted favorably with the quadrupole moment of CO_2, resulting in the solubility of Fluorel at lower temperatures where polar interactions are suspected to be magnified[36,41,42]. The effect of polarity and the dipole-quadropole interactions was observed by McHugh et al in a study of the fluorination of poly(isoprenes)[43]. The McHugh group also studied the benefits of polar character in a variety of fluorinated hyrdrocarbon polymers[44]. This dipole-quadrupole interaction allows for favorable polymer-CO_2 interactions, which in combination with low polymer-polymer interactions will allow the polymer to dissolve in CO_2 at lower pressures. In addition to fluorinated compounds, Hoefling and colleagues found silicone-based amphiphiles to exhibit CO_2 miscibility at temperatures up to 313 K and at pressures of less than 40 MPa[45]. Silicone-based polymers (see **Figure 3**), poly(dimethylsiloxanes), have also been found to dissolve in CO_2 at low pressures [46,47].

While very successful at lowering cloud point pressures of polymers, fluorinated amphiphiles carry with them economic drawbacks. Seeing this shortcoming, researchers began to search for non-fluorous functional groups that could have the effect of lowering miscibility pressures similar to the extent of the fluorous compounds. In order to design a polymer that was likely to exhibit low miscibility pressures in CO_2, several factors had to be taken into account. As noted previously and seen numerous times in the literature, most polymers must have a low T_g and CED to exhibit CO_2 miscibility down to low pressures[32,48]. In addition to having limited self-interactions, the polymer must interact

favorably with CO_2. In the case of McHugh's work with fluoropolymers, polarity provided the dipole-quadrupole interactions necessary for dissolution in CO_2[36,42-44]. For non-fluorous polymers, the focus of interaction between CO_2 and the polymer became the Lewis acid/base interactions, since carbon dioxide has been shown to act as a Lewis acid[3]. Kazarian et al used FT-IR to determine that electron rich functional groups such as the carbonyl group exhibited specific interactions (Lewis acid-base) with CO_2. This study presented the evidence for the Lewis acid-base interactions between the electron donor (Lewis base on polymer) and the electron acceptor (Lewis acid carbon in CO_2)[49]. Given this information about the carbonyl group, many researchers began to see the potential of a Lewis base in creating a non-fluorous CO_2-phile. Using this information, many polymers consisting of only carbon, hydrogen, and oxygen were dissolved in CO_2[36,50,51]. Fink and colleagues produced a work that investigated the effect that various side chains had on the miscibility pressure of poly(dimethylsiloxanes) in CO_2[52]. By placing different side chains and varying amounts of those side chains onto a constant chain-length silicon backbone, the effects of each chain and the extent of substitution could be independently observed. Using a carbonyl group, a Lewis base to promote polymer-CO_2 interactions, as an electron donor group and copolymers of ethers and CO_2, Sarbu and colleagues produced non-fluorous polymers with low miscibility pressures[50,51]. Polyethers were also successfully studied for their CO_2 solubility by Drohmann and Beckman[53]. McHugh et al investigated the effects of placing the carbonyl group in the backbone rather than as part of a side chain[54]. Though many functional groups containing a Lewis base have been effective in lowering the cloud point pressure of non-fluorous polymers, incorporating the acetate group as a side chain

of a hydrocarbon chain [poly(vinyl acetate)] (see **Figure 4**) currently yields the most versatile non-fluorous CO_2-philic polymer as it is miscible with CO_2 at relatively low pressures at high molecular weights and weight percentages[55]. Wallen et al has investigated the interactions between CO_2 and the methyl acetate group on sugars. The work speculates that not only is there a Lewis acid/base interaction between the carbonyl and the carbon in CO_2, but there is also a weaker, complementary hydrogen bonding interaction (see **Figure 5**) from the methyl protons and the oxygen in CO_2. The results give a possible explaination as to why the acetate group has proven to be the most effective Lewis base in lowering miscibility pressures of polymers[56,57]. It is upon these works that the current work is based.

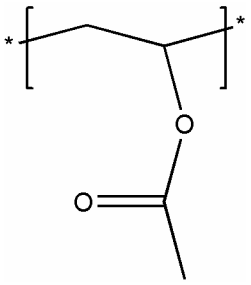

Figure 4: Poly(Vinyl Acetate)

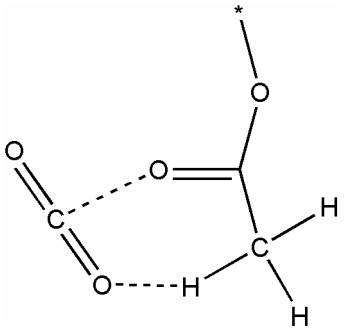

Figure 5: Proposed CO_2-Acetate Interaction[56,57]

3.0 RESEARCH OBJECTIVES

The purpose of this work was to systematically examine the effects of Lewis base groups on the miscibility pressures of polymers in CO_2 by noting the effects of small changes in side chain or backbone composition. The ultimate goal of the project is to develop a polymer made from only carbon, hydrogen and oxygen that exhibits solubility in CO_2 at pressures similar to that of the known fluorinated CO_2-philes. Lewis base groups were placed on various pre-made oligomers, and they were compared to each other as well as to various degrees of substitution of the same group. Also, several purchased polymers were tested to observe their behavior in CO_2. This research had the following goals:

1) To investigate the effects on miscibility pressures in CO_2 resulting from the placement of ketones, ethers, hydrocarbon branching, silicon branching, and alkane side chains on a poly(dimethylsiloxane) (PDMS) backbone with 25 repeat units.
2) To investigate the effect of molecular weight on miscibility pressures in CO_2 of PDMS and poly(propylene oxide) (PPO).
3) To investigate the effect of miscibility pressures in CO_2 resulting from the placement of acetate and ethyl ether Lewis base side chains on a polyether backbone.
4) To investigate the effect of miscibility pressures in CO_2 resulting from replacing the hydroxyl end groups of the substituted and unaltered poly(propylene oxide) with acetate-functional groups.

5) To determine the importance of the polymer-CO_2 interactions versus the polymer self-interactions by comparing PPO to a polymer lacking Lewis base groups but having a low T_g and CED, poly(propylene) (PP).
6) To find a correlation between the work done on the PDMS and the PPO backbones and gain fundamental knowledge concerning the use of Lewis base side chains to lower the miscibility pressures in CO_2 of non-fluorous polymers.
7) To determine whether the acetate group is the most effective Lewis base that can be employed on a non-fluorous polymer for the purpose of lowering miscibility pressures in CO_2.

4.0 EXPERIMENTAL METHODOLOGY

4.1 Materials

Argon was purchased from Praxair of Danbury, CT at 99.99% purity. The copolymers of methylhydrosiloxane [a) 3.5 mole%, b)6.5 mole %, c) 16.5 mole%, and d) 27.5 mole%] and dimethylsiloxane, polydimethylsiloxanes (MW = 1250, 2000, and 3780), and platinum-(vinyl tetramethyldisiloxane) catalyst in xylene (low color) were purchased from Gelest of Morrisville, PA. The poly(epichlorohydrin) mixture (85% poly(epichlorohydrin), 15% 1,3-Dioxolane) was obtained from 3M with the poly(epichlorohydrin) having an approximate molecular weight of 2400. Low molecular weight atactic poly(propylene) (MW 425 and 1000) was obtained from Sunoco Chemicals. Anhydrous solvents, all materials to be grafted to the polymers, and all other chemicals were purchased from Aldrich and used without purification unless otherwise noted.

4.2 Analyses

All ^{1}H-NMR spectra were obtained using a Bruker DMX 300 instrument with a deuterated chloroform solvent containing tetramethylsilane as an internal reference. FT-IR spectra were taken on a Matson Instruments Research Series FT-IR.

4.3 Synthesis of Grafted MethylHydrosiloxane-Dimethylsiloxane Copolymers

Grafted copolymers were synthesized according to the procedure used by Fink et al[52] (see **Figure 6**). The glassware was oven-dried overnight and purged with ultra-high purity argon before use. In a typical experiment 10 g (27.6 mmol) of copolymer(16.5% MethylHydrosiloxane – 83.5% Dimethylsiloxane) and 2.39 g (27.8 mmol) allyl ethyl ether were charged into a 500 ml three-neck, round-bottomed flask. The system was then equipped with a magnetic stir-bar, a condenser, and an argon feed. 60 mL of anhydrous toluene and 100 mg of platinum-vinyl tetramethyldisiloxane complex in xylene (low color) were added to the reaction mixture. The solution was stirred for 3 – 4 hours at room temperature under an argon atmosphere. Then, it was heated to 45 °C and stirred overnight. During heating the color of the solution turned a slight brownish-yellow. The completion of the reaction was verified by the disappearance of the Si-H band at 2157^{-1} using FT-IR (see **Figure A1** in **Appendix A**). 0.3 g of decolorizing carbon was added to the hot solution, and the mixture was stirred at 65 °C for 1 – 2 hours. The solution was then filtered while hot. Upon evaporation of the solvent under reduced pressure, a slightly yellow copolymer was isolated.

Table 1 shows a summary of the syntheses conducted using the siloxane backbone. Each siloxane oligomer had 25 repeat units. The table displays the number of substituted side chains, the structure of the side chain, the amount of polymer used, and the amount of side chain base material used. The volume of solvent, the duration of reaction, the temperature, and amount of catalyst remained constant through all reactions.

Table 1: Synthesis of Grafted MethylHydrosiloxane-Dimethylsiloxane Copolymers			
Reactive Sites	**Side Chain**	**mmol Si-H**	**mmol allyl compound***
1	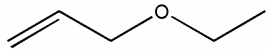	2.68	6.40
2		5.42	12.7
5		27.7	27.8
11		32.2	39.0
1	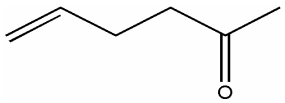	2.70	3.37
2		5.42	5.82
5		27.6	27.6
11		63.5	71.3
25		82.0	82.9
1	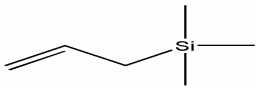	2.70	3.25
1	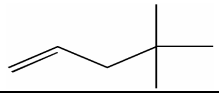	2.67	3.57
5	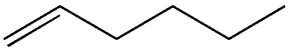	14.1	16.1
5	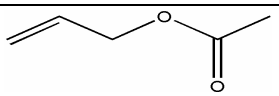	27.6	27.6
* In some cases an excess was used to ensure complete conversion			

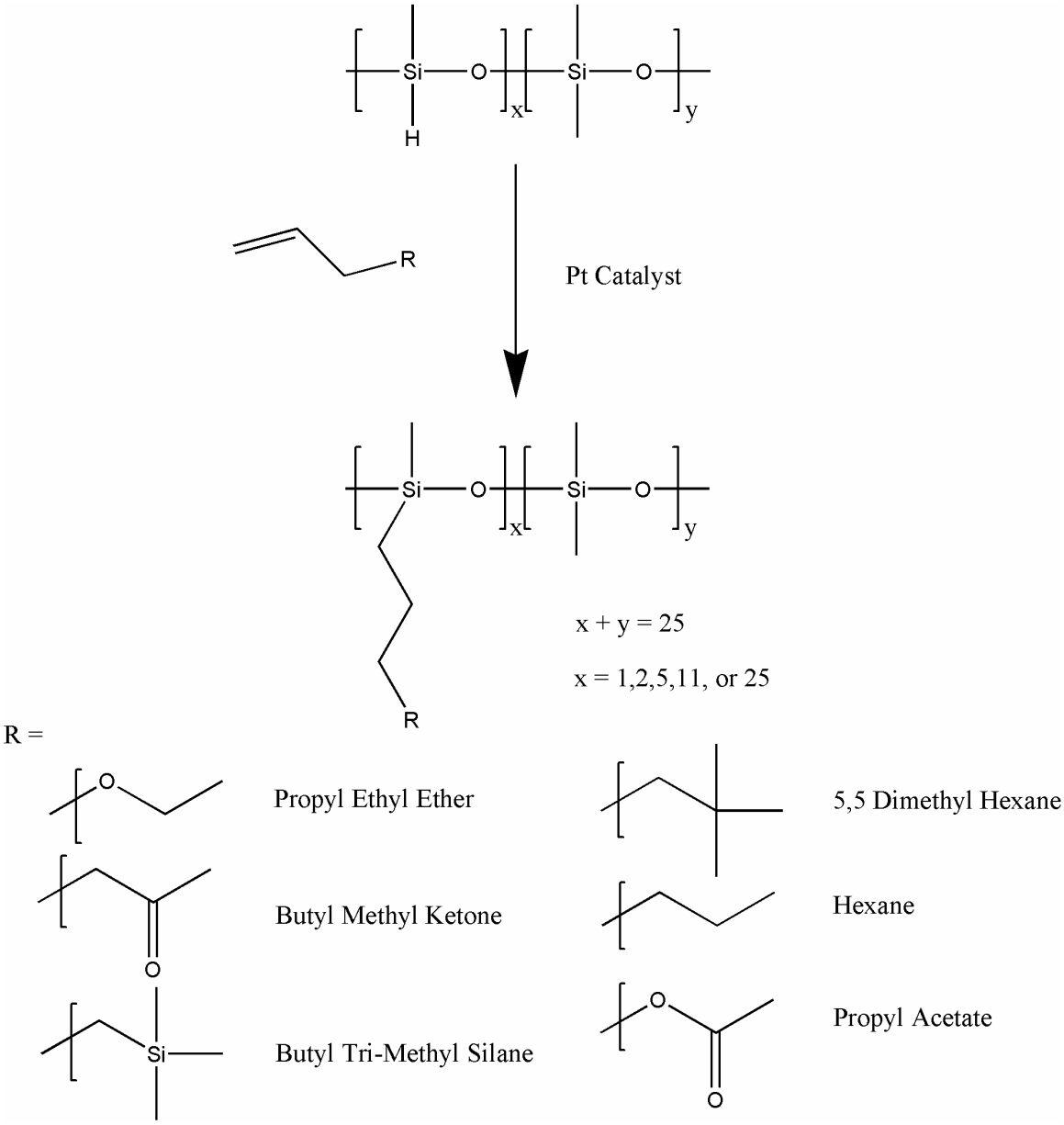

Figure 6: Silicon Backbone Reaction Mechanism

The various siloxane polymers were characterized using ^{1}H-NMR (see **Figures B1 – B7** in **Appendix B**). The complete removal of starting material was verified by the disappearance of the allyl double bond peaks that are typically between 5 and 6 ppm. Following is the ^{1}H-NMR (300 MHz, $CDCl_3$) peak data for each of the grafted side chains on the silicon-backbone polymers. **MethylHydrosiloxane:** δ 0.11 (Si-*CH*$_3$), 4.70 (s, Si-*H*). **Propyl ethyl ether:** δ 0.11 (Si-*CH*$_3$), 0.63 (Si-*CH*$_2$-CH_2), 1.31 (t, -O-CH_2-*CH*$_3$), 1.75 (-Si-CH_2-*CH*$_2$-CH_2-), 3.49 (-O-*CH*$_2$-CH_3), 3.59 (Si-CH_2-CH_2-*CH*$_2$-O-). **Butyl methyl ketone:** δ 0.11 (Si-*CH*$_3$), 0.52 (t, Si-*CH*$_2$-CH_2), 1.36 (-Si-CH_2-*CH*$_2$-CH_2-), 1.61 (Si-CH_2-CH_2-*CH*$_2$-), 2.14 (s, -CH_2-CO-*CH*$_3$), 2.42 (t, -*CH*$_2$-CO-CH_3). **Butyl tri-methyl silane:** δ 0.14 (Si-*CH*$_3$), 0.55 (Si-*CH*$_2$-CH_2-CH_2-*CH*$_2$-Si), 1.41 (Si-CH_2-*CH*$_2$-*CH*$_2$-CH_2-Si). **5,5 dimethyl hexane:** δ 0.11 (Si-*CH*$_3$), 0.56 (Si-*CH*$_2$-CH_2), 0.94 (s, C-*CH*$_3$), 1.40 (Si-CH2-*CH2*-*CH2*-*CH2*-C). **Hexane:** δ 0.11 (Si-*CH*$_3$), 0.55 (Si-*CH*$_2$-CH_2), 0.94 (-CH_2-*CH*$_3$), 1.33 (Si-CH_2-*CH*$_2$-*CH*$_2$-*CH*$_2$-*CH*$_2$-CH_3). **Propyl acetate:** δ 0.11 (Si-*CH*$_3$), 0.38 (Si-*CH*$_2$-CH_2), 1.50 (Si-CH_2-*CH*$_2$), 1.83 (s, -O-CO-*CH*$_3$), 3.82 (Si-CH_2-CH_2-*CH*$_2$-O*).*

4.4 Partial Reduction of Poly(epichlorohydrin) to form Epichlorohydrin/Propylene Oxide Copolymers

In order to achieve varying degrees of substitution with a polyether backbone, poly(epichlorhydrin) was first reduced to a poly(epichlorohydrin)/poly(propylene oxide) copolymer using lithium aluminum hydride ($LiAlH_4$). This allowed for the replacement with methyl groups of a known amount of chloride groups (see **Figure 7**). The remaining chloride groups were later allowed to react in a grafting mechanism to incorporate functional side chains onto the polymer chain (see **Figures 8 and 9**). The degree of the reduction can be directly controlled by the amount of lithium aluminum hydride ($LiAlH_4$) added to the reaction. The degrees of reduction used in this work and the corresponding amounts of reducing agent are shown in **Table 2**. The glassware was oven-dried overnight and purged with ultra-high purity argon before use. As adapted from an existing procedure[58], in a typical reaction (**Figure 7**) 6.30 g (57.9 mmol CH_2-Cl) of polymer mixture (85% poly(epichlorohydrin) (PECH) – 15% dioxolane) was charged into a 500 ml three-neck, round-bottomed flask. The system was then equipped with a magnetic stir-bar, a condenser, and an argon feed. 50 ml of anhydrous THF was added to completely dissolve the polymer mixture. After dissolution, 58 mL (58.0 mmol) $LiAlH_4$ (1.0 M in THF) was added to the flask dropwise. The solution was heated to 45 °C and stirred for 3 days. After cooling, the excess $LiAlH_4$ was eliminated with approximately 55 mL of a (1:1) mixture of THF/DI H_2O mixture. This mixture was added dropwise with a syringe since the result was rapid hydrogen gas formation. To complex the aluminum salts, 16.26 g (57.6 mmol) of potassium sodium tartrate was added. The

mixture was stirred for 30 minutes, and the salts were then removed by filtration. To ensure the complete removal of the salts, the THF/H_2O mixture was evaporated under reduced pressure, and the sample was dissolved in toluene. After a second filtration, the toluene and any residual 1,3-dioxolane from the original polymer mixture were removed under reduced pressure, and the product formed was a very pale-yellow, transparent, viscous liquid. The polymer was characterized by ^{1}H-NMR analysis, and the CH_3 peak was clearly visible in the NMR spectrum at about 1.1 ppm (see **Figure B8** in **Appendix B**). **Partially reduced PECH:** δ 1.16 (-*CH_3*), 3.65 (-*CH_2*-*CH*-O), 3.65 (-*CH_2*-Cl).

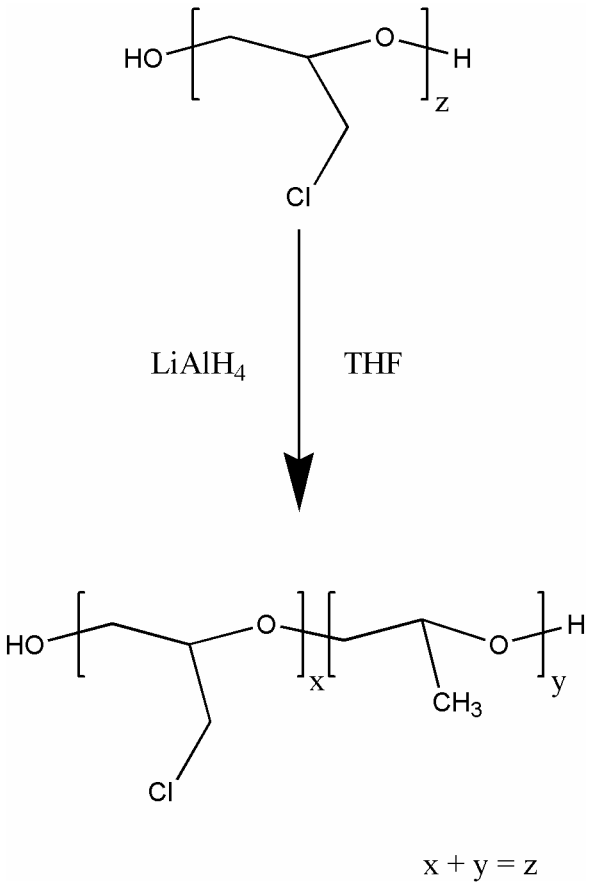

Figure 7: Reduction of Poly(epichlorohydrin)

Table 1: Reduction of Poly(epichlorohydrin)				
Reaction Composition		Integration Results		
mmol Repeat Units	mmol LiAlH4	Backbone Peak	Methyl Peak	% Reduction
321	80	1	0.21	31
317	165	1	0.42	54
421	360	1	0.57	69
222	165	1	0.59	71
381	400	1	0.81	85
187	195	1	0.99	100

Complete conversion was verified by the integration of the CH_3 peak at about 1.1 ppm and the backbone carbon peaks between 3.4 and 3.8 ppm. The ratio of these peaks (see **Table 2**) was used to determine the approximate degree of reduction. The peak ratios and corresponding degrees of reduction were calculated by the following equation:

$$\frac{BackbonePeak}{MethylPeak} = \frac{5x + 3y}{3y} \tag{4-1}$$

where x is the ratio of unreduced repeat units (containing five protons) and y is the ratio of reduced repeat units (containing three protons that contribute to the backbone peak and the three methyl protons). x and y must add up to 1. Solving these equations for y gives the approximation for the degree of reduction.

4.5 Synthesis of Acetate-functionalized Poly(propylene oxide)

Acetate functional poly(propylene oxide) was synthesized according to the procedure used by Cohen[59]. The glassware was oven-dried overnight and purged with ultra-high purity argon before use. (Note: A large excess (see **Table 3**) of potassium acetate was used in all cases to ensure a complete reaction.) In a typical experiment 4.7 g (15.3 mmol CH_2-Cl) of partially reduced PECH (30%) was charged into a 500 ml three-neck, round-bottomed flask and mixed with approximately 50 mL of DMF. The system was then equipped with a magnetic stir-bar, a condenser, and an argon feed and heated to 135 °C. After the dissolution of the polymer, 10.5 g (107 mmol) potassium acetate was added to the solution. The solution was stirred overnight under an argon atmosphere. During the reaction, the solution became cloudy from KCl salt precipitation. The reaction was then cooled, and the polymer was precipitated in DI water. The polymer was washed with DI water, and the water/DMF mixture was decanted several times. To remove the residual water, the polymer was dissolved in toluene and dried over magnesium sulfate ($MgSO_4$). The solution was filtered through Whatman #1 filter paper, and the toluene was removed under reduced pressure, yielding a yellow, transparent, viscous liquid. **Table 3** shows a summary of the syntheses conducted to graft the acetate onto the poly(propylene oxide). The table displays the percentage of acetate substitution, the base polymer used, the amount of polymer used, and the amount of acetate salt used. The duration of reaction and the temperature remained constant through all reactions. **Figure 8** illustrates the reaction scheme.

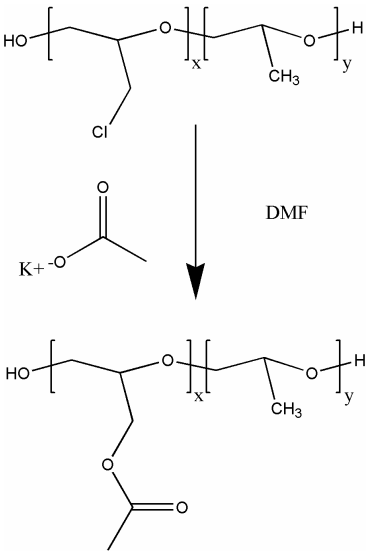

Figure 8: Synthesis of Acetate-Functional PPO

Table 3: Synthesis of Acetate-functional Poly(propylene oxide)			
Starting Polymer (Theoretical)	**Reaction Composition**		**% Acetate (Actual)**
	mmol CH_2-Cl	**mmol KAc**	
85% Reduced PECH	12.8	52.0	12
71% Reduced PECH	16.5	50.9	22
54% Reduced PECH	30.4	103	44
31% Reduced PECH	40.0	107	69
0% Reduced PECH	64.4	124	100

To verify the acetate-substituted product, the ^{1}H-NMR spectra were analyzed for the appearance of the Ac-CH_3 peak at 2.1 ppm. The CH_2 protons in the acetate chain were seen in a doublet at 4.1 - 4.2 ppm which should integrate at two-thirds of the peak at 2.1 ppm. To determine the degree of acetylation and to verify the original approximation for degree of reduction, the Ac-CH_3 peak at 2.1 ppm was compared to the methyl peak in the PPO repeat unit at 1.1 ppm (see **Figure B9** in **Appendix B**). The sum of the integrations should be one, with the integration of the peak at 2.1 indicating the percentage of repeat units with acetate substitution. Due to the isolation of the peaks and clear integration results, this method is more accurate than the method used to determine the degree of reduction and was the method used for the final results. **Acetate Grafted PPO:** δ 1.13 (-CH_2-CH(-*CH_3*)-O-), 2.07 (s, -O-CO-*CH_3*), 3.64 (-*CH_2*-*CH*-O-), 4.17 (d, -*CH_2*-O-CO-CH_3).

4.6 Synthesis of Methyl Ether-Functionalized Poly(propylene oxide)

The glassware was oven-dried overnight and purged with ultra-high purity argon before use. (Note: A large excess of sodium methoxide was used (see **Table 4**) in all cases to ensure a complete reaction.) In a typical experiment 7.10 g (13.3 mmol CH_2-Cl) of partially reduced PECH (88% reduced) was charged into a 500 ml three-neck, round-bottomed flask and mixed with approximately 50 mL of chloroform. The system was then equipped with a magnetic stir-bar, a condenser, and an argon feed. After the dissolution of the polymer, approximately 65 mL (32.5 mmol) of sodium methoxide (NaOMe) solution (0.5 M in methanol) was added to the solution. The solution was stirred overnight under an argon atmosphere at 35 °C. During the reaction, the solution became cloudy with NaCl salt precipitation. The reaction was then cooled, and the chloroform/methanol solvent mixture was removed under reduced pressure. The polymer was dissolved in toluene, and the salt was filtered through Whatman #1 filter paper out of the mixture. The toluene was removed under reduced pressure, yielding a yellow, transparent, viscous liquid.

Table 4 shows a summary of the syntheses conducted to graft the methyl ether onto the poly(propylene oxide). The table displays the percentage of ether substitution, the base polymer used, the amount of polymer used, the amount of ether salt used, and the volume of chloroform added. The duration of reaction and the temperature remained constant through all reactions. **Figure 9** illustrates the reaction scheme.

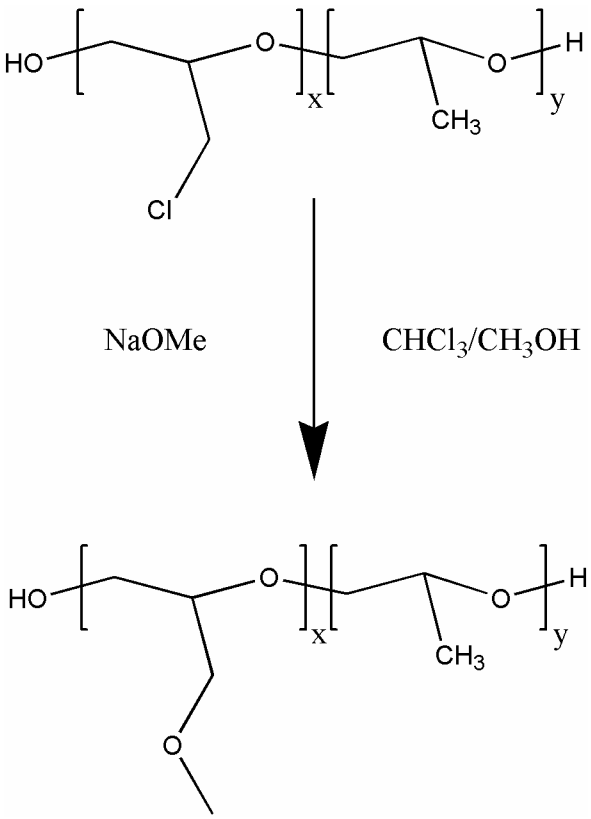

Figure 9: Synthesis of Methyl Ether-Functional PPO

Table 4: Synthesis of Methyl Ether-Functional Poly(propylene oxide)				
Starting Polymer	**Reaction Composition**			**% Ether**
(Theoretical)	**mmol CH_2-Cl**	**mmol NaOMe**	**mL Chloroform**	**(Actual)**
85% Reduced PECH	13.3	32.5	50	12
71% Reduced PECH	22.7	45.0	100	22
50% Reduced PECH	18.1	25.0	75	44
0% Reduced PECH	78.1	80.0	100	100

To characterize the ether-substituted product, the ^{1}H-NMR spectra were analyzed in a similar manner to the analysis of the partially reduced PECH. The CH_2 and CH_3 protons in the methyl ether chain show up in the same location as the backbone protons of the PECH. To verify the addition of the ether chains, the ratio of the methyl group peak from the reduced repeat units at 1.1 ppm and the broad PECH/ether peaks from 3.4 to 3.8 ppm was taken (see **Figure B10** in **Appendix B**). The new ratio was compared to the original degree of reduction ratio and showed that the appropriate amount of protons was attached to the polymer backbone. The peak ratios and corresponding degrees of reduction calculated by the following equation:

$$\frac{(Backbone + Ether)Peak}{MethylPeak} = \frac{8x + 3y}{3y} \tag{4-2}$$

where x is the ratio of ether-substituted repeat units (containing eight protons) and y is the ratio of reduced repeat units (containing three protons that contribute to the backbone peak and the three methyl protons). The sum of x and y must be one. Solving these equations for x verified the degree of substitution. There was one case in which this method could not be applied. For the 100% ether substituted PECH, there was no methyl peak at 1.1 ppm since none of the repeat units had been reduced. In this case the weight of the sodium chloride salt byproduct was taken, and its molar equivalence to the polymer reactant was used to verify the completed reaction. **Methyl Ether Grafted PPO:** δ 1.14 (-CH_2-CH(-*CH_3*)-O-), 3.71 (-*CH_2*-*CH*(-*CH_2*-O-*CH_3*)-O-).

4.7 Capping of the Hydroxyl End Groups of Select PECH/PPO Polymers

The glassware was oven-dried overnight and purged with ultra-high purity argon before use. (Note: A large excess of acetyl chloride was used in all cases to ensure a complete reaction.) In a typical experiment 10.51 g (10.5 mmol -OH) of PPO (MW 2000) was charged into a 500 ml three-neck, round-bottomed flask and mixed with approximately 100 mL of toluene. The system was then equipped with a magnetic stir-bar, a condenser, and an argon feed. After the dissolution of the polymer, approximately 3 mL (42.2 mmol) of acetyl chloride (AcCl) and approximately 3 mL (21.5 mmol) of triethylamine were added to the solution. The solution was stirred overnight under an argon atmosphere at room temperature. During the reaction, the solution became cloudy with salt precipitation. The reaction was then filtered twice through Whatman #1 filter paper to remove the salt; the toluene, excess acetyl chloride, and excess triethylamine (TEA) were removed under reduced pressure. The capped polymers showed no physical differences from their uncapped counterparts, appearing as yellow, viscous oils.

Table 5 lists the polymers that were capped at 100% conversion. The duration of reaction and the temperature remained constant through all reactions. **Figure 10** illustrates the reaction scheme.

Table 5: Polymers Capped with Acetate
100% Acetate Substituted PECH
PPO (MW 2000)
12% Acetate Substituted PECH
12% Methyl Ether Substituted PECH
PECH

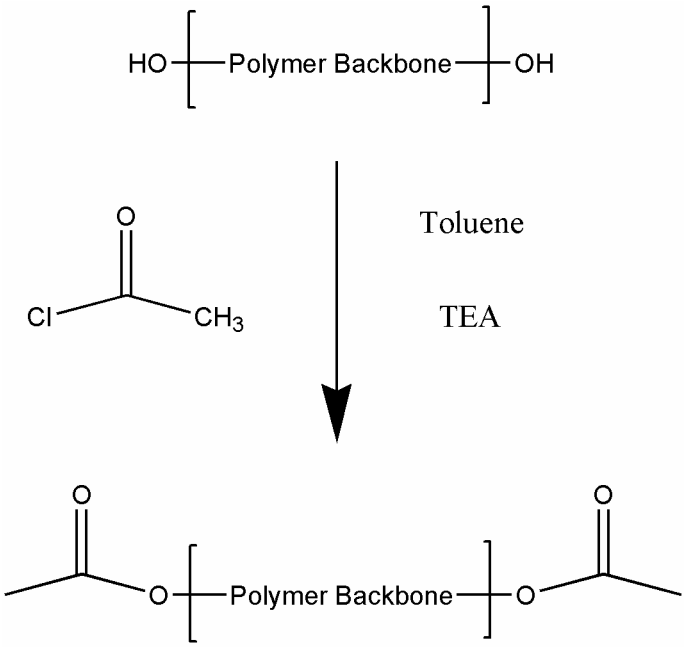

Figure 10: Capping of PECH/PPO Polymers with the Acetate Group

To verify the completion of the reaction, a FT-IR spectrum was taken. The -OH peaks at 1080^{-1}, 1060^{-1}, and a broad peak at approximately 3500^{-1} disappeared as the hydroxyl groups were replaced by the acetate. There was still a residual peak near 3500^{-1} as there was water present. On the polymers without acetate substitution in the backbone, the methyl protons on the acetate end groups were easily visible in the ^{1}H-NMR spectrum at 2.1 ppm (see **Figure B11** in **Appendix B**).

4.8 Purification of Low Molecular Weight Poly(propylene)

The solvents were removed from a solution of poly(propylene) (MW 425) oligomer in hexane and water. A ^{1}H-NMR spectrum of the sample verified the removal of the solvents. The PP (MW 1000) was received as an amorphous, white solid mixed with crystalline beads of high molecular weight PP. An included GPC spectrum provided by Sunoco Chemicals indicated that a majority of the sample had a molecular weight of 1000. The mixture was placed in hexane which dissolved the PP 1000, while the high molecular weight material remained as an insoluble solid. The high molecular weight material was filtered through Whatman #1 filter paper out of the solution, and the hexane was removed under reduced pressure. The product was pure poly(propylene) at the desired molecular weight of approximately 1000.

4.9 Synthesis of Low Molecular Weight Poly(acetaldehyde)

Acetaldehyde was polymerized according to a procedure used by Vogl[60]. The glassware was oven-dried overnight and purged with ultra-high purity argon before use. 20 mL (356.8 mmol) of acetaldehyde was charged into a 200 ml volumetric flask and mixed with approximately 10 mL of ethyl ether. The system was then equipped with a magnetic stir-bar and purged with argon. The flask was lowered into a mixture of dry ice and acetone and brought to a temperature of approximately -78°C. After the cooling of the mixture, approximately 0.15 mL (0.95% wt. %) of concentrated hydrochloric acid (HCl) solution (aqueous) was added to the flask. The solution was stirred and the cold bath maintained for four hours. To cap and stabilize the polymer, 80 mL (843.8 mmol) of acetic anhydride and 10 mL (123.6 mmol) of pyridine were added to the reaction, and the system was allowed to slowly warm to room temperature overnight. The polymer was precipitated in ice water and extracted in a separatory funnel with chloroform. The chloroform/polymer solution was dried over magnesium sulfate ($MgSO_4$) and filtered through Whatman #1 filter paper. The chloroform was removed under reduced pressure, yielding a yellow, transparent, viscous liquid. Poly(acetaldehyde) is not stable and can begin to depolymerize in a solvent or when heated. Therefore the ^{1}H-NMR spectrum will show trace amounts of monomer due to dissolution in chloroform. The product was verified by ^{1}H-NMR (see **Figure B13** in **Appendix B**). **Poly(acetaldehyde):** δ 1.35 (-CH(-*CH*$_3$)-O-), 5.04 (-*CH*(-CH_3)-O-). **Trace Acetaldehyle:** δ 2.22 (CHO-*CH*$_3$-), 9.80 (*CH*O-CH_3-). **Acetate End Groups:** δ 2.10 (-O-CO-*CH*$_3$).

4.10 Phase Behavior Determination

All phase behavior measurements were made in a D. B. Robinson high pressure view cell (see **Figure 11**). In a typical experiment the clear view cell was charged with 0.5 to 1.0 g of polymer sample, mixing balls were added, and the lid of the vessel was sealed. All experiments in this work were conducted at room temperature (~295 K). Oil was introduced into the vessel to lift the piston and remove all atmospheric air, and the cell was filled with a predetermined amount of CO_2 to obtain the desired weight percentage of polymer. The CO_2 input was monitored at the pump by observing the volume that entered the cell at a constant pressure. The density of the CO_2 at the given conditions was calculated using an equation of state obtained from the International Thermodynamic Tables of the Fluid State[61] and integrated by Newton's method. After closing the CO_2 feed, the pressure in the vessel was raised by adding oil with a high pressure syringe pump until the polymer dissolves in the carbon dioxide [up to a maximum of 7000 psi (48.26 MPa)]. After dissolution, the oil was removed from the cell to slowly drop the pressure until a cloud point could be visually obtained. Cloud point measurements were taken as the pressure of the clear one-phase solution dropped and a cloud of polymer came out of solution, yielding an opaque two-phase mixture. The data point used was the pressure at which the mixture had 10% of its original transparency. After the cloud point was verified by several readings, the pressure was lowered, and more CO_2 was added until the next desired weight fraction of polymer was reached. The pressure in the cell was raised again, and the process was repeated until a sufficient amount of cloud point

data was obtained. The resulting data was graphed to form a cloud point curve showing the pressure at various weight percentages with an error of +/- 1 MPa.

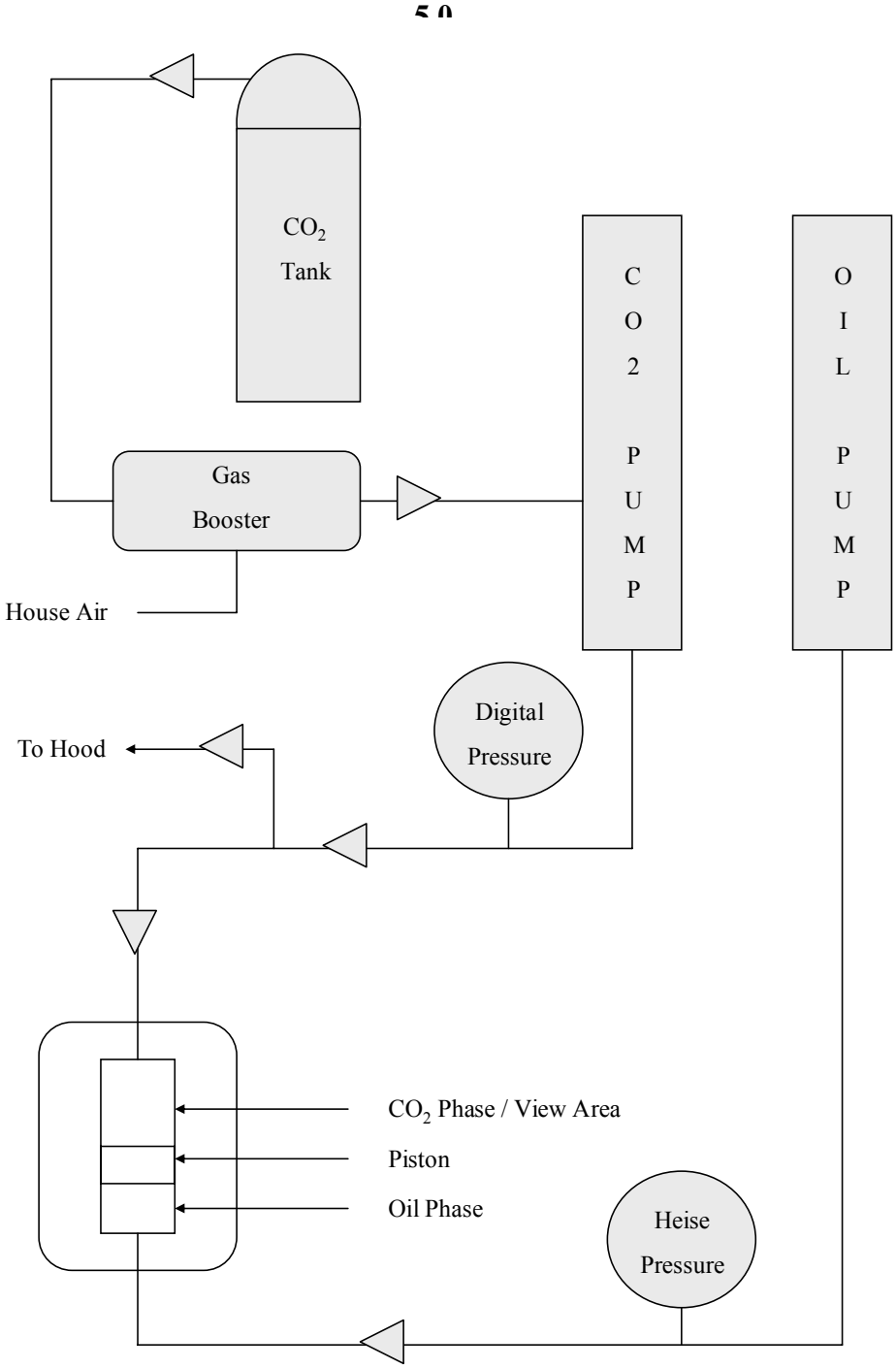

Figure 11: High Pressure Equipment for Phase Behavior Determination

5.0 RESULTS AND DISCUSSION

5.1 The Effect of Grafted Side Chains on a PDMS Backbone

Model silicon oligomers made from dimethylsiloxane and hydromethylsiloxane were purchased at a total chain length of 25 repeat units. 5 unique oligomers were used with varying hydromethyl composition so that through hydrosilation samples with one, two, five, eleven, or twenty-five side chains were produced. Monitoring the reaction with FT-IR (see **Figure A1** in **Appendix A**) ensured complete conversion of the hydromethyl groups. All grafted side chains included a propyl spacer between the functional group and the PDMS backbone and totaled six atoms in length, with the exception of the branched samples which had a length of five atoms

.

5.1.1 Phase Behavior of PDMS with Grafted Ketone

Ketone groups were grafted onto all five oligomers, giving a full range of degrees of substitution. The one and two substituted ketone-siloxanes gave the best CO_2 solubility while increasing the degree of substitution to five and eleven increased the miscibility pressure of the polymer (see **Figure 12**). Substituting all 25 repeat units with a ketone group resulted in a polymer that was completely insoluble within the limits of the available equipment (48.26 MPa). This set of results was the first to show that there is an optimal amount of substitution for a given side chain. In the case of the ketone, the optimum was one or two substitutions or 4% - 8%. Addition of more ketone groups

raised the cloud point pressure of the polymer. There are several reasons for this. First the addition of a six carbon chain with an oxygen atom added to the overall molecular weight of the oligomer, decreasing the entropy of mixing. According to the group contribution model developed by van Krevelen[62], the addition of a side chain tended to stiffen the polymer structure allowing less freedom of movement and increasing the cohesive energy density (CED). The cohesive energy density of the base PDMS is very low (Surface Tension: 19.9 mN/m @ 20 °C)[32], approaching the low cohesive energy density of the most CO_2-philic fluoroacrylates (Surface Tension of poly(1,1-dihydrodecafluorooctyl acrylate): 10 mN/m @ 20 °C)[32], and the addition of the Lewis base containing or branching groups lifted the overall cohesive energy density of the polymer. The ketone groups did have a Lewis base in the carbonyl oxygen, but the interactions between the base and CO_2, while important, were not enough to overcome the other negative effects. A certain amount of the CED increase could be balanced by the Lewis base interaction with CO_2, but after a certain point (5-substituted ketone) the effect from the higher cohesive energy density began to be dominant, finally leading to insolubility when all 25 repeat units were substituted.

5.1.2 Phase Behavior of PDMS with Grafted Ethyl Ether

Ethyl ether functional groups were grafted onto four of the five available oligomers, excluding the full 25 repeat unit substitution. As with the ketone substitution, the ether-substituted oligomer had an optimal degree of substitution (see **Figure 13**). The two-ether substitution (8%) was the optimal amount of ether content, and when the number of substituted units was increased to five and eleven, the cloud point pressure of the ethyl ether PDMS polymer became dramatically worse, narrowly remaining within the boundaries of the equipment (48.26 MPa). While the one substituted ethyl ether siloxane did not differ as drastically, it was clearly inferior to the 8% ethyl ether substitution. As with the grafted ketones, the cohesive energy density effects appeared to be the dominant characteristic over the Lewis acid/base interactions between the ether oxygen and the CO_2.

Figure 12: Phase Behavior of Ketone Substituted PDMS

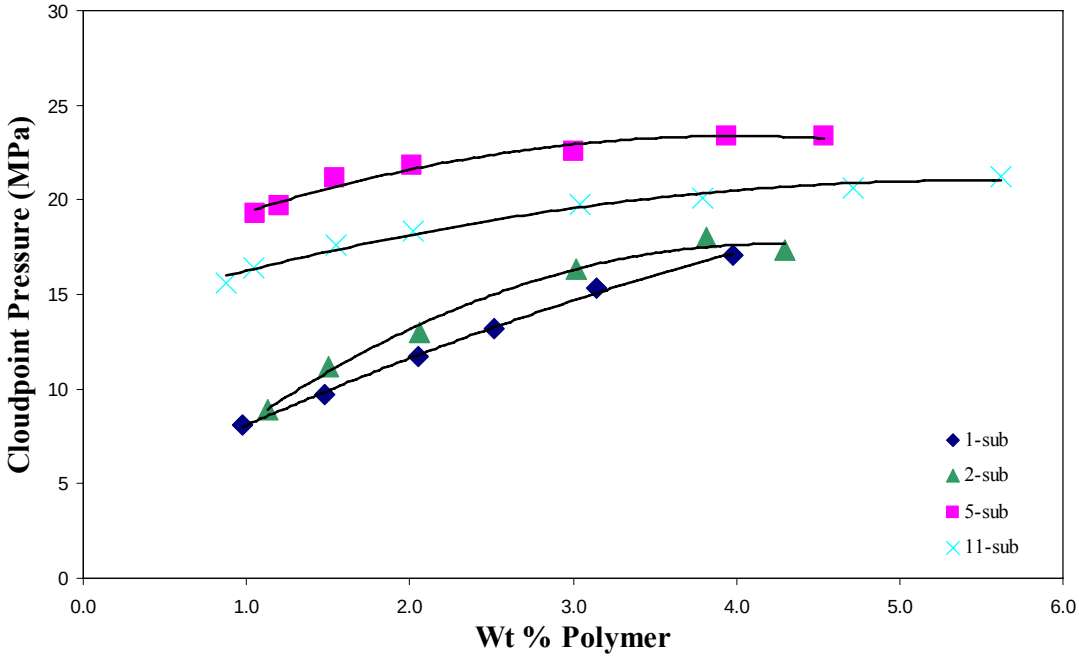

Figure 13: Phase Behavior of Ethyl Ether Substituted PDMS

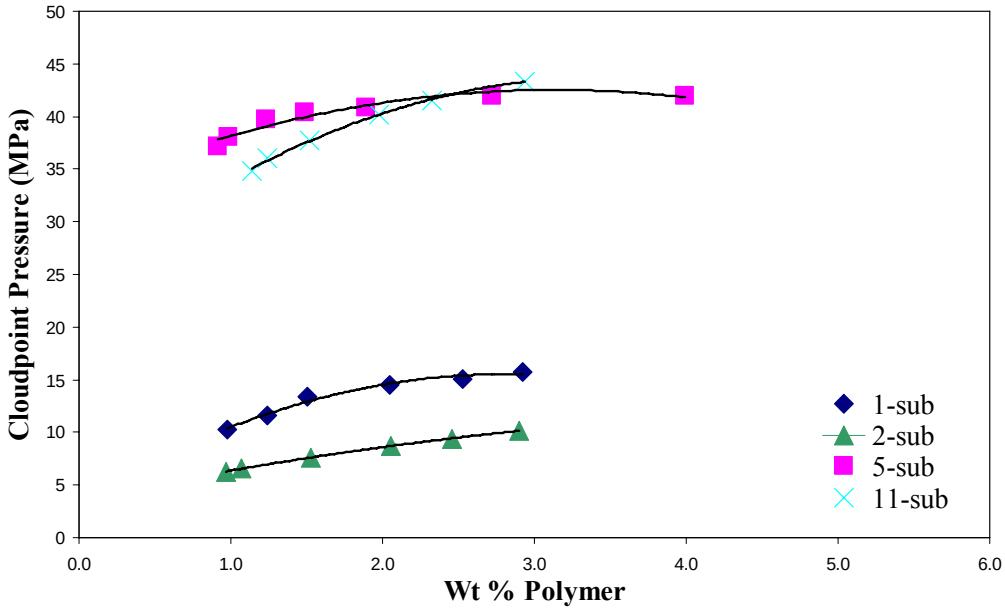

5.1.3 Phase Behavior of PDMS with Grafted Hydrocarbon Branching

Two forms of a tri-methyl branched group, one with carbon at the center and one with silicon at the center, were grafted onto a silicon oligomer with one hydromethyl reactive site. The results on cloud point pressure of placing these groups were compared to the miscibility pressures of the unaltered oligomer containing one Si-H group. At all observed concentrations, there was very little difference between the polymers with branching groups and the unmodified polymer (see **Figure 14**). Despite elevating the cohesive energy density[62], the addition of the branched groups also contributed to the overall free volume by incorporating more end groups. This drop in T_g was able to compensate for the decrease in flexibility. Also, there was only one group added per oligomer so the effect of the increased CED was not overwhelming. There was no difference between the branching groups themselves; whether silicon or carbon was the central atom for the branching area, the miscibility pressure of the polymer was not affected. The Si-H group did not interact favorably with CO_2, and this became more obvious as the Si-H concentration within the polymer was increased. As more hydromethyl groups were left unaltered, the miscibility pressure of the oligomer became steadily higher. In other work done on this project by co-worker, Sevgi Kilic, it was clear that having two Si-H groups in the oligomer greatly increased the cloud point pressure of the oligomer[47].

Figure 14: Phase Behavior of Branching Group Substituted PDMS

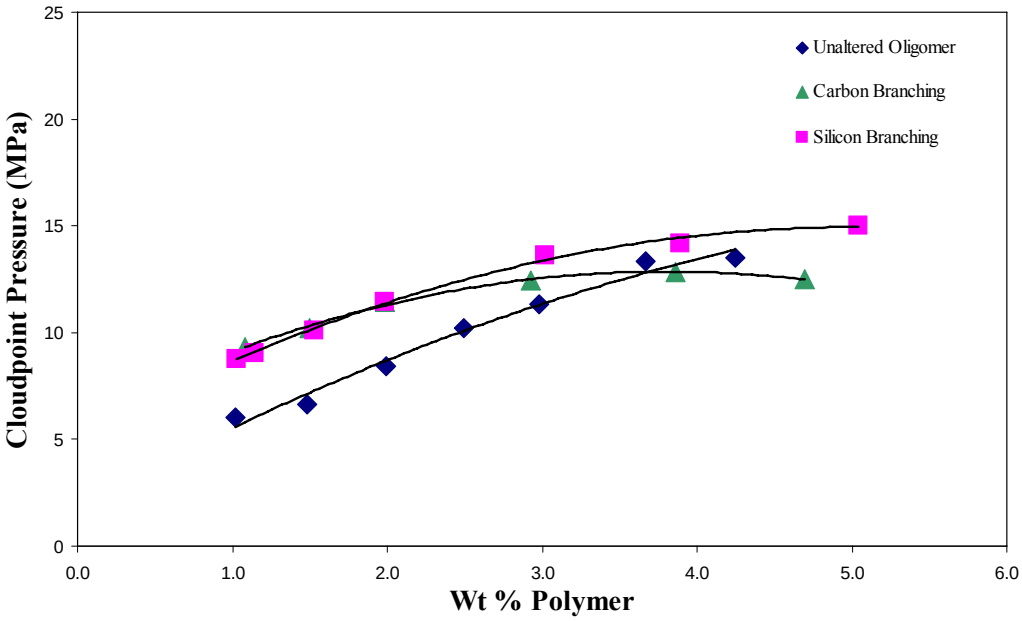

5.1.4 Phase Behavior of PDMS with Grafted Acetate and Hexane

In a previous work[52] on this subject, the effects of grafting a hydrocarbon chain, hexane, and an acetate group onto PDMS were observed. In this work, that data was verified for the five-substituted PDMS sample. The hexane chain was a very poor addition as it added cohesive energy density to the polymer[62] without the benefit of extra branching groups or a Lewis base site. The acetate group[47] performed well as the Lewis base interactions with CO_2 allowed for increased solubility (see **Figure 15**). In this work, only the five-substituted acetate was observed. In efforts made by group member, Sevgi Kilic, five-substituted (20%) acetate was found to be the amount of substitution that allowed for optimal solubility[47]. At this degree, the adverse effect of the hydrocarbon

on the cohesive energy density achieved the most favorable balance with the positive effects of the acetate Lewis base interactions with the solvent, carbon dioxide. With fewer acetate groups, there was less Lewis acid/base interaction resulting in higher cloud point pressures, and with more acetate substitution, the interaction with CO_2 was not strong enough to counterbalance the negative effects from the increased cohesive energy density[62]. This comparison clearly showed the vast decrease in cloud point pressure resulting from the incorporation of a Lewis base group in the side chain.

5.1.5 The Effect of Molecular Weight on the Phase Behavior of PDMS

As previously stated, increasing the molecular weight of a polymer results in a drop in the change in entropy of mixing and therefore increased cloud point pressures in CO_2. This was confirmed with a molecular weight analysis of various PDMS samples. Oligomers of increasing molecular weights (1250, 2000, and 3780) were evaluated for cloud point pressure (see **Figure 16**), and they behaved as predicted. Though the increase in cloud point pressure was not staggering, there was a slight and steady increase as more repeat units were added to the oligomer. This study proved that while molecular weight made a difference in the CO_2 solubility of the polymer, it did not have the radical effect that were seen when a Lewis base was added or when the cohesive energy density was altered.

Figure 15: Phase Behavior of 5-Substituted Hexane and Acetate Substituted PDMS

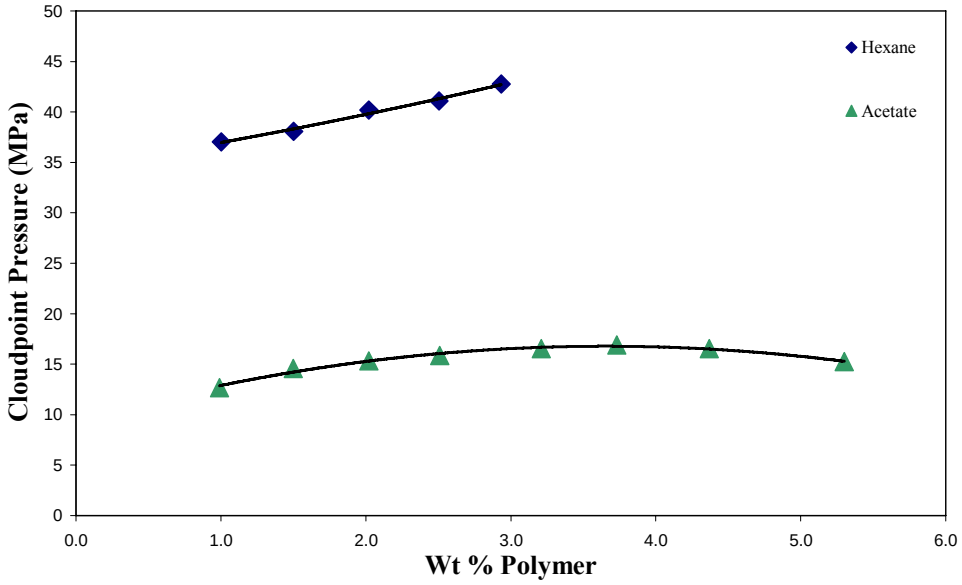

Figure 16: Molecular Weight Effects on PDMS Solubility in Carbon Dioxide

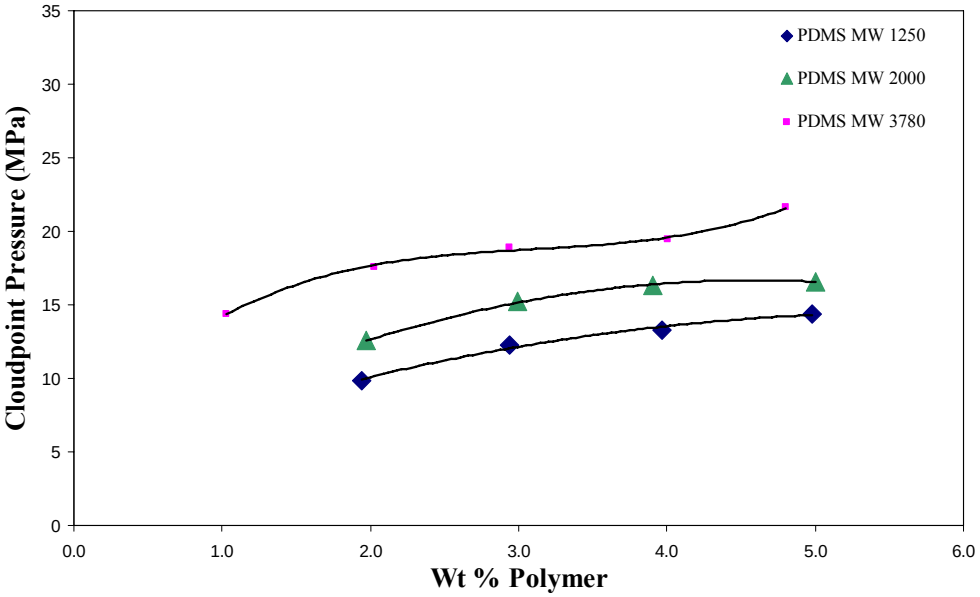

5.1.6 Comparison of Grafted Lewis Base Chains on PDMS

As stated previously, the carbonyl group interacts favorably with CO_2[55]. To evaluate whether the CO_2 interactions are caused by the acetate group as a whole or simply the carbonyl itself, the acetate grafted PDMS was compared to the ketone grafted PDMS (see **Figure 17**) with five repeat units substituted. While both groups contain a carbonyl group, the acetate group also has an oxygen in the grafted chain. It was hypothesized that the reason that acetate group interacted more with the CO_2 was because the oxygen atom allowed the carbonyl group to rotate more freely in the acetate than the CH_2 group allows the carbonyl in a ketone to rotate[47]. This allowed the carbonyl group to rotate to the most optimal position for interaction with CO_2. The barriers to rotation for the C-O and C-C bonds were found to be 1.1 and 3.0 kcal/mole respectively[63].

Figure 17: Acetate vs. Ketone (5-sub) Grafted PDMS

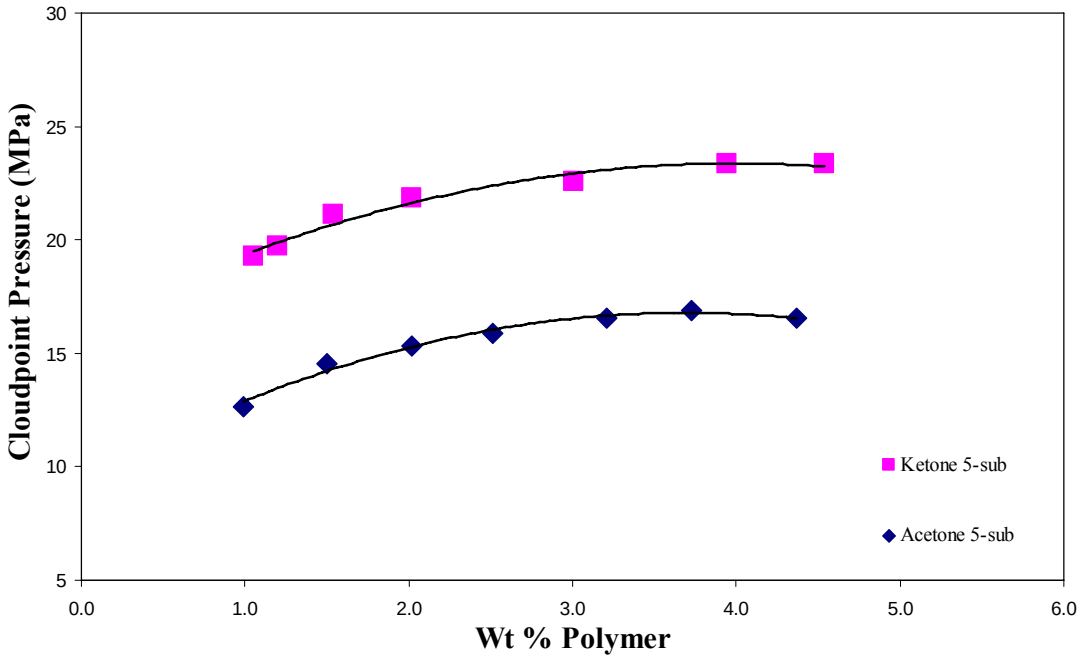

With two repeat units on the PDMS substituted, the ether group allows for lower miscibility pressures than ketone or acetate (see **Figure 18**). This is near the optimal amount of substitution for ketone and ether, while acetate requires more of a presence on the polymer chain to lower cloud point pressures to a minimum. When comparing the optimal degree of substitution of all tested functional groups (see **Figure 19**), the 2-substituted ether allows for the lowest miscibility pressures. This corresponds to calculations done by fellow group member, Yang Wang. His work for Dr. Karl Johnson indicates that the binding energy between CO_2 and a carbonyl oxygen is almost equal to the binding energy between CO_2 and the ether oxygen[47]. This new assertion was later tested on a polyether backbone (see **Section 5.6**).

Figure 18: Comparison of Acetate, Ketone, and Ether Groups Substituted on Two Repeat Units of PDMS

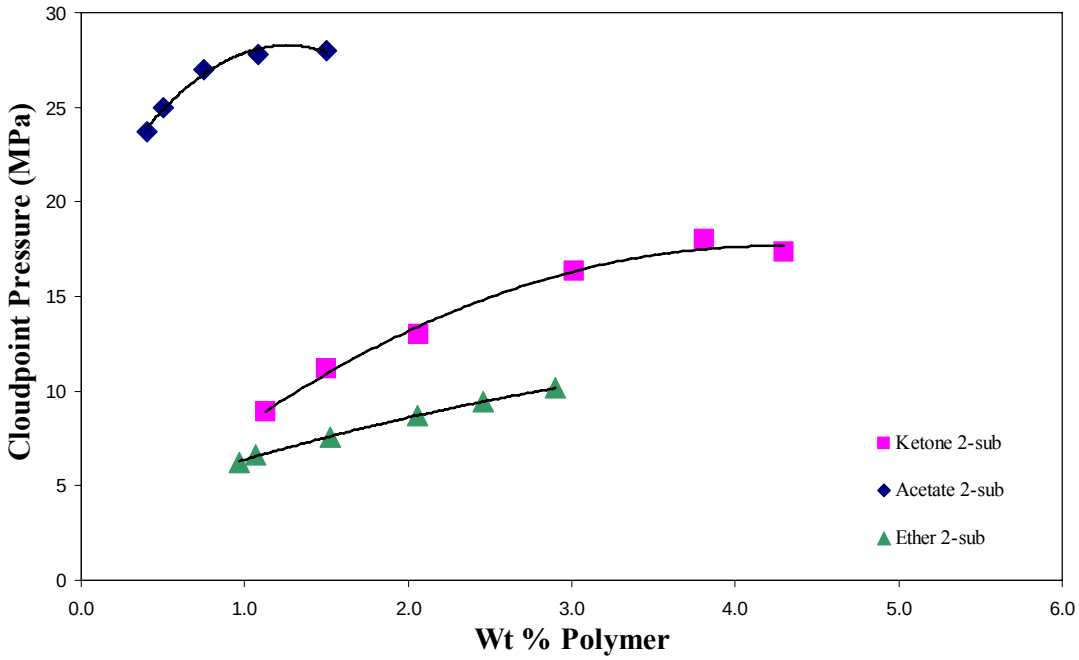

Figure 19: Comparison of the Optimal Substitution of Grafted Side Chains on PDMS

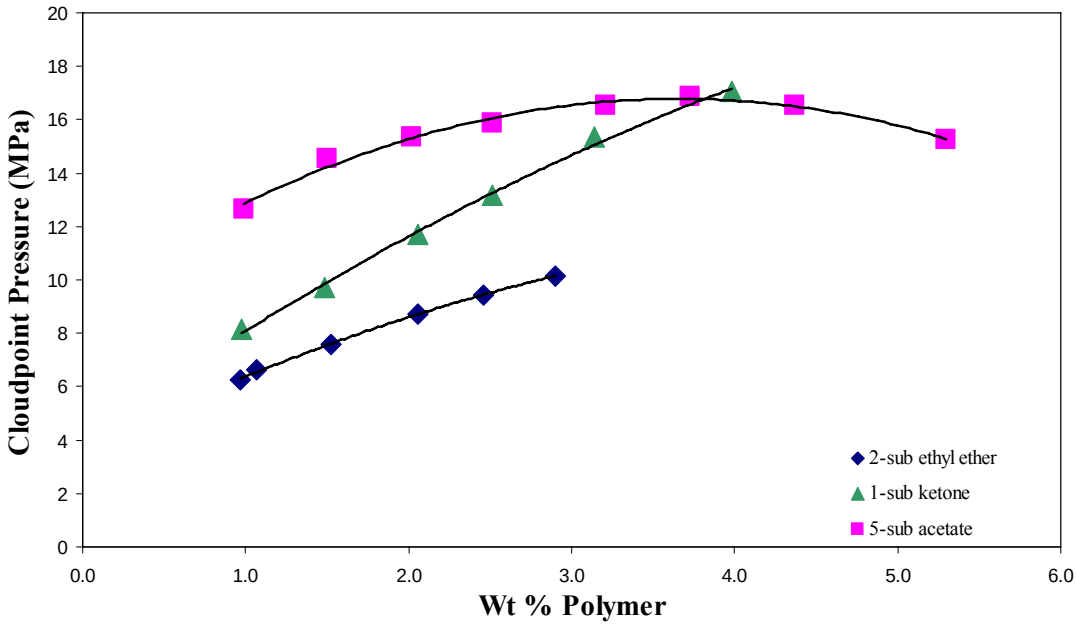

5.2 The Effect of Grafted Side Chains on a Polyether Backbone

The overall goal of this work is to develop a polymer that will be miscible with CO_2 down to low pressures and contain only carbon, hydrogen, and oxygen. Given the lessons from the study of grafted materials on a siloxane backbone, a similar study on a polyether backbone was undertaken. The model compound in the non-fluorous study was a polyether. The starting material was poly(epichlorohydrin) (PECH) which when reduced completely became poly(propylene oxide) (PPO) with hydroxyl end groups. The PECH was obtained at an approximate molecular weight of 2400, and this weight was verified by ^{1}H-NMR peak analysis (see **Figure B12** in **Appendix B**). In this procedure, the hydroxyl end groups of the PECH were capped with acetate groups. The CH_3 protons from the ends of these groups were visible in the ^{1}H-NMR at about 2.1 ppm, while the backbone protons gave a broad peak from 3.4 to 3.8 ppm. The integral ratio of these peaks was used to determine the number of the repeat units and then the approximate molecular weight. The following equation was used to verify the molecular weight of the PECH:

$$\frac{BackbonePeak}{AcetatePeak} = \frac{5x}{6} \tag{5-1}$$

where x is the total number of repeat units (containing five protons), and the six represents the two three-proton end groups on each polymer. Using this equation it was determined that the polymers had about 28 repeat units at a molecular weight of 92.5 each, giving an overall molecular weight of about 2600. The PECH was reduced to various degrees, and the effect of grafting acetate and methyl ether side chains to the polyether backbones was observed.

5.2.1 Phase Behavior of PPO with Grafted Acetate

Since acetate has proven to be an effective Lewis base side chain, it was chosen to be grafted onto a polyether backbone and evaluated to determine if it would have the same CO_2 solubility effects as observed on the siloxane backbone. The acetate groups were grafted onto the repeat units in the following degrees: 12%, 22%, 44%, 68%, and 100%. The oligomer with 22% of the repeat units containing grafted acetate was the most CO_2-philic of the five samples (see **Figure 20**), though even the best acetate-substituted polymer had higher cloud point pressures than those of the base PPO polymers having no acetate substitution. This percentage of substitution is comparable to the optimal degree of acetate composition on the PDMS backbone, giving credibility to the results of the siloxane backbone study. As seen in the results of the acetate substituted PDMS, having too few acetate side chains resulted in a cohesive energy density increase[62] without the benefit of multiple Lewis base sites. On the other hand, if there were too many acetate groups, the polymer was stiffened, and the Lewis acid/base interactions were not strong enough to overcome the increase in CED. Grafting acetate groups onto approximately 20% of the repeat units, allows for the optimal balance between polymer-polymer and polymer-CO_2 interactions, yielding the lowest cloud point pressures.

5.2.2 Phase Behavior of PPO with Grafted Methyl Ether

Given the work of Yang Wang stating that an ether group may interact with CO_2 as well as an acetate group, a methyl ether group was chosen as a second Lewis base to graft

onto a polyether backbone. Given the simplicity of the structure and the incorporation of an ether-oxygen as the electron-rich donor, the structure was assumed to interact favorably with CO_2. The ether groups were grafted onto the repeat units in the following degrees: 12%, 22%, 44%, and 100%. None of the four samples were miscible with CO_2 to the limits of the equipment (48.26 MPa). Given their close proximity, it was hypothesized that the backbone oxygen would not allow the ether oxygen to interact with CO_2 and vice versa, as the oxygen atoms on the polymer repelled the oxygen atoms on the carbon dioxide when the carbon in CO_2 attempted to interact with either oxygen (see **Figure 21**). Since the CO_2 needed to interact with the oxygen atoms in order to draw the molecule into solution, the solubility of the polymer may have been greatly reduced because the oxygen atoms on all of the grafted repeat units were inaccessible. The 12% substituted PPO partially dissolved at the limits of the equipment, but as the degree of substitution rose, the polymers showed no tendency to dissolve at all. It should be noted that the structure of the methyl-ether-substituted PPO closely resembles a branched poly(ethylene oxide) (PEO), which is known to exhibit poor solubility in CO_2[53]. Also worth noting was the insolubility of low molecular weight poly(acetaldehyde). This sample also had oxygen atoms in close proximity and was not miscible with CO_2 to the pressure limits of the equipment and down to 0.7 weight percent.

Figure 20: Phase Behavior of Acetate Substituted PPO

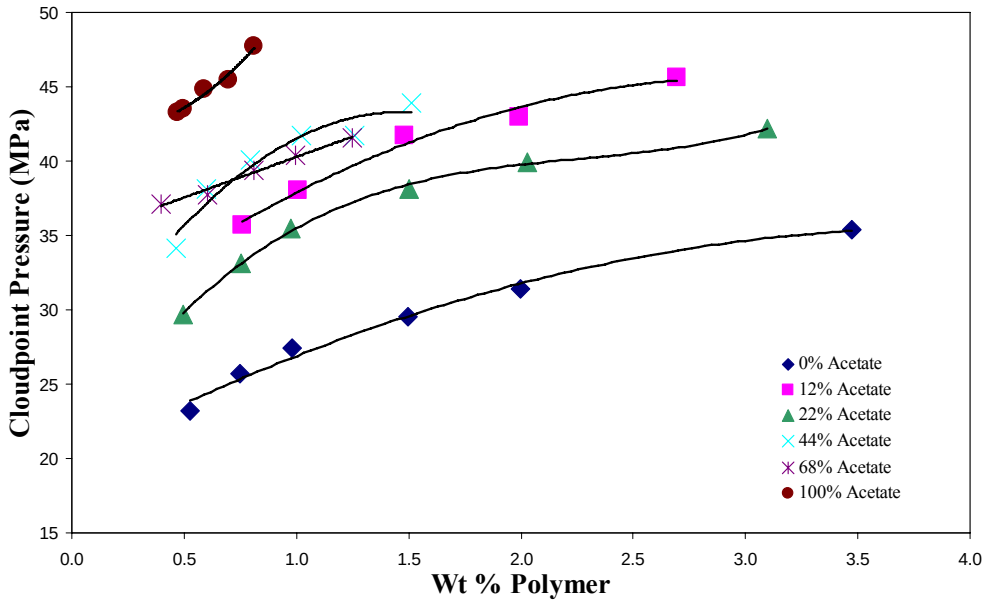

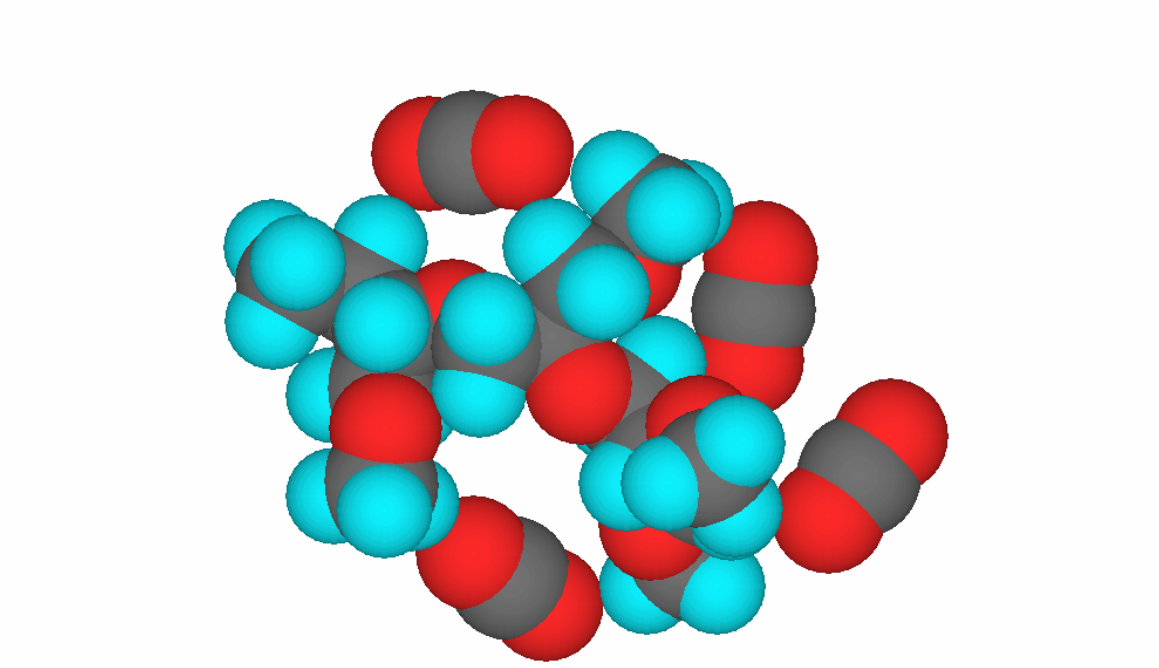

Figure 21: Hypothesized Steric Hindrance in 3 Repeat Units of Ether-Substituted PPO

5.3 The Effect of End Group Capping on PPO Polymers

The hydroxyl end groups had a detrimental effect on the solubility of the PPO polymers in CO_2 because they can hydrogen bond to each other, increasing their polymer-polymer interactions. This behavior was observed in similar work examining the effects of hydroxyl end groups observed on poly(isobutylene)[33] and on poly(ethylene oxide)[21]. To determine the effect that this phenomenon had on the polymers, the hydroxyl groups were reacted with acetyl chloride, leaving a CO_2-philic acetate group on the ends of the polymer chain. PPO (MW 2000) with no side chains was tested as well as the 12% acetate, 100% acetate, and 12% ether samples (see **Figure 22**). While the ether sample was not miscible as capping did not improve the insoluble polymer enough to bring it into solution, the acetate polymers were more CO_2-philic when capped with end groups. The degree of acetate substitution did not affect the cloud point pressure drop obtained by capping the end groups as all polymers exhibited a drop of 500 to 1000 psi (3.4 to 6.9 MPa) when capped.

Figure 22: The Effect of End Group Capping on Acetate-Substituted PPO

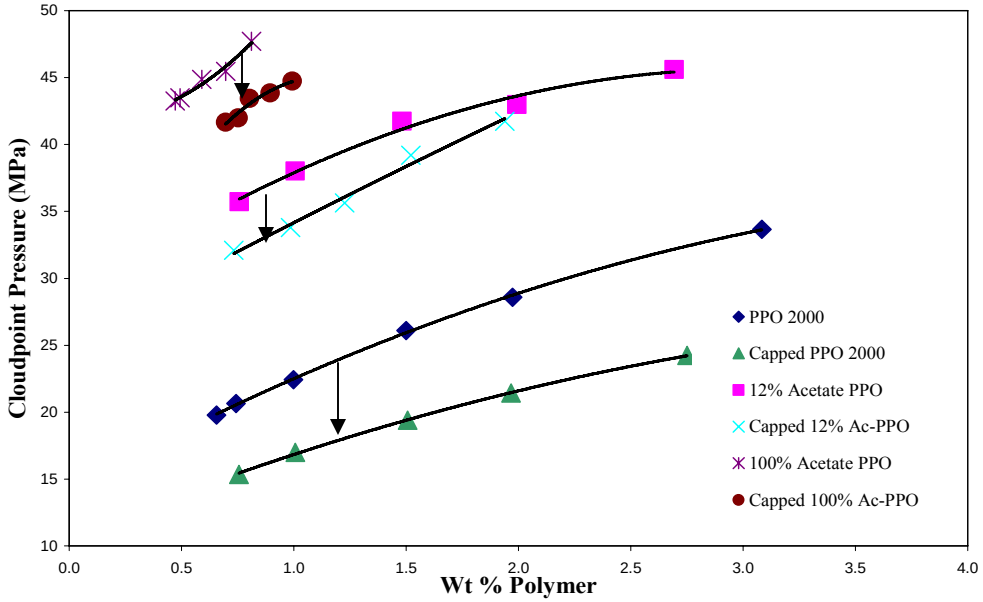

Figure 23: Molecular Weight Effects on PPO Solubility in Carbon Dioxide

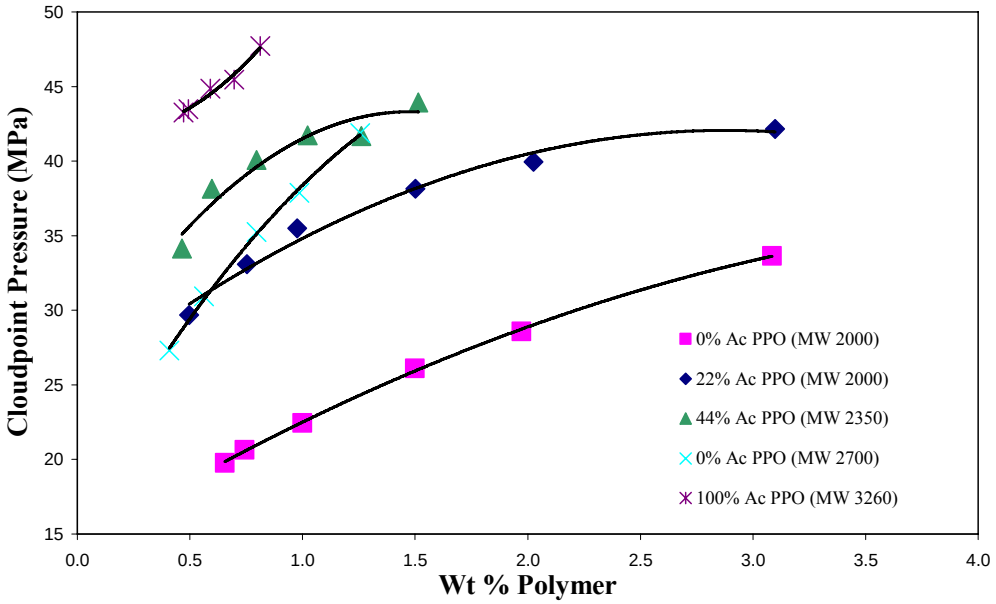

5.4 The Effect of Molecular Weight on the Phase Behavior of PPO

Increasing the molecular weight of a polymer resulted in a drop in entropy of mixing and therefore decreased CO_2 solubility. This was confirmed with a molecular weight analysis of two PPO samples. Two polymers of differing molecular weights (2000 and 2700) were evaluated for cloud point pressure (see **Figure 23**), and they behaved as predicted. With the 35% increase in molecular weight from the PPO 2000 to the PPO 2700, the cloud point pressure increased substantially. The effect of molecular weight was much more pronounced for the non-fluorous polymers than it was in the siloxane samples. The PPO did not have the low cohesive energy density (Surface tension: 31.5 mN/m @20°C)[32] necessary to overcome the negative entropic effects caused by increased molecular weight. When comparing the acetate-grafted PPO on a molecular weight basis with unaltered PPO, it was seen that the polymers with acetate did not favorably compare to the base PPO polymer. At a molecular weight of 2000, the acetate-grafted polymer (22% Ac) had a cloud point pressure of about 10 MPa higher than that of the base PPO. The acetate-grafted polymer at a molecular weight of 2360 (44% Ac), showed a slightly higher cloud point pressure than an unaltered PPO with a molecular weight of 2700. The polymer with all of the repeat units grafted with acetate had the highest molecular weight (MW 3260) and had a higher cloud point pressure than the other polymers in the comparison.

5.5 Phase Behavior of Poly(propylene)

Poly(propylene) (PP) was chosen as an appropriate hydrocarbon counterpart to PPO as it had almost the same repeat unit with the lack of one oxygen atom. The PP was tested to determine the effects of oxygen in the backbone on the miscibility pressure in CO_2. PP at a molecular weight of 425 (about 10 repeat units) had relatively high cloud point pressures in CO_2 (see **Figure 24**). At the next available molecular weight increment (MW 1000), the PP was insoluble at the limits of the equipment (48.26 MPa). Despite the low T_g and CED (-10 °C and a surface tension of 29.4 mN/m[32], respectively) of PP, it was evident that the lack of oxygen in the backbone harmed the solubility of the oligomer just as the suspected blocking of the backbone oxygen atoms in the methyl-ether substituted PPO severely debilitated the solubility of that polymer. In comparison the PPO, which has an ether group in the backbone, had a significantly lower cloud point curve than PP at the same molecular weight of 425[53]. At a molecular weight of 1000, the PP was not miscible with the CO_2 at the limits of our equipment (48.26 MPa), while the PPO dissolved in carbon dioxide at moderate pressures of 20 to 25 MPa from 0.6 to 1 weight percent[53]. The benefits of adding a Lewis base group were very obvious when comparing PP (MW = 425) and PVAc (MW = 3090)[55]. The miscibility pressures of these polymers were similar at one weight percent even with the PVAc having over seven times the molecular weight. At higher weight concentrations, the cloud point pressure of PP rose dramatically while the PVAc curve remained relatively flat. Placing the carbonyl group as a Lewis base in the backbone can lower the miscibility pressure of a non-fluorous polymer, though not to the extent seen when placing the group in a side chain

(PVAc). At 308 K, poly(lactide) (PLA) at a molecular weight of 128,500 at five weight percent will dissolve in CO_2 at about 140 MPa[54]. Under the same conditions and with the same molecular weight, PVAc exhibits a cloud point pressure of 70 MPa[55]. Poly(propylene) is not the only hydrocarbon to have high miscibility pressures in CO_2. At 4.82 wt. percent and at ~383K, poly(isobutylene) (MW 1000) has a cloud point pressure of about 190 MPa[33].

Figure 24: Cloud Point Effects of Lewis Base Groups on a Polymer

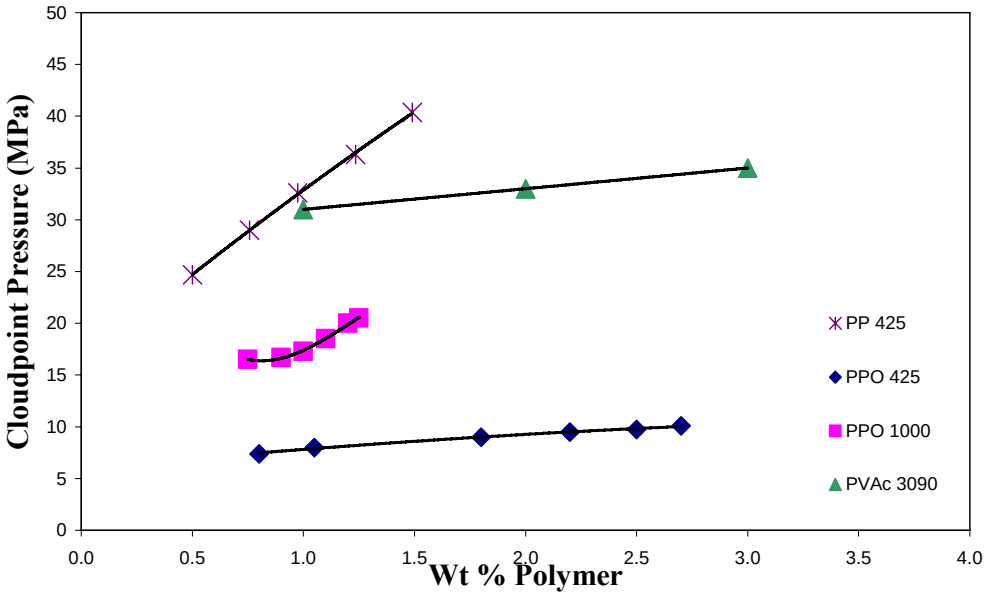

5.6 Phase Behavior of Poly(ethyl vinyl ether)

To further compare the effects of an ether-group and an acetate-group as functional Lewis base side chains, poly(ethyl vinyl ether) (PEVE) was purchased from Aldrich at a molecular weight of 3700. When tested, the polymer had higher cloud point pressures than PVAc[55] with a similar molecular weight of 3090 (see **Figure 25**). While the PEVE exhibited a comparable cloud point pressure to PVAc at lower concentrations, the PVAc had lower miscibility pressures as the weight concentration rose. However, the comparison was effectively equal as the molecular weight of the PVAc was lower than that of the PEVE, and the PVAc had about 17 fewer repeat units. This result was very important as it provided supporting evidence to the research by group member, Yang Wang, stating that the ether group was as effective as the acetate group for the purpose of

Figure 25: Phase Behavior Comparison of Ether and Acetate Containing Polymers

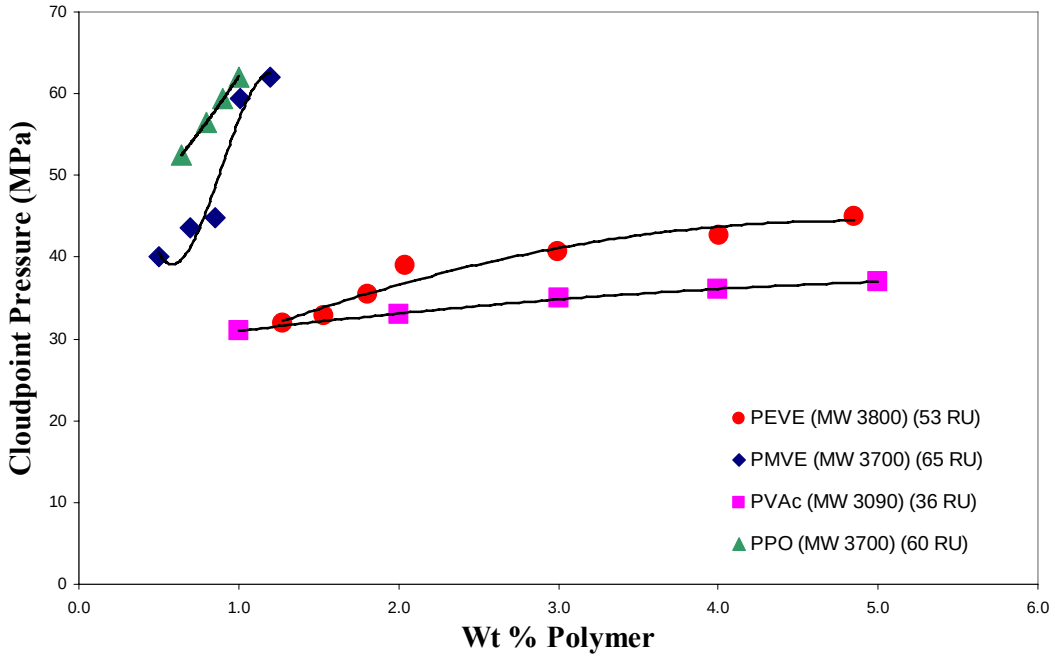

interacting with CO_2. The PEVE had much lower miscibility pressures than that of poly(methyl vinyl ether) (PMVE), which was tested by group member, Sevgi Kilic. This large disparity was attributed to the increase in free volume and hence lower T_g provided by the additional CH_2 spacer in PEVE. The T_g of PEVE is -43°C, and the T_g values for PEVE are generally lower than those of PMVE[64]. The PMVE had a similar cloud point curve to PPO with acetate capped end groups (also tested by Sevgi Kilic) at approximately the same molecular weight. Though not clearly superior, the PMVE had lower miscibility pressures than PPO, which has the same repeat unit composition. The only difference between the polymers is that the ether linkage is in the side chain of PMVE, while the PPO has ether in the backbone.

6.0 CONCLUSIONS

In the investigation of grafted side chains, it was found that each Lewis base group had an optimal degree of substitution on the PDMS polymers. In the case of the acetate group, the optimum (~20%) acetate substitution (excluding the base polymer) seen on the PDMS polymer was duplicated on the PPO backbone. The presence of an optimal amount of substitution is not a new discovery as it was observed on fluorinated polymers as reported by Beckman et al[37]. In each case there is a balance between the effect of the Lewis base interactions with CO_2 and the increase in cohesive energy density and T_g.

While very important, the T_g and CED of a polymer are not the dominant factors in governing the miscibility of the polymer in CO_2. The need for a Lewis base bonding site on the polymer was obvious in this study. When comparing PP to PPO, this fact was quite apparent. The oxygen atom in PPO enabled that polymer to dissolve in CO_2 at much higher molecular weights than the pure hydrocarbon, even though PP has a low T_g and a lower CED than PPO (see **Table 6**). Adding the acetate group yielded an even larger cloud point pressure difference despite the fact that PP has a far lower T_g and CED than PVAc.

Table 6: Selected Physical Properties of Polymers[32,64,65]

Polymer ---	Tg ° C	Surface Tension mN/m @ 20 °C
PP	-31	29.4
PPO	-83	31.5
PVME	-31	31.8
PEVE	-43	36.0
PVAc	32	36.5

While very important, Lewis base groups must be placed onto the polymer judiciously. As hypothesized in the case of methyl ether substituted PPO, having oxygen

atoms in close proximity serves to repel CO_2 rather than facilitate interactions that would lower miscibility pressures. The base polymer, PPO, is miscible with CO_2 as is the methyl ether group which can be seen in the PMVE sample. However, when combined, the oxygen atoms are too closely aligned in space to interact with the carbon dioxide solvent. Also adding credibility to the spacing argument is the insolubility of poly(acetaldehyde), which arranges oxygen atoms in close spatial proximity.

Replacing the hydroxyl end groups with acetate groups resulted in lower cloud point pressures for the polymers. The grafted side chains did not appear to have any effect on the extent to which the miscibility pressure was lowered as each polymer was improved by approximately the same amount. When deriving the most CO_2-philic polymer, the hydroxyl groups must be converted to a structure that interacts more favorably with carbon dioxide and less favorably with end groups on other polymer chains.

The addition of the acetate Lewis base group was proven effective in lowering miscibility pressures of a polymer in CO_2, but there is now a challenge to the fact that acetate aids in lowering cloud point pressures more than any other Lewis base. Both simulation calculations and experimental results have shown that an ethyl ether may be just as effective at forming a Lewis acid/base bond with CO_2 as the acetate group.

7.0 RECOMMENDED FUTURE WORK

To further validate the findings made in this work, there are several experiments to be undertaken. First, the acetate group displayed an optimal low cloud point pressure at about 20% acetate substitution on both the siloxane and polyether backbones. While PVAc is known to be an excellent non-fluorous CO_2-phile, the effects of a 20% acetate-substituted hydrocarbon backbone should be investigated. This may be accomplished by co-polymerizing isobutylene[66] and (trimethylsiloxy)ethylene[67], removing the protecting silyl group, and acetylating to yield poly(vinyl acetate-co-isobutylene) (see **Figure 26**).

The spacing hypothesis posed to explain the lack of miscibility of the ether-substituted ether in CO_2 can be further supported by the synthesis of similar polymers with more space between the oxygen atoms. Polymers with one more carbon spacer than PPO (see **Figure 27**) can be synthesized by polymerizing 4 member oxetanes[68,69]. Additionally, it would be interesting to observe the effects of spacing in the grafted side chain, though the means to create such a polymer are not currently known (see **Figure 28**).

In addition to the materials that support the conclusions of this work, there are other materials that should be tested. Nitrogen as a Lewis base should be fully investigated on both the ether and hydrocarbon backbones. Both methyl amine and imidazole should be tested (see **Figure 29**) to determine whether or not nitrogen, a strong Lewis base, can aid in the lowering of the cloud point pressure of a polymer more than acetate or ether. Imidazole provides an exposed nitrogen atom that is not

surrounded by methyl groups, eliminating steric interference in the CO_2 – Lewis base interactions. It has also been thought that CO_2 could position itself on the side of the ring to chelate between the two nitrogen atoms of imidazole.

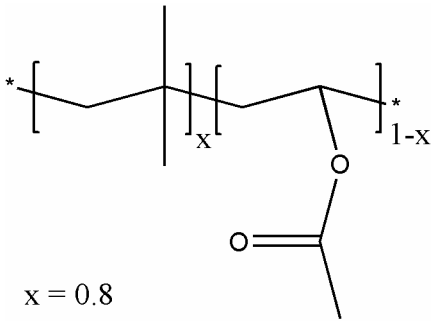

Figure 26: Poly(vinyl acetate-co-isobutylene)

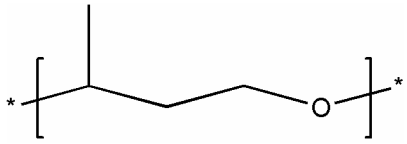

Figure 27: Poly(2-methyltrimethylene oxide)

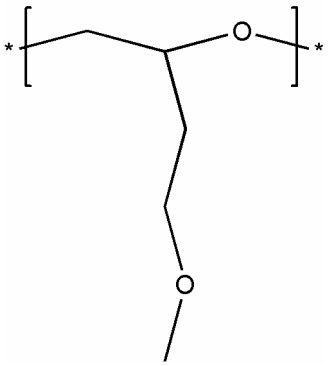

Figure 28: Ethyl Methyl Ether Substituted PPO

Methyl branching increases the free volume and has proven to aid in dissolving polymers in CO_2, as seen in a poly(ethylene oxide)/poly(propylene oxide) comparison[53]. To increase the methyl branching 2-methyl-2-butene oxide can be polymerized[70] to form a PPO analog with additional methyl groups on the backbone carbon chain (see **Figure 30**).

In addition, simulation work done by Dr. Johnson's group at the University of Pittsburgh has shown that CO_2 should bond strongly with an acetate-like structure that contains a CH_2 spacer between the ether oxygen and carbonyl group (see **Figure 31**). According to the initial simulations, the group seems to chelate CO_2 between the oxygen atoms. If successful, this would be a very important development as it would be the first time that simulations have directed experimental work in this field.

Finally, work by Dr. Johnson has also revealed that a sulfonyl group should interact with CO_2 more strongly than a carbonyl oxygen. Experimental investigation into this structure (see **Figure 32**) should be undertaken to evaluate the effects of replacing carbon with sulfur in an acetate group. Again, this would be an experimental study that was aided by simulation work.

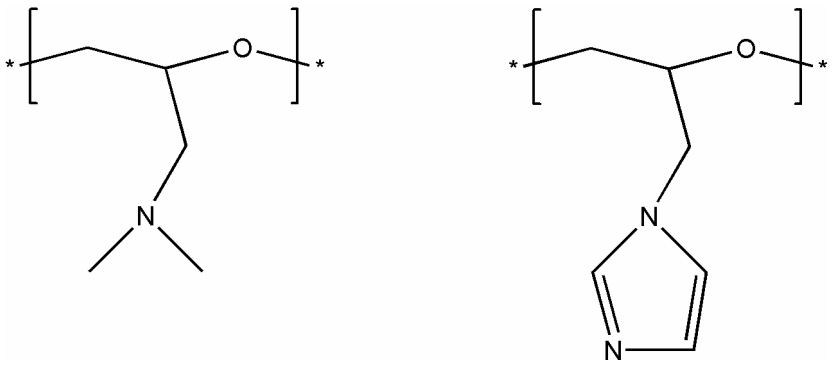

Figure 29: Grafted Nitrogen Lewis Base Groups

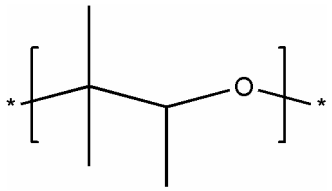

Figure 30: Poly(2-methyl-2-butene oxide)

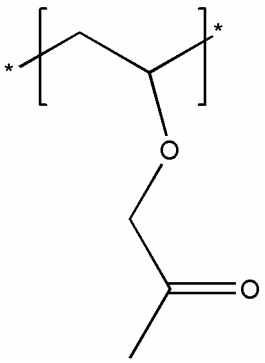

Figure 31: Poly(vinyl ether methyl ketone)

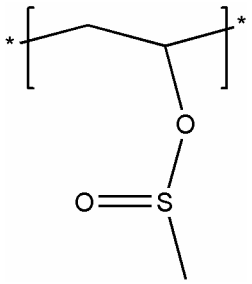

Figure 32: Poly(vinyl sulfonate)

8.0 APPENDIX A: FT-IR SPECTRUM

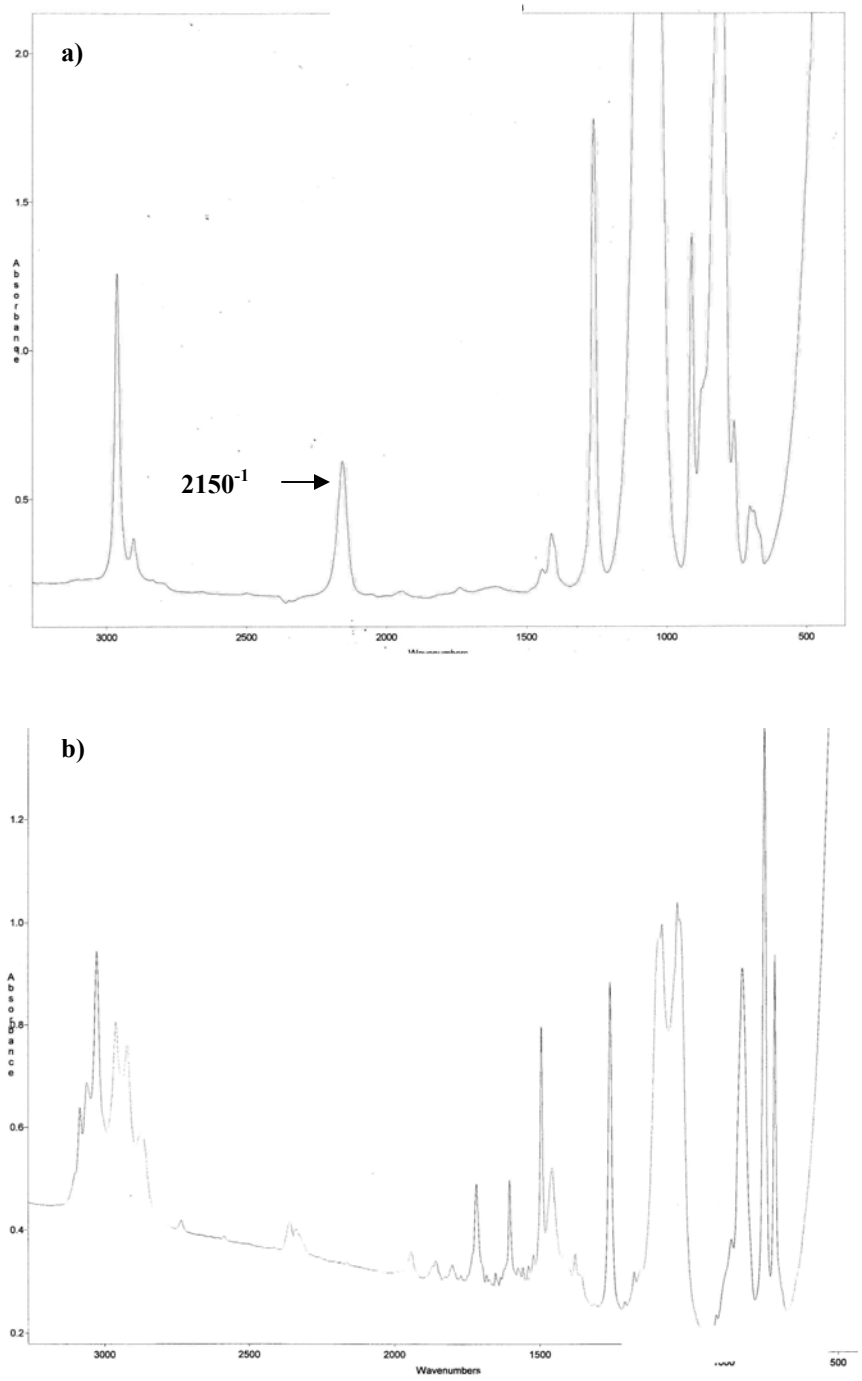

Figure A1: The Monitoring of the Silicon Reaction by FT-IR through the disappearance of the Si-H peak at 2150^{-1}. **a)** Before Reaction. **b)** After Reaction

9.0 APPENDIX B: ^{1}H-NMR SPECTRA

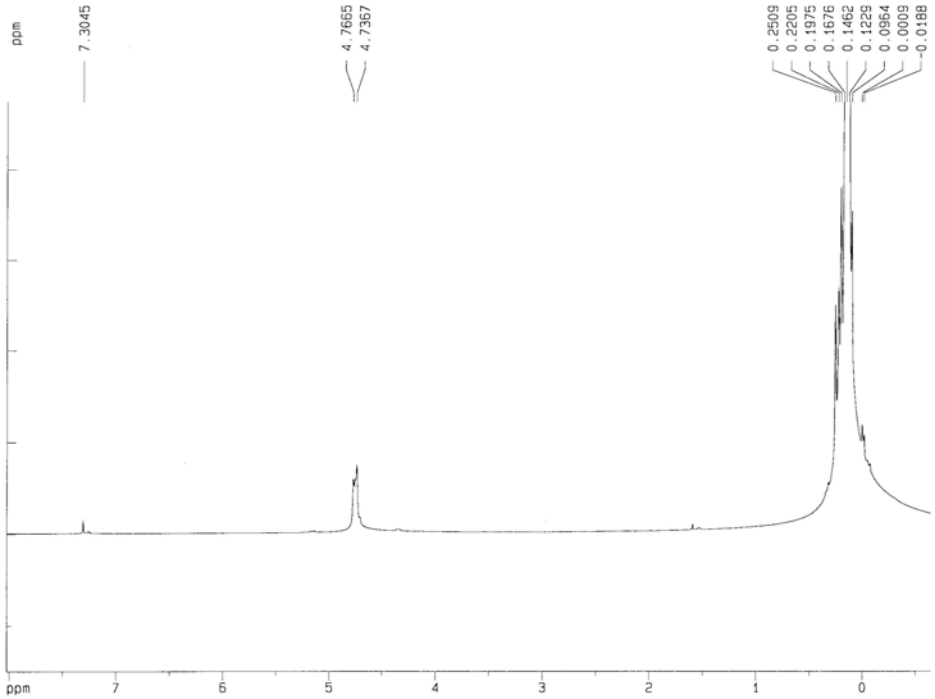

Figure B1: ^{1}H-NMR Spectrum for Silicon Polymer

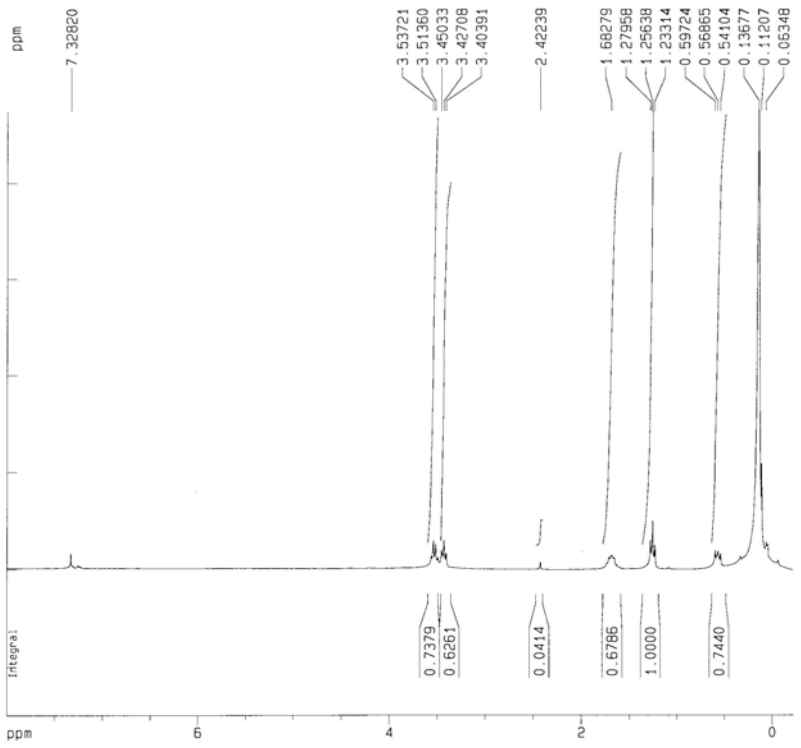

Figure B2: ^{1}H-NMR Spectrum for Propyl Ethyl Ether Substituted PDMS

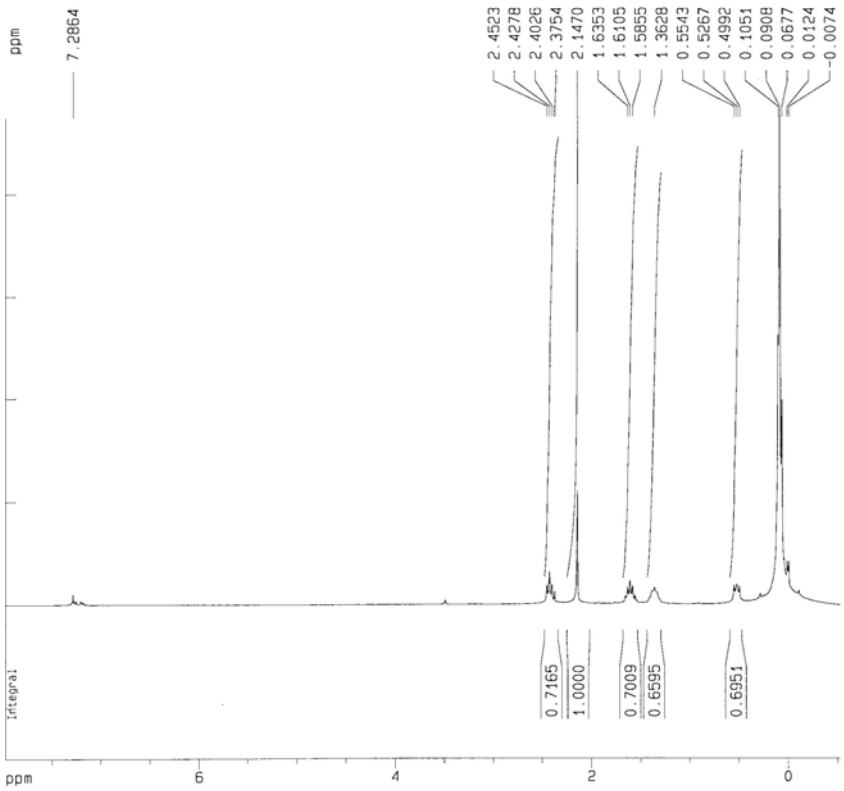

Figure B3: [1]H-NMR Spectrum for Butyl Methyl Ketone Substituted PDMS

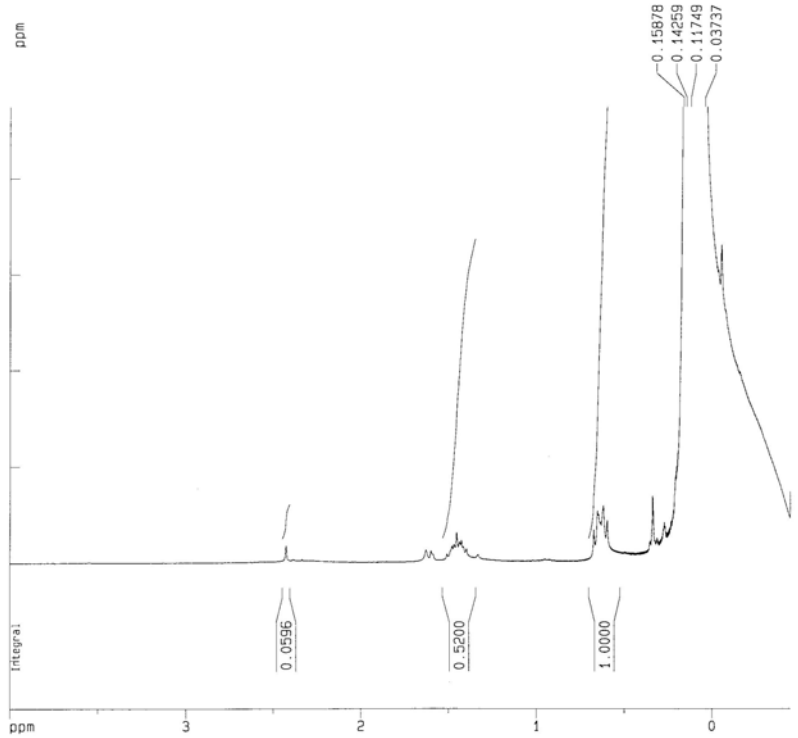

Figure B4: [1]H-NMR Spectrum for Butyl Tri-Methyl Silane Substituted PDMS

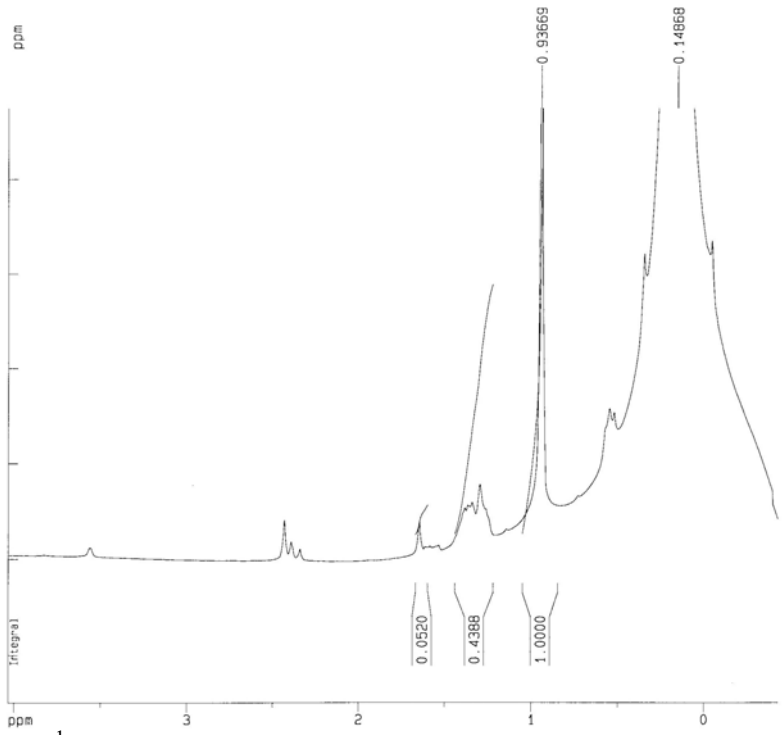

Figure B5: [1]H-NMR Spectrum for 5,5 Dimethyl Hexane Substituted PDMS

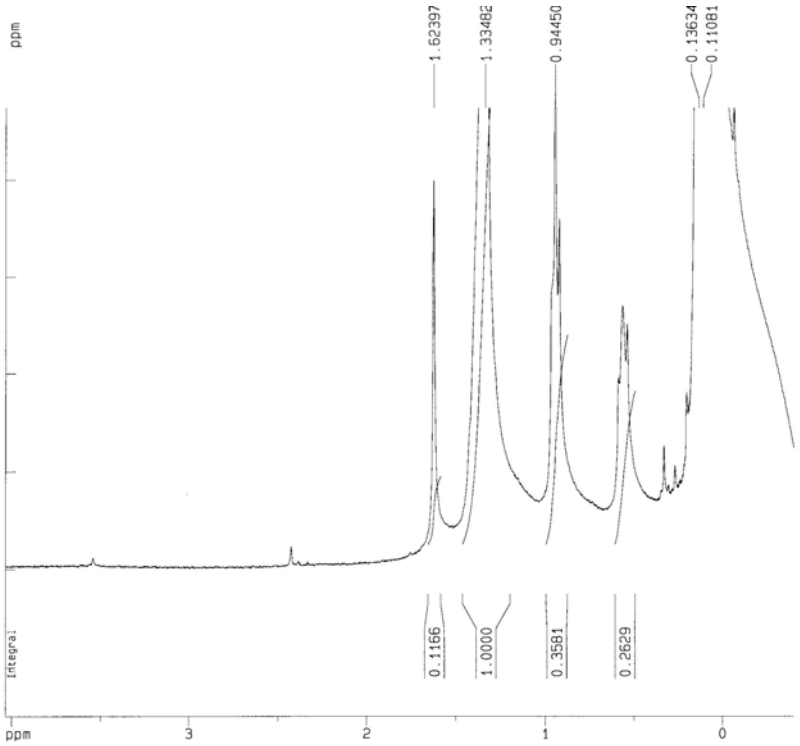

Figure B6: [1]H-NMR Spectrum for Hexane Substituted PDMS

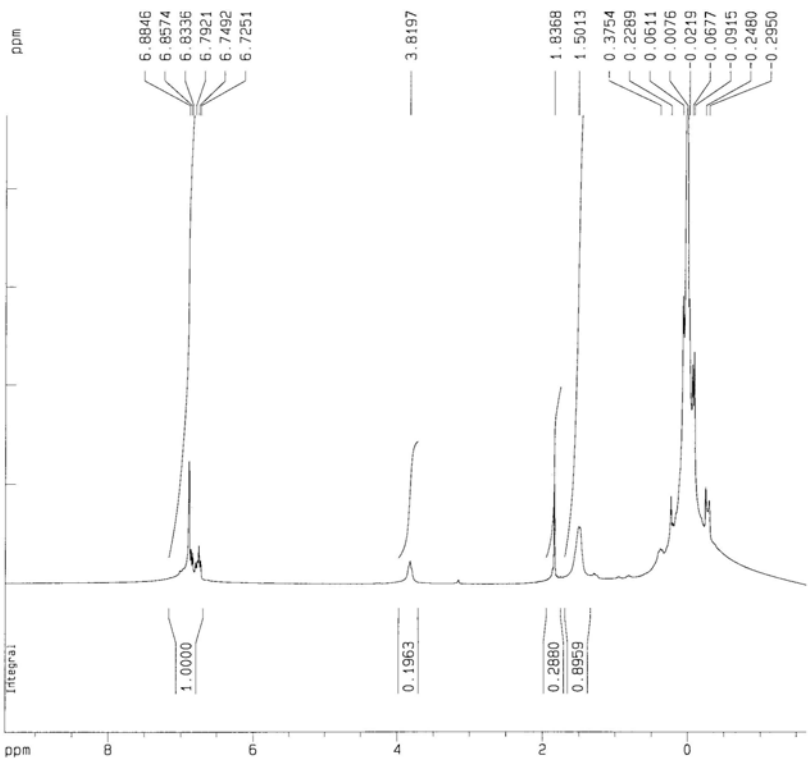

Figure B7: ^{1}H-NMR Spectrum for Propyl Acetate Substituted PDMS

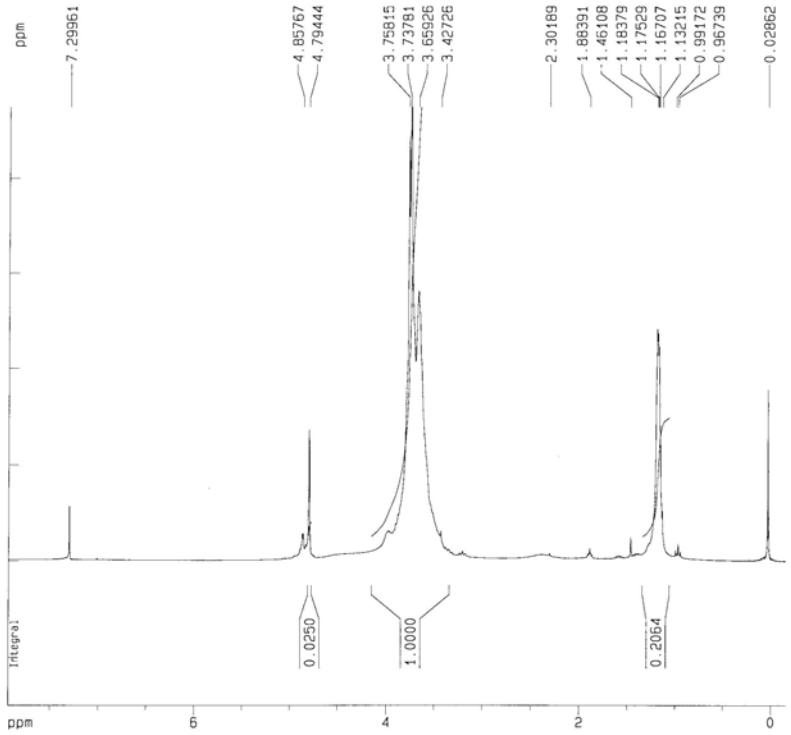

Figure B8: ^{1}H-NMR Spectrum for Partially Reduced PECH

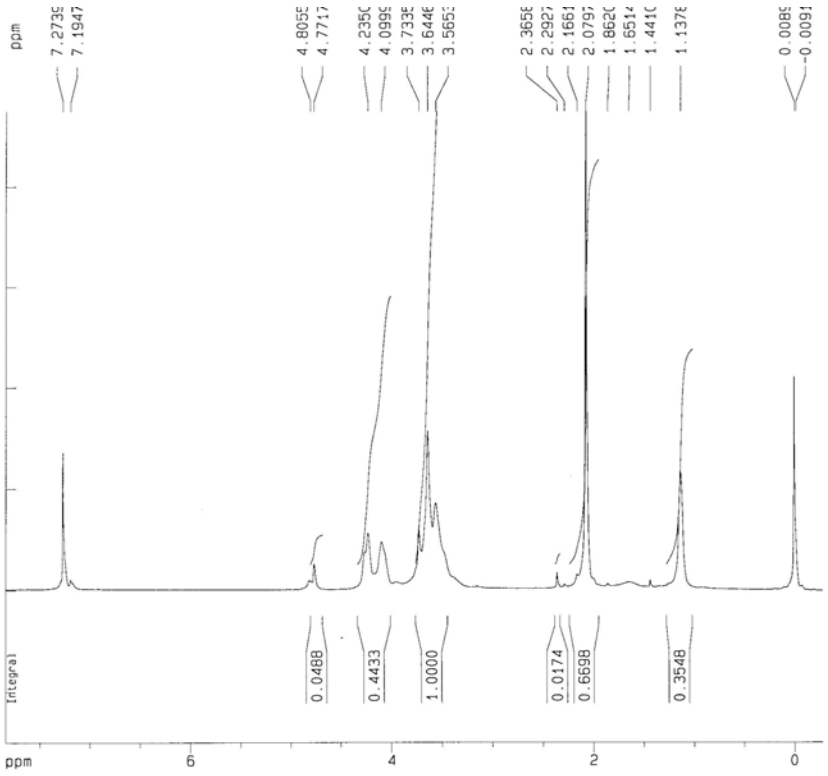

Figure B9: [1]H-NMR Spectrum for Acetate Substituted PPO

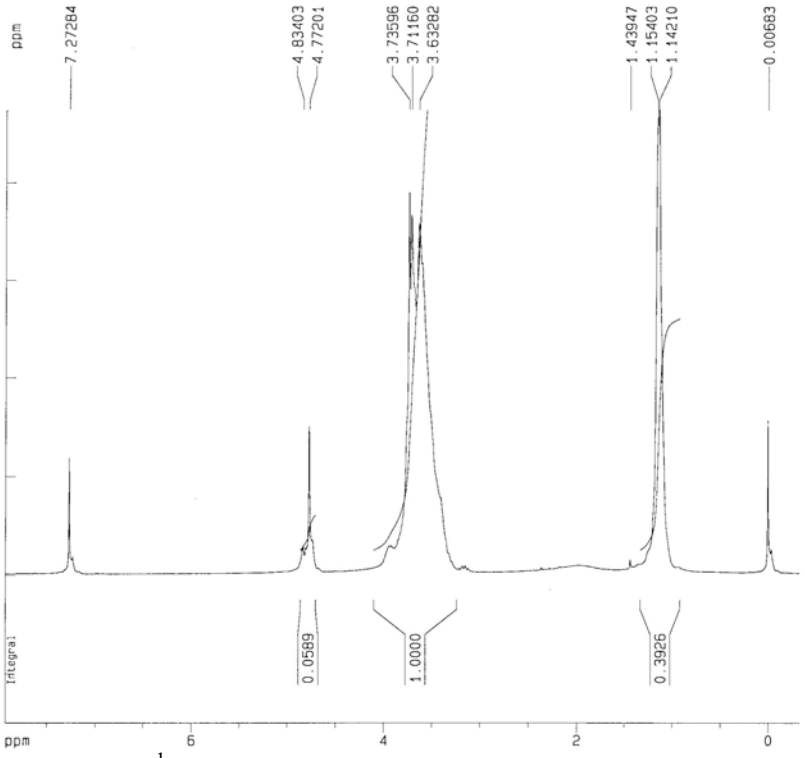

Figure B10: [1]H-NMR Spectrum for Methyl Ether Substituted PPO

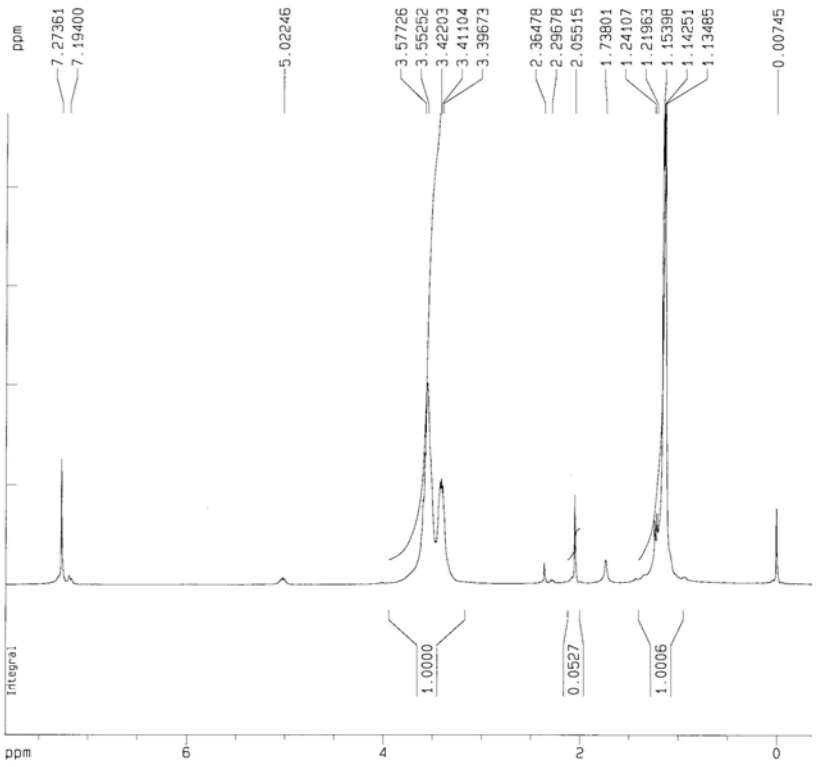

Figure B11: [1]H-NMR Spectrum for PPO with Acetate-Functional End Groups

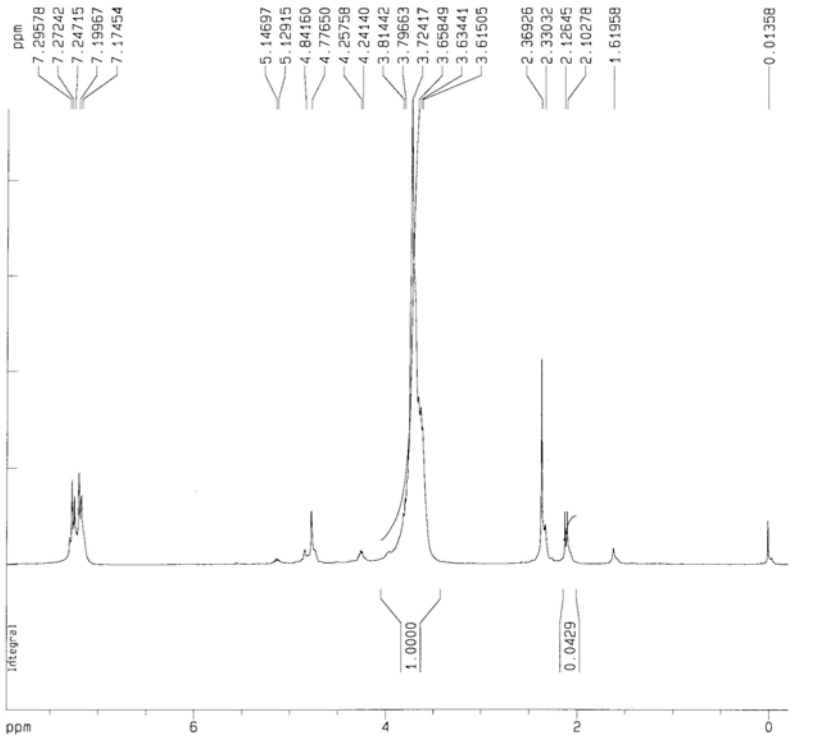

Figure B12: [1]H-NMR Spectrum for PECH with Acetate-Functional End Groups

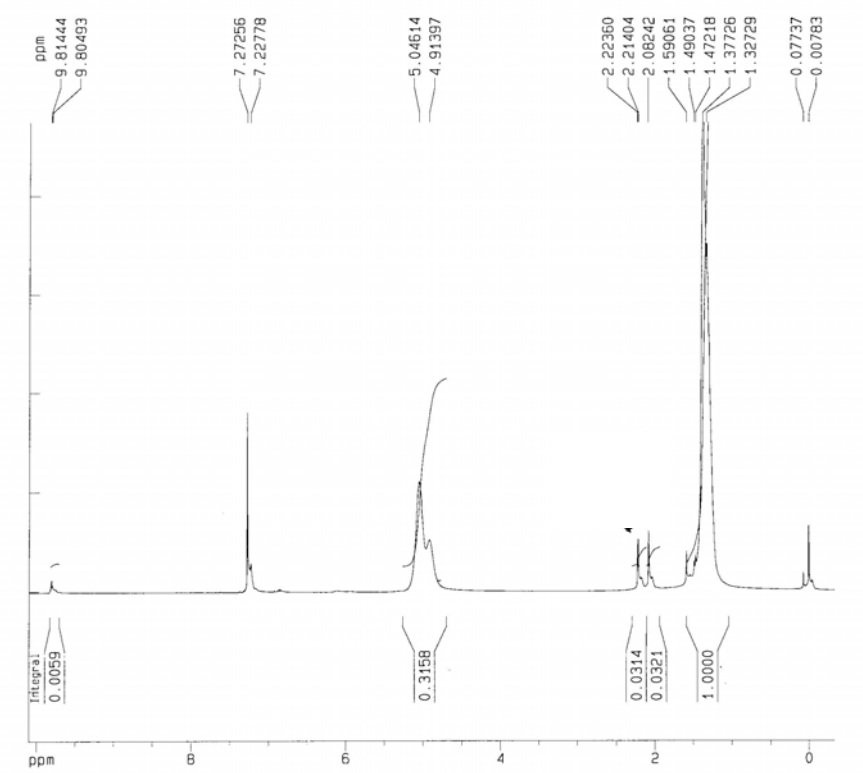

Figure B13: ^{1}H-NMR Spectrum for Poly(acetaldehyde)

10.0 REFERENCES CITED

1. Eckert, C. A.; Knutson, B. L.; Debenedetti, P. G. *Nature.* **1996**, 383, 313.

2. Consani, K. A.; Smith, R. D. *J. Supercritical Fluids.* **1990**, 3, 51.

3. O'Shea, K. E.; Kirmse, K. M.; Fox, M. A.; Johnston, K. P. *J. Phys. Chem.* **1991**, 95, 7863.

4. Johnston, K.P.; Lemert, R.M. *Encylclopedia of Chemical Processing and Design.* Mcketta, J.J., Ed.; Marcel Dekker: New York, **1996**. 1.

5. Harrison, K.; Goveas, J.; Johnston, K.P.; O'Rear, E.A. *Langmuir.* **1994**, 10, 3536.

6. DeSimone, J.M.; Guan, Z.; Elsbernd, C.S. *Science.* **1992,** 267, 945.

7. Hsaio, Y. L.; Maury, E. E.; DeSimone, J. M.; Mawson, S. M.; Johnston, K. P. *Macromolecules.* **1995**, 28, 8519.

8. Adamsky, F. A.; Beckman, E. J. *Macromolecules.* **1994,** 27, 312.

9. Ghencu, E.; Russell, A. J.; Beckman, E. J. *Biotechnol. Bioeng.* **1998,** 58, 572.

10. Johnston, K. P.; Harrison, K. L.; Clarke, M. J.; Howdle, S.; Heitz, M. P.; Bright, F. V.; Carlier, C.; Randolph, T. W. *Science.* **1996,** 271, 624.

11. Yadzi, A. V.; Beckman, E. J.; *Ind. Eng. Chem.* **1997,** 36, 2368.

12. Atkins, P. *Physical Chemistry,* 6th ed. W. H. Freeman and Company: New York, **1998**.

13. Jessop, P. G.; Ikariya, T.; Noyori, R. *Chem. Rev.* **1999,** 99, 475.

14. DeSimone, J. M.; Maury, E. E.; Menceloglu, Y. Z.; McClain, J. B.; Romack, T. J.; Combes, J. R. *Science.* **1994,** 265, 356.

15. Super, M.; Berluche, E.; Costello, C.; Beckman, E. *Macromolecules.* **1997,** 30, 368.

16. Cooper, A. *Green Chem.* **1999,** 1, G167.

17. Matsuyama, K.; Mishima, K.; Umemoto, H.; Yamaguchi, S. *Environ. Sci. Technol.* **2001,** 35, 4149.

18. Beuermann, S.; Buback, M.; Nelke, D. *Macromolecules.* **2001,** 34, 6637.

19. Baradie, B.; Shoichet, M. S. *Macromolecules.* **2002,** 35, 3569.

20. Beueermann, S.; Buback, M.; Isemer, C.; Lacik, I.; Wahl, A. *Macromolecules.* **2002,** 35, 3866.

21. Lepilleur, C.; Beckman, E. J. *Macromolecules.* **1997,** 30, 745.

22. Shiho, H.; DeSimone, J. M. *J. Poly. Sci. Part A.* **2000,** 38, 1146.

23. Christian, P.; Howdle, S. M.; Irvine, D. J. *Macromolecules.* **2000,** 33, 237.

24. Carson, T.; Lizotte, J.; DeSimone, J. M. *Macromolecules.* **2000,** 33, 1917.

25. Yazdi, A. V.; Lepilleur, C.; Singley, E. J.; Liu, W.; Adamsky, F. A.; Enick, R. M.; Beckman, E. J. *Fluid Phase Equilibria.* **1996,** 117, 297.

26. Li, J.; Beckman, E. J. *Ind. Eng. Chem. Res.* **1998,** 37, 4768.

27. Ghenciu, E. G.; Beckman, E. J. *Ind. Eng. Chem. Res.* **1997,** 36, 5366.

28. Hancu, D.; Beckman, E. J. *Ind. Eng. Chem. Res.* **1999,** 38, 2833.

29. Hancu, D.; Beckman, E. J. *Ind. Eng. Chem. Res.* **2000,** 39, 2843.

30. Glebov, E. M.; Yuan, L.; Krishtopa, L. G.; Usov, O. M.; Krasnoperov, L. N. *Ing. Eng. Chem. Res.* **2001,** 40, 4058.

31. Tepper, G.; Levit, N. *Ind. Eng. Chem. Res.* **2000,** 39, 4445.

32. O'Neill, M. L.; Cao, Q.; Fang, M.; Johnston, K. P.; Wilkinson, S. P.; Smith, C. D.; Kerschner, J. L.; Jureller, S. H. *Ind. Eng. Chem. Res.* **1998,** 37, 3067.

33. Gregg, C. J.; Stein, F. P.; Radosz, M. *Macromolecules.* **1994,** 27, 4981.

34. Hoefling, T.; Stofesky, D.; Reid, M.; Beckman, E.; Enick, R. M. *J. Supercrit. Fluids.* **1992,** 5, 237.

35. Mertdogan, C. A.; Byun, H.; McHugh, M. A.; Tuminello, W. H. *Macromolecules.* **1996,** 29, 6548.

36. Rindfleisch, F.; DiNoia, T. P.; McHugh, M. A. *J. Phys. Chem.* **1996,** 100, 15581.

37. Lepilleur, C.; Beckman, E. J.; Schonemann, H.; Krukonis, V. J. *Fluid Phase Equilibria.* **1997,** 134, 285.

38. Mesiano, A. J.; Enick, R. M.; Beckman, E. J.; Russell, A. J. *Fluid Phase Equilibria.* **2001,** 178, 169.

39. McHugh, M. A.; Park, I.; Reisinger, J. J.; Ren, Y.; Lodge, T. P.; Hillmyer, M. A. *Macromolecules.* **2002,** 35, 4653.

40. Sanchez, I. C.; Panayiotou, C. G. *Models for Thermodynamic and Phase Equilibria Calculations.* Sandler, S., Ed. Dekker: New York, **1993.**

41. Prausnitz, J. M.; Lichtenthaler, R. N.; Azevedo, E. G. *Molecular Thermodynamics of Fluid Phase Equilibria,* 2nd ed. Prentice Hall: Englewood Cliffs, NJ, **1986**.

42. Mertdogan, C. A.; DiNola, T. P.; McHugh, M. A. *Macromolecules.* **1997,** 30, 7511.

43. McHugh, M. A.; Park, I-H.; Reisinger, J. J.; Ren, Y.; Lodge, T. P.; Hillmyer, M. A. *Macromolecules.* **2002,** 35, 4653.

44. McHugh, M. A.; Garach-Domech, A.; Park, I-H.; Li, D.; Barbu, E.; Graham, P.; Tsibouklis, J. *Macromolecules.* **2002,** 35, 6479.

45. Hoefling, T. A.; Newman, D. A.; Enick, R. M.; Beckman, E. J. *J. Supercrit. Fl.* **1993,** 6, 165.

46. Bayraktar, Z.; Kiran, E. *J. Appl. Poly. Sci.* **2000,** 75, 1397.

47. Kilic, S.; Michalik, S.; Enick, R.; Beckman, E. J. *To be Submitted to Ind. Eng. Chem Res.* **2003.**

48. Luna-Bárcenas, G.; Mawson, S.; Takishima, S.; DeSimone, J. M.; Sanchez, I. C.; Johnston, K. P. *Fluid Phase Equilibria,* **1998,** 146, 325.

49. Kazarian, S. G.; Vincent, M. F.; Bright, F. V.; Liotta, C. L.; Eckert, C. A. *J. Am. Chem. Soc.* **1996,** 118, 1729.

50. Sarbu, T.; Styranec, T. J.; Beckman, E. J. *Ind. Eng. Chem. Res.* **2000,** 39, 4678.

51. Sarbu, T.; Styranec, T. J.; Beckman, E. J. *Nature.* **2000,** 405, 165.

52. Fink, R.; Hancu, D.; Valentine, R.; Beckman, E. J. *J. Phys. Chem.* **1999,** 103, 6441.

53. Drohmann, C.; Beckman, E. J. *J. Supercritical. Fluids.* **2002,** 22, 103.

54. Conway, S. E.; Byun H-S.; McHugh, M. A.; Wang, J. D.; Mandel, F. S. *J. Appl. Polym. Sci.* **2001,** 80, 1155.

55. Shen, Z.; McHugh, M. A.; Xu, J.; Belardi, J.; Kilic, S.; Mesiano, A.; Bane, S.; Karanikas, C.; Beckman, E.; Enick, R. *Polymer.* **2003,** 44(5), 1491.

56. Raveendran, P.; Wallen, S. L. *JACS.* **2002,** 124, 12590.

57. Blatchford, M. A.; Raveendran, P.; Wallen, S. L. *JACS.* **2002,** 124, 14818.

58. Krishnamurthy, S.; Brown, H. C. *J. Org. Chem.* **1982,** 47, 276.

59. Cohen, H. L. *J. Poly. Sci: Poly. Chem. Ed.* **1975,** 13, 1993.

60. Vogl, O. *J. Polym. Sci., Part A-2.* **1964,** 2, 4591.

61. Angus, S.; Armstrong, B.; de Reuck, K. M. *International Thermodynamic Tables of the Fluid State; v. 3 Carbon Dioxide.* Pergamon Press: Oxford, New York, **1976.**

62. van Krevelen, D. W. *Properties of Polymers, 3rd ed.* Esevier: New York, **1990.**

63. Streitwieser, A.; Heathcock, C. H. *Intro. Org. Chem.* MacMillan Publishing Co.: New York, **1976.**

64. Lal, J.; Trick, G.S. *J. Polym. Sci., Part A-2*. **1964,** 2, 4559.

65. Brandrup, J.; Immergut, E. H.; Grulke, E. A., ed. *Polymer Handbook, 4th ed.* Josh Wiley & Sons, Inc.: New York, **1999.**

66. Chung, T. C.; Kumar, A.; Rhubright, D. *Polymer Bulletin.* **1993,** 30, 385.

67. Murahashi, S.; Nozakura, S.; Sumi, M. *J. Polym. Sci., Part B.* **1965,** 3, 245.

68. Oguni, N.; Hyoda, J. *Macromolecules,* **1980,** 13, 1687.

69. Kops, J.; Spanggaard, H. *Macromolecules,* **1982,** 15, 1200.

70. Field, N. D.; Kieras, J. A.; Borchert, A. E. *J. Polym. Sci., Part A-1.* **1967,** 5, 2179.

Section 3 High CO_2 Solubility of Per-acetylated Compounds

Over the past several years there has been intense interest in the use of supercritical carbon dioxide ($scCO_2$) as an environmentally friendly solvent for laboratory and industrial applications.[1] However, a critical factor in limiting the use of $scCO_2$ is its weak solvent strength relative to organic liquids. This hurdle has led to the investigation of CO_2-philic groups that enhance the solubility of $scCO_2$ insoluble derivatives. Currently the most widely used class of $scCO_2$ solubilizing groups are perfluorinated ester or ether derivatives.[2] While these CO_2-philes have found widespread application in surfactants and additives, their use is limited by prohibitive cost, lack of availability in bulk quantity, and environmental and biological persistence.

From a theoretical analysis[3] of the origin of fluoroalkane CO_2-philicity we proposed that similarly electronegative oligo-carbonate and oligo-ester derivatives would make useful substitutes, as demonstrated by the high CO_2 solubility of poly(ether-carbonate).[4] We have also observed that the addition of acetate side chains to silicone dramatically increased its CO_2 solubility,[5] while others have noted the remarkable solubility of poly (vinyl acetate) in CO_2 relative to other non-fluorous homopolymers.[6] All of these examples are based on polymeric derivatives that, while useful, did not fulfill our search for a non-fluorinated small molecule derivative that could be attached to a given compound to increase its solubility in CO_2. An alternative approach to constructing molecular subunits with multiple ester functionalities could involve the acetylation of oligo-hydroxyl derivatives (see poly(vinyl acetate) above). A ready source of multi-hydroxylated compounds is the family of mono-, di- and oligosaccharides. These can be readily converted to their per-acetylated derivatives, (**Figure 1**) which should have a similar density of electronegative groups (and hence CO_2 solubility) to perfluorohydrocarbons.

To test our hypothesis we determined the CO_2 solubility of commercially available sorbitol hexaacetate (**1**) and β-D-galactose pentaacetate (**2**). These materials were combined with liquid CO_2 at sub-critical (T<304 K) and supercritical (T>304 K) temperatures in a high pressure, windowed, variable-volume cell. The high pressure single phase solutions were gradually expanded until a second phase appeared. If the second phase was not a solid, the system was further expanded until particles of **1** and **2** appeared at the three phase pressure. At lower pressures CO_2 rich vapor co-existed withthe solid phase of **1** or **2**. Upon removal of the CO_2 the final form of the solid obtained was also noted. The results (summarized in **Table 1** and **Figure 2**) indicate that both **1** and **2** were soluble in CO_2 at low pressures and both exhibit three phase equilibria. At 5 wt%, the phase behavior results for **1** and **2** were nearly identical. While sorbitol hexaacetate (**1**) was recovered as powder at the end of the experiment, β-D-galactose pentaacetate (**2**) formed a fragile foam with a fibrillar morphology and a density of 0.09 g/ml.

Encouraged by the low pressures required to dissolve **1** and **2** in dense CO_2, we prepared a series of test compounds in which CO_2 insoluble amines were functionalized by per-acetoxy alkyl chains (analogous to the frequently used perfluorinated alkyl esters) to assess any improvement in solubility. In particular, the per-acetylated amides of D-gluconic acid with 1-octylamine, 1,8-diaminooctane and 1,4-aminomethylbenzene (compounds **3**, **4** and **5**, respectively) were prepared by ring opening reaction of the amine with gluconolactone followed by per-acetylation with acetic anhydride. Phase behavior results (**Table 1)** demonstrate that each of the amides exhibited CO_2 solubility. While compound **3** was readily

---

† Yale University
‡ University of Pittsburgh

[1] (a) Eckert, C.A.; Knutson, B.l.; Debenedetti, P.G. Nature, **1996**, *373*, 313. (b) Wells, S. L.; DeSimone, J.M. *Angew. Chem., Int. Ed.* **2001**, *4*0, 518. (c) Mesiano, A.J.; Beckman, E.J.; Russell, A.J. *Chem. Rev*., **1999**, *99*, 623.

[2] (a) DeSimone, J.M.; Keiper, J.S. *Curr. Opin. Solid State Mater. Sci.*, **2001**, *5*, 333. (b) Shi, C.; Huang, Z.; Kilic, S.; Xu, J.; Enick, R. M.; Beckman, E. J.; Carr, A. J.; Melendez, R. E.; Hamilton, A. D.*Science* **1999**, *286*, 1540-1543.

[3] Diep, P;, Jordan, K.D;, Johnson, J.K;, Beckman, E.J. *J. Phys. Chem A.* **1998**, *102*, 2231.

[4] Sarbu, T.; Styranec, T.; Beckman, E.J. *Nature*, **2000**, *405*, 165.

[5] Fink, R.; Hancu, D.; Valentine, R.; Beckman, E.J. *J. Phy. Chem.B*, **1999**, *103*, 6444.

[6] Rindfleisch, F.; DiNoia, T.; McHugh, M.; *J. Phys. Chem.,* **1996,** *100,* 15581.

soluble in CO_2 at 298 K, compounds **4** and **5** were less soluble in CO_2, exhibiting high bubble point pressures at supercritical temperatures. Even though compounds **4** and **5** were initially insoluble in CO_2 at 298 K, a single phase could be obtained at elevated temperature and pressure, and a cloud point was eventually determined by cooling to 298 K followed by expansion until a second phase appeared.

An even more challenging test was the cyclic heptasaccharide, β-cyclodextrin. This molecule contains 21-hydroxyl groups surrounding a central cavity. The peracetylated derivative, β-cyclodextrin heneicosaacetate (**6**) showed outstanding solubility in liquid and $scCO_2$ over a very broad range of compositions (**Table 1** and **Figure 2**). The two phase boundary for this per-acetylated heptasaccharide (**6**), was observed at higher pressures compared to the per-acetylated monosaccharide (**2**) because of the increase in molecular weight. However, **6** was more soluble than the much smaller functionalized amides **4** and **5**, because of the absence of highly CO_2-phobic amide functionality. As the CO_2 was evacuated from the top of the cell at the end of the experiment, the β-cyclodextrin heneicosaacetate (**6**) formed a fragile, fibrillar foam with a density of 0.06 g/ml.

The limit of this strategy was reached with the attempted dissolution of cellulose triacetate **7** (n = ~180) in CO_2. The high molecular weight (103,000) of this per-acetylated polysaccharide rendered it completely insoluble in CO_2 over the 298 – 448 K temperature range at pressures up to 52 MPa. No evidence of polymer dissolution swelling, softening, melting, or foam generation was detected.

In summary, these results represent a significant step in the design of non-fluorous CO_2-philic agents. High solubility in $scCO_2$ can be achieved with a range of peracetylated sugars, from mono-saccharides to cyclodextrin. This strategy will permit not only the construction of simple and biodegradable CO_2-additives but also a unique opportunity to investigate host-guest interactions in $scCO_2$.

Acknowlegement. We are grateful for the financial support provided by DOE and NSF under the grants 400937-1 and CHE-0131477 respectively.

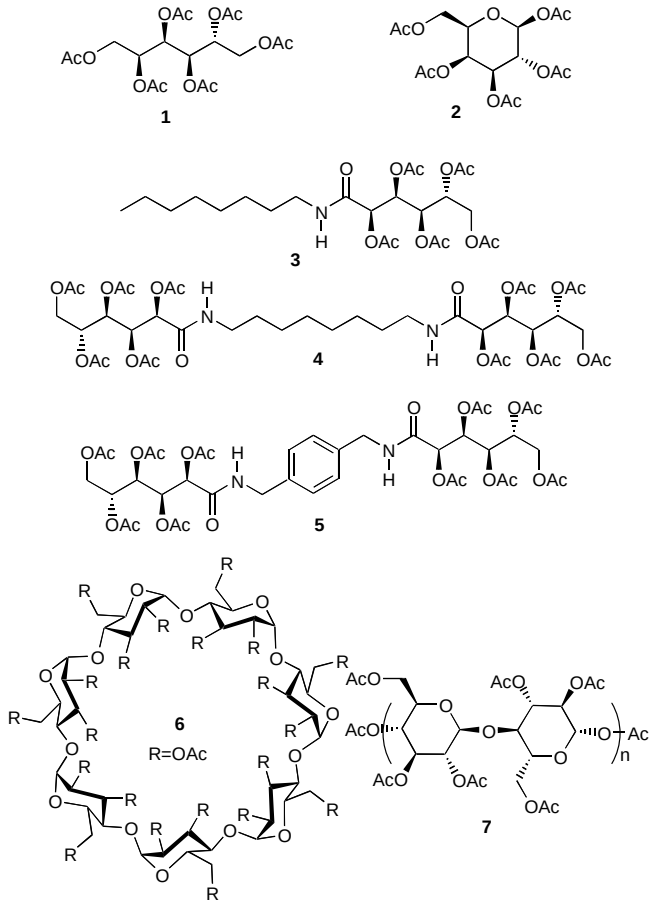

Figures 1: Per-acetylated sugars tested for solubility in Carbon dioxide.

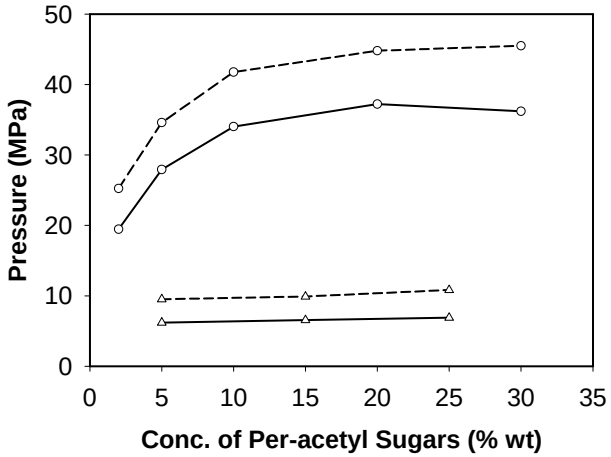

Figure 2: Phase diagrams for the solubility of acetylated sugars **2** (Δ) and **6** (O) in CO_2 at 298 K (solid line) and 313 K (dashed line). The area above each of the curves represents a single phase region.

Table 1: Phase behavior of acetylated sugars in liquid (T < 304 K) and $scCO_2$.(T > 304 K)

Acetyl sugar	% (wt)	T (K)	3 phase pressure (MPa)	2 phase pressure (MPa)	state of material after CO_2 venting
1	5	298	3.58	6.34[a]	powder
1	5	313	4.48	8.98 [a]	powder
2	5-25	298	5.17	Fig. 2 [a]	foam
2	5-25	313	8.27	Fig. 2 [a]	foam
3	1	298	5.51	6.55 [a]	powder
4	2	298	-	37.22[b]	powder
4	2	323	-	37.91 [b]	powder
4	2	343	-	42.74 [b]	powder
5	1	298	-	37.91 [b]	powder
5	1	338	-	41.36 [b]	powder
5	1	353	-	41.42 [b]	powder
6	2-30	298	5.52	Fig. 2 [a]	foam
6	2-30	313	8.27	Fig. 2 [a]	foam
7	1	448	insoluble	insoluble	-

[a] Bubble point pressure. [b] Cloud point pressure

Section 4. Novel Phase Behavior of CO_2-Philic Solids

The CO_2-Maltose Octaacetate System Illustrates a Novel Phase Behavior Diagram for Solids That Melt in Near- or Supercritical Fluids

Lei Hong [a], Mark C. Thies [b], Robert M. Enick [a]

[a] Department of Chemical and Petroleum Engineering, Oak Ridge University Faculty Participation, 1249 Benedum Engineering Hall, University of Pittsburgh, PA 15261, USA

[b] Department of Chemical Engineering, Clemson University, 127 Earle Hall, Clemson, SC 29634-0909, USA

Abstract

Sugar acetates, poly(fluoroalkyl acrylate), and poly(vinyl acetate) have melting points greater than the critical point of CO_2, yet liquefy at sub-critical temperatures in liquid CO_2. These compounds are also considered to be CO_2-philic because they exhibit high solubilities (i.e., >10 wt %) in liquid CO_2. Although limited portions of the phase behavior for binary mixtures of these compounds with CO_2 have been previously reported, their global pressure-temperature (PT) projection has yet to be elucidated or classified. In this study, a complete Pxy diagram for the CO_2 (1)-maltose octaacetate (2) system at 298 K has been measured. The diagram is characterized by numerous multiphase regions, including five two-phase regions (VL_1, L_1L_2, L_2S, VL_2, and VS) and two three-phase pressures (VL_1L_2 and VL_2S). Limited Pxy measurements have also been made at lower temperatures to determine whether LLE behavior re-emerges at lower temperatures. The global PT phase behavior for this system, which to our knowledge has yet to be reported in the literature, has fluid-phase behavior analogous to a Type V

system as defined by Scott and Van Konynenburg. However, the system also exhibits VL_2S behavior, with the three-phase line bounded by the triple point of maltose octaacetate at higher temperatures and a quadruple point at low temperatures near the triple point of CO_2. Although exemplified by CO_2-solid binary mixtures, this type of phase behavior may also be exhibited in mixtures of solids with other near-critical or supercritical solvents.

(Keywords: Carbon dioxide, maltose octaacetate, liquid-liquid equilibria, solid-fluid equilibria, melt, CO_2-philic)

Introduction

Several highly CO_2-philic polymers, including poly(fluoroalkyl acrylate) [1, 2], poly(perfluoroether) [3], and poly(dimethyl siloxane) [4, 5], have been incorporated into copolymers, surfactants, and chelating agents to enhance their CO_2 solubility. More recently, hydrocarbon-based CO_2-philes have been examined, including low molecular weight poly(propylene oxide) [4], branched alkyls [6], poly(ether-carbonate) [7], sugar acetates [8, 9], cyclic sugar acetates [10], and poly(vinyl acetate) [11, 12].

Many of these compounds, including poly(fluoroalkyl acrylate), sugar acetates, and poly(vinyl acetate), are solid at ambient temperatures, but melt in liquid CO_2 and also exhibit very high CO_2 solubilities (>10 wt %). Most prior phase behavior studies of these systems have concentrated on the CO_2-rich liquid (L_1) – CO_2-phile-rich liquid (L_2) phase boundary at CO_2-phile loadings between 1 and 30 wt %. For example, cloud-point pressures have been presented for mixtures of CO_2 with several sugar acetates, including

1,2,3,4,6-pentaacetyl α-D-glucose at 313 K [8], 1,2,3,4,6-pentaacetyl β-D-glucose at 313 K [8], 1,2,3,4,6-pentaacetyl β-D-galactose at 313 K [8, 9] and 298 K [9], β-cyclodextrin heneicosaacetate at 298 K and 313 K [9, 10], and α-cyclodextrin octadecaacetate and γ-cyclodextrin tetracosaacetate [10] at 298 K and 313 K. Liquid-liquid cloud points have also been presented for mixtures of CO_2 with poly(vinyl acetate) oligomers (Mw = 12500, 17000) that are solids at 298 K [12]. Pressure-composition diagrams (albeit limited to a narrow range of compositions in the L_1L_2, VL_2, and VL_1 two-phase regions and at the three-phase VL_1L_2 line) have been recently presented for the CO_2-poly(heptadecafluorodecyl acrylate) binary [13]. This fluoroalkyl acrylate homopolymer has a melting point of 351 K. In each of these examples, the neat CO_2-philes are solids (S); therefore, *four* phases (S, L_1, L_2, V) must be represented on a complete pressure-composition diagram. However, no such representations have yet to be reported in the literature. Furthermore, no single P-T projection for binary or pseudo-binary mixtures containing CO_2 [14, 15, 16, 17] can be used to predict the phase behavior of the binary systems under investigation. The commonly used Van Konynenberg and Scott-type diagrams are inappropriate because their PT projections correspond to systems generated from the Van der Waals equation of state, therefore solid phases were not considered. The CO_2-solid phase diagrams presented by McHugh and Krukonis [16] do not correspond to solids that are CO_2-philic enough to melt in the presence of liquid CO_2. Rowlinson [18] presented PTx diagrams for systems that exhibited a wide range of phase behavior, including critical phenomena, LLE, and immiscible solids, but no polymeric systems were discussed.

The objective of this study is to present pressure-composition diagrams and PT projections characteristic of binary mixtures of CO_2 with CO_2-philic solids that melt in the presence of dense CO_2. A per-acetylated disaccharide, maltose octaacetate, was selected as a candidate because of the high degree of CO_2 solubility previously reported for sugar acetates.

Experimental

Materials

β-D-maltose octaacetate [99+%, Sigma, T_m = 428 - 430 K], the structure showed in Figure 1, was used as received. CO_2 [99.99%, Coleman grade] was obtained from Penn Oxygen.

Phase Behavior

Bubble- and dew-point loci were determined using a non-sampling technique involving isothermal compression and expansion of binary mixtures of known overall composition. This method is also known as the synthetic method and is described in detail elsewhere [3, 9, 12]. A short summary of the procedure is presented below.

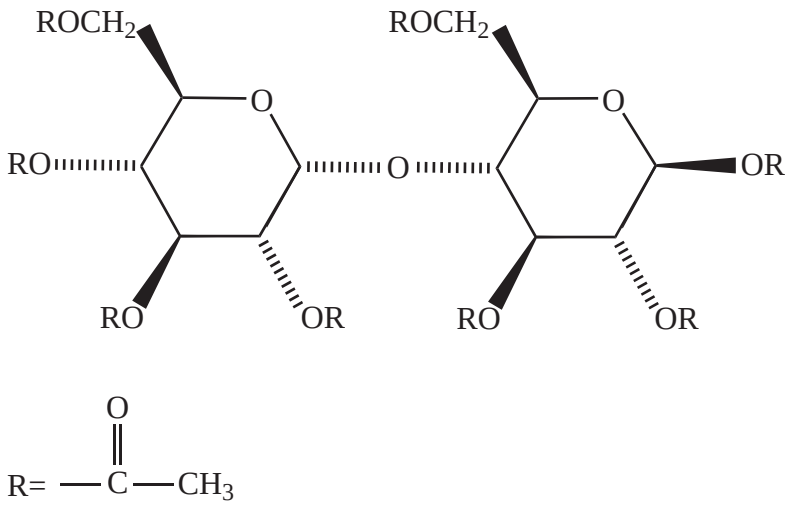

Figure 1

Structure of β-D-maltose octaacetate.

A specified amount of the sugar acetate (e.g., 2.0000 ± 0.0001 g) was introduced to the sample volume of a high pressure, windowed, stirred, variable-volume view cell (DB Robinson & Assoc., 3.18 cm ID, ~120 cm^3 working volume). In this cell, the sample volume is separated from the overburden fluid by a steel cylinder (floating piston) that retains an O-ring around its perimeter. The O-ring permits the cylinder to move while retaining a seal between the sample volume and the overburden fluid. After purging with carbon dioxide at 0.2 MPa, the sample volume was minimized by displacing the floating piston to the highest possible position within the cell that did not result in the compaction of the sugar acetate particles. High pressure liquid carbon dioxide (295 K, 13.78 MPa) was then introduced to the sample volume as the silicone oil overburden fluid was withdrawn at the equivalent flow rate using a dual-proportioning positive displacement pump (DB Robinson). This technique facilitated the isothermal, isobaric addition of a known volume of CO_2 (e.g., 20.44 ± 0.01 cm^3) into the sample volume. The mass of CO_2

introduced was determined from the displaced volume, temperature, and pressure using an accurate equation of state for carbon dioxide [19]. Based on uncertainties associated with measurement of temperature, pressure, volume and the precision of the equation of state, compositions were accurate to within 1% of the specified value (e.g. 10.00 ± 0.1wt %). The sugar acetate-CO_2 mixture was then compressed to 62 MPa. At these elevated pressure conditions, either a single, transparent liquid phase or solid-liquid equilibrium was observed. The sample volume was then slowly expanded, and observations of two-phase or three-phase equilibrium were recorded. Bubble points were characterized by the co-existence of a minute amount of vapor phase in equilibrium with the liquid phase. Dew points were designated as the pressure at which it was no longer possible to see through the solution. After maintaining the sample volume under quiescent conditions for 30 minutes, it was observed that several drops of liquid would slowly accumulate at the bottom of the sample volume. Three-phase pressures were characterized either by VLL or VLS equilibrium. Two- and three-phase boundaries were reproduced several times to within approximately ± 0.1 MPa, as measured with a Heise pressure gauge accurate to within ± 0.07 MPa for data to 70 MPa. Temperatures were measured with a type K thermocouple to an accuracy of ± 0.2 K.

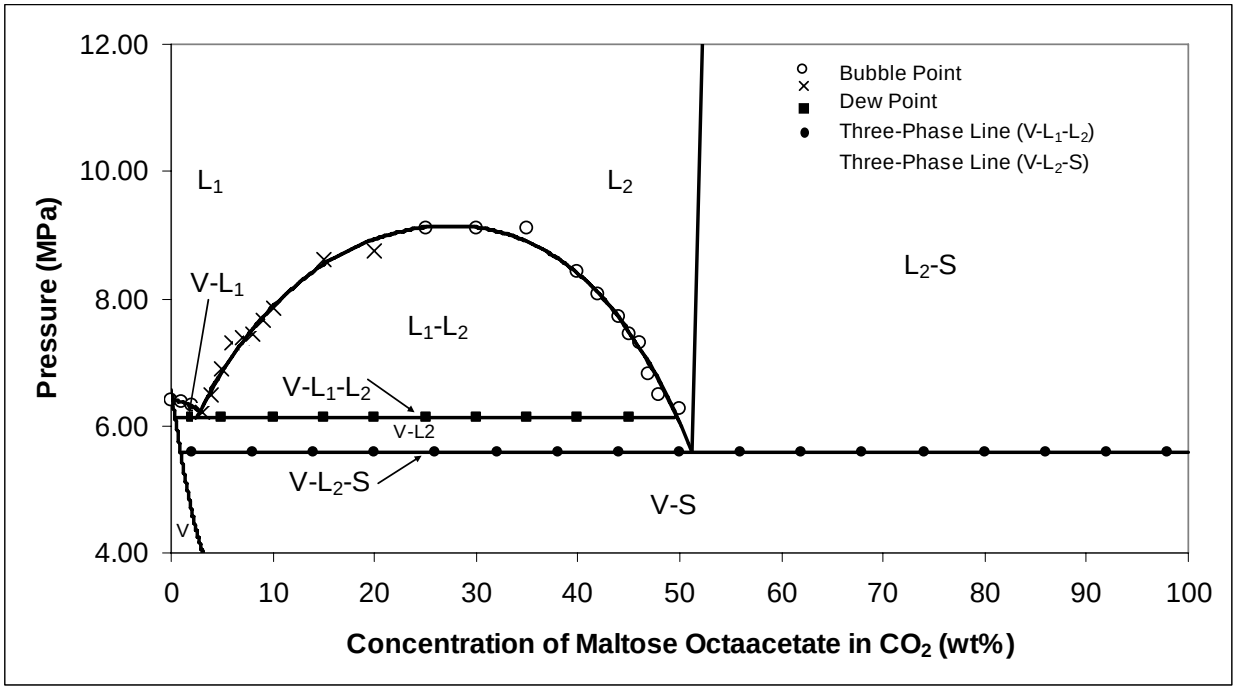

Figure 2

Pressure-composition diagram for the carbon dioxide (1) – maltose octaacetate (2) binary at 298 K

Results

Pressure – Composition Diagram

The pressure-composition diagram for CO_2-maltose octaacetate is illustrated in Figure 2. As discussed below, it is characterized by five two-phase regions and two three-phase pressures.

VL_1 Expansion of the CO_2-rich liquid, L_1, resulted in VL_1 equilibria. The small VL_1 region (approximately 3 wt % or less maltose octaacetate) is bounded by the CO_2 vapor

pressure, the VL_1 bubble-point locus, a VL_1 dew-point locus (but no dew-point data was measured for this region), and the three-phase VL_1L_2 line.

L_1L_2 Expansion of single-phase liquids that contained higher concentrations of maltose octaacetate (3-52 wt % maltose octaacetate) resulted in the occurrence of either a dew point (3-24 wt % maltose octaacetate) or a bubble point (25-52 wt % maltose octaacetate) of a L_1L_2 liquid-liquid region (L_1 is richer in CO_2 than L_2). The red color (associated with critical opalescence) and slow phase segregation of the liquid phases associated with the 25 wt % mixture bubble point indicated that this composition was close to the critical-point composition. The L_1L_2 region is bounded by the two-phase boundary and the VL_1L_2 line.

L_2S Solid-liquid (L_2) equilibrium was observed at maltose octaacetate concentrations greater than ~50 wt % and pressures above the three-phase VL_2S line because all of the maltose octaacetate could not be dissolved in the acetate-rich L_2 phase. Expansion of these two-phase mixtures resulted in the formation of CO_2-rich vapor bubbles at the VL_2S three-phase pressure. The L_2S region is bounded by a steep cloud-point curve (but no data was collected along this boundary), the neat maltose octaacetate boundary (conc. = 100%), and the VL_2S line.

VL_2 Isobaric expansion of the three-phase VL_1L_2 mixture resulted in the depletion of the CO_2-rich L_1 phase and the growth of the V and L_2 phases. Pressure decreased upon expansion when the L_1 phase was no longer present and the mixture entered the VL_2 two-

phase region. The pressure range of the VL_2 region was narrow, as further expansion led to the occurrence of the S phase. The VL_2 two-phase region is bounded by the VL_1L_2 and VL_2S three-phase loci, and the VL_2 bubble- and dew-point loci (however, no data were collected on these short two-phase boundaries).

VS Isobaric expansion of three phase VL_2S mixtures resulted in the reduction in the L_2 phase volume. The system pressure began to diminish only when the L_2 phase was gone, leaving the vapor and solid phases in equilibrium. The VS region is bounded by the VL_2S three-phase line, the neat solid boundary (conc. = 100%), the vapor pressure of solid octaacetate at 298 K, and the VS dew-point locus.

VL_1L_2 and VL_2S Three-Phase Lines The pressure-composition diagram of the CO_2-maltose octaacetate binary mixture exhibits both vapor-liquid-liquid and vapor-liquid-solid three-phase lines at 298 K. The pressure difference between these two three-phase lines is only 0.6 MPa, so isothermal expansions must be conducted slowly and carefully to attain two-phase VL_2 equilibria. Although Pxy diagrams with multiple three-phase pressures have been previously reported for binary mixtures containing carbon dioxide, these systems have not included vapor-liquid-liquid equilibria. For example, the CO_2-biphenyl system exhibits gas-liquid-solid and fluid-liquid-solid equilibria at temperatures greater than the minimum temperature of the SLV line and the upper critical end point [16, 20].

PT Projection

The features found in Figure 2 can be used to generate a PT projection of the global phase behavior for the CO_2-maltose octaacetate system over a broad temperature range. For example, Figure 2 contains (in order of decreasing pressure) a L_1L_2 critical point (the critical point would be located close to the 24 wt % bubble-point datum), the CO_2 vapor pressure, a VL_1L_2 three-phase pressure line, a VL_2S three-phase pressure line, and (at a very low pressure value not measured or shown in Figure 2) the maltose octaacetate SV sublimation point. Our proposed pressure-temperature projection for the CO_2-maltose octaacetate binary is illustrated in Figure 3 (The axes of this figure are not drawn to scale in order to make the figure more legible.). The pressure-composition data illustrated in Figure 2 correspond to the dashed-line isotherm at 298 K shown in Figure 3. Beginning at high pressures in the one-phase region, we follow the isotherm to lower pressures, intersecting in order the L_1L_2 critical-point locus, the CO_2 vapor pressure curve, the VL_1L_2 three-phase line, the VL_2S three-phase line, and the maltose octaacetate SV sublimation curve, corresponding to the data shown in Figure 2. Figure 3 also illustrates that the triple-point temperature of the maltose octaacetate, roughly 428 K (based on its melting-point range), is greater than the critical temperature of CO_2, 304.2 K. The lower critical end point (LCEP) temperature of 291 K was estimated by cooling 5% maltose octaacetate – 95% CO_2 and 2.5% maltose octaacetate – 97.5% CO_2 mixtures to sub-ambient temperatures until no evidence of a VL_1L_2 phase was observed. Further cooling to 253 K did not result in the re-occurrence of either L_1L_2 or V L_1L_2 equilibria.

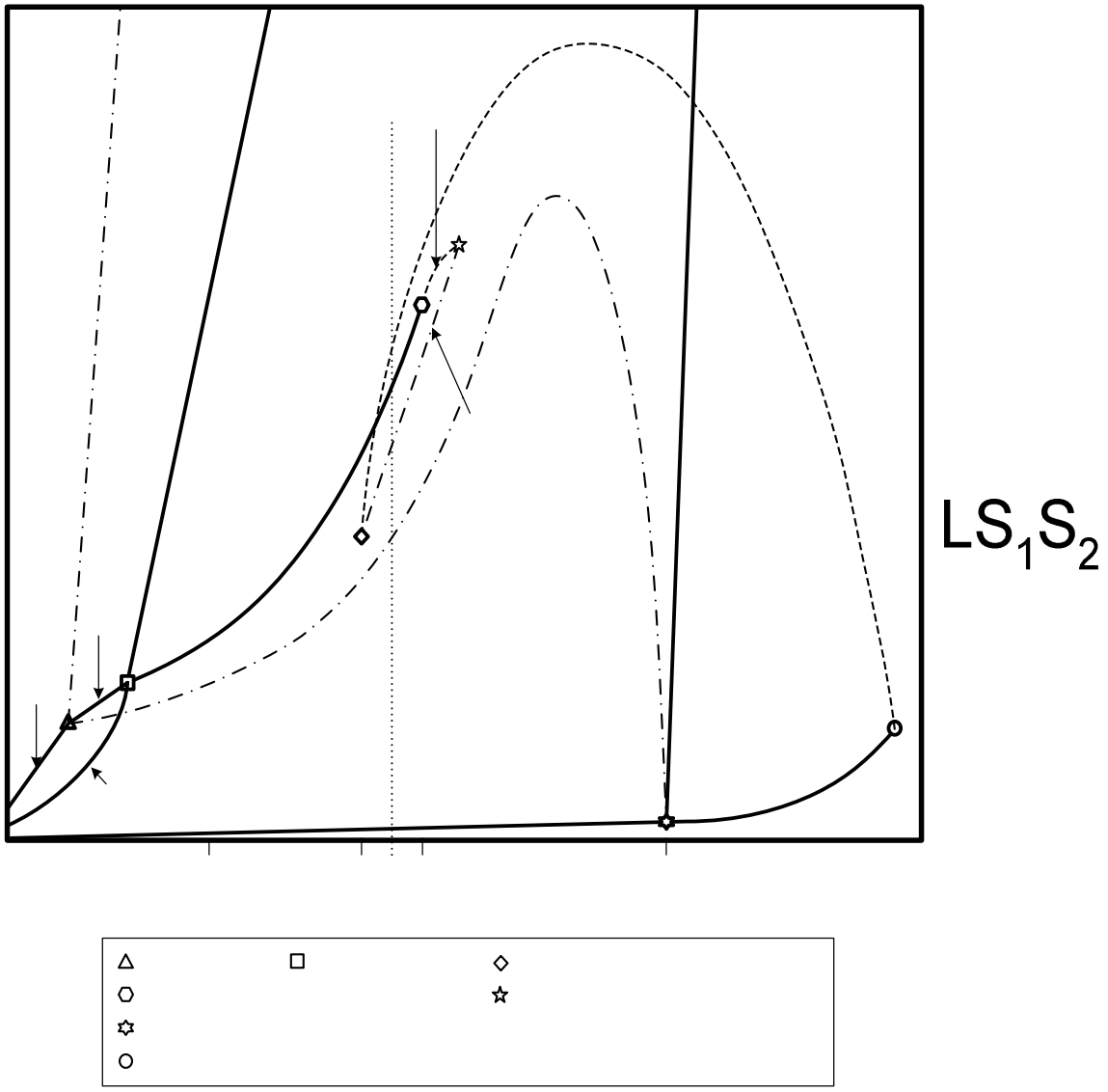

Figure 3

Proposed PT Projection for CO_2-Philic Solids that Melt in Dense CO_2

Continuing with Figure 3, the LL critical locus originates at the LCEP, transitioning to a fluid-liquid critical locus at temperatures above the critical temperature of CO_2 before terminating at the critical point of the maltose octaacetate. A short L_1V critical locus originates at the critical point of CO_2 and ends at an upper critical end point (UCEP)

P (MPa)

referred to as the K point. The VL_1L_2 three-phase line terminates at one end at the LCEP and at the other end at the K point. The VL_2S locus originates at low temperatures at a quadruple point (Q Point) of solid CO_2, solid maltose octaacetate, liquid, and vapor and ends at the triple point of the maltose octaacetate. Given the narrow pressure gap between the VL_1L_2 and VL_2S lines in Figure 2, it is likely that the VL_2S locus increases in pressure with temperature, remaining slightly below the VL_1L_2 line before rapidly decreasing in pressure with increasing temperature at a temperature greater than the K point and below the maltose octaacetate triple point [21].

Conclusions

The phase behavior that can exist between CO_2 and a CO_2-philic solid that melts in the presence of liquid CO_2 has been determined. At temperatures between the LCEP and the K point, the pressure-composition diagram is characterized by five two-phase regions and two three-phase lines. The pressure-temperature projection of the binary has the fluid-phase features of a Scott and Van Konynenburg Type III or V system, but also includes a VL_2S line that extends from the triple point of the CO_2-philic solid to a VLS_1S_2 quadruple point at very low temperatures. This type of phase behavior, which to our knowledge has heretofore not been previously reported, is likely to be observed for other highly CO_2-soluble solids that melt in liquid CO_2, including poly(vinyl acetate), poly(fluoroalkyl acrylate), and other sugar acetates. The high solubility of maltose octaacetate in CO_2 can be explained by the interaction between a Lewis base (carbonyl groups of maltose octaacetate) and Lewis acid (CO_2). This same mechanism was previously illustrated by Sarbu [7] and Raveendran [8].

References

[1] J.M. DeSimone, Z. Guan, C.S. Elsbernd, Science, 257 (1992) 945-947.

[2] J.B. McClain, D. E. Betts, D.A. Canelas, E.T. Samulski, J.M. DeSimone, J.D. Landona, G.D. Wignall, Proceedings of the 1996 Spring Meeting of the ACS, Division of Polymeric Materials: Science and Engineering, New Orleans, LA., 1996, Vol. 74, 234-235.

[3] R. Enick, E.J. Beckman, A. Yazdi, V. Krukonis, H. Schonemann, J. Howell, Journal of Supercritical Fluids, 13 (1998) 121-126.

[4] M. O'Neill, Q. Cao, M. Fang, K.P. Johnston, S. Wilkinson, C. Smith, J. Kerschner, S. Jureller, Ind. Eng. Chem. Res., 37 (1998) 3067-3079.

[5] Z. Bayraktar, E. Kiran, Journal of Applied Polymer Science, 75 (2000) 1397-1403.

[6] J. Eastoe, A. Paul, S. Nave, D. Steytler, B. Robinson, E. Rumsey, M. Thorpe, R. Heenan, JACS, 123 (2001) 988-989.

[7] T. Sarbu, T. Styranec, E. Beckman, Nature, 405 (2000) 165-168.

[8] P. Raveendran, S.L. Wallen, JACS Communications, 124 (2002) 7274-7275.

[9] V. Poltluri, J. Xu, R. Enick, E. Beckman, A. Hamilton, Organic Letters, 4 (2002) 2333-2335.

[10] V. Potluri, A.D. Hamilton, C.F. Karanikas, S.E. Bane, J. Xu, Fluid Phase Equilibria, (submitted for publication).

[11] F. Rindfleisch, T.P. DiNoia, M.A. McHugh, J. Phys. Chem., 100 (1996) 15581-15587.

[12] Z. Shen , M.A. McHugh, J. Xu, J. Belardi, S. Kilic, A. Mesiano, S. Bane, C. Karnikas, E. Beckman, R. Enick; Polymer, 44 (2003) 1491-1498.

[13] A. Blasig, C. Shi, R. Enick, M. Thies, I&ECR. 41 (2002) 4976 – 4983.

[14] P.H. Van Konynenberg, R.L. Scott, Philo. Trans. R. Soc. London, Ser. A, 298, 495-540, 1980.

[15] A. Van Pelt, C.J. Peters, J. de Swaan Arons, J. Chem. Phys. 95 (1991) 7569-7575.

[16] M.A. McHugh, V.J. Krukonis, Supercritical Fluid Extraction, Principles and Practice, 2nd Edition, Butterworth-Heinemann, Boston, 1994, pp. 45-71.

[17] C.F. Kirby, M.A. McHugh, Chem. Rev., 99 (1999) 565-602.

[18] J.S. Rowlinson, Liquids and Liquid Mixtures, 2nd edition, Butterworths, London, 1969, Chapter 6.

[19] R. Span, W. Wagner, J. Phys. Chem. Ref. Data, 25 (1996) 1509–1596.

[20] M.A. McHugh, An Experimental Investigation of the High Pressure Fluid Phase Equilibrium of Highly Asymmetric Binary Mixtures, Ph.D. Dissertation, University of Delaware, 1981.

[21] H.G. Donnelly, D.L. Katz, Ind. Eng. Chem. 46 (1954) 511.

Section 5. Use of Molecular Modeling to Design CO_2 Soluble Polymers

Supercritical carbon dioxide was used as a reaction media to synthesize statistically random copolymers of tetrafluoroethylene (TFE) and vinyl acetate (VAc) with similar molar mass and 7-to-63 mol% TFE content. The 19 mol% TFE copolymer exhibited the highest solubility in CO_2 whereas copolymers with 12-to-27 mol% TFE exhibited lower, but, similar levels of solubility in CO_2. Copolymers with up to 27 mol% TFE were more soluble in CO_2 than PVAc. However, the 47 mol% TFE copolymer only dissolved in CO_2 at elevated temperatures and it was less soluble than PVAc, whereas the 63 mol% TFE copolymer did not dissolve in CO_2 even at temperatures in excess of 144 °C and pressures of 210 MPa. The molecular modeling results show that the interaction of CO_2 with acetate side group was not affected by presence of fluorine in the polymer backbone, therefore the enhanced solubility of the semi-fluorinated copolymers is attributable to the enhanced binding between CO_2 and the semi-fluorinated backbone of the copolymer when the CO_2 molecule can access both the fluorinated (Lewis base) and hydrogenated (Lewis acid) parts of the backbone simultaneously.

Introduction

Poly(tetrafluoroethylene-co-vinyl acetate) (Poly(TFE-co-VAc)) is a fluoropolymer with potential applications in the coatings, optical and biomedical fields.[1-3] Poly(TFE-co-VAc) can be synthesized via free radical copolymerization of tetrafluoroethylene (TFE) and vinyl acetate (VAc) in dense carbon dioxide, with the composition of the TFE-VAc copolymer being controlled by the ratio of monomers in the feed.[4] Although a small concentration of fluorosurfactant was added to the monomers and CO_2 in an initial study

of this polymerization, subsequent trials without surfactant yielded copolymers of similar polydispersity and greater molar mass, implying that the surfactant is not necessary for solubility of the macroradical chains.[5] Based on reactivity ratios, Poly(TFE-co-VAc) is a random copolymer because TFE cross-propagates with VAc, and VAc propagates randomly. Hydrolysis of VAc to vinyl alcohol (VA) yields the predicted decrease in copolymer molar mass to form poly(TFE-co-VAc-co-VA), suggesting that the copolymer was linear [4,5]. This is in contrast to Poly(TFE-co-VAc) prepared by emulsion, where a precipitous drop in molar mass is observed upon hydrolysis due to ester groups in the backbone. The high yield and high molar mass of the TFE-VAc copolymers provided indirect evidence that poly(TFE-co-VAc) is CO_2 soluble at reaction conditions of 45 °C and 20-to-23 MPa and loadings of 20% w/v. Since the polymerization was conducted in a vessel that did not permit detection of the phase behavior, the actual CO_2-solubility of these polymers was not determined.

The phase behavior of the homopolymers of each monomer has been previously established. Poly(vinyl acetate), PVAc, is a non-crystalline, low T_g polymer that exhibits the greatest degree of CO_2-solubility associated with any high molecular weight oxygenated hydrocarbon homopolymer that has yet been identified, although it is far less CO_2-philic than fluoroacrylate or siloxane-based polymers.[6,7] This high degree of CO_2 solubility has been attributed to a weak complex that forms between CO_2 and the readily accessible acetate group.[6,7] PTFE is a crystalline polymer that is insoluble in CO_2 and organic solvents, although it does dissolve at high temperature in high molecular weight fluorocarbon solvents.[8] Poly(tetrafluoroethylene-co-19.3 mol% hexafluoropropylene) (FEP_{19}) is a nonpolar fluorocopolymer that has similar properties to PTFE, but FEP_{19} is highly branched and therefore has normal melting point at ~145°C whereas PTFE has a melting point in excess of 300°C. It has been demonstrated that FEP_{19} can dissolve in supercritical CO_2 at temperatures in excess of 185°C and pressures of approximately 100 MPa.[8-10] If the TFE segments in FEP_{19} are replaced with vinylidene fluoride (VF), this VF-HFP copolymer remains in solution to very low temperatures since the polar character of the VF group interacts with the quadrupole of CO_2.[11]

The experimental objective of this study is to determine if random copolymers of TFE and VAc are indeed CO_2-soluble at levels in excess of those exhibited by PVAc homopolymer containing a comparable number of repeat units. The precise reasons for the enhanced solubility of partially fluorinated polymers relative to their hydrocarbon analogues are not entirely understood. Therefore, molecular modeling is used to characterize the CO_2-polymer interactions in the CO_2-PVAc and CO_2-poly(TFE-co-VAc) systems. There have been a number of different efforts to model the thermodynamic properties of polymer-CO_2 mixtures. Generally speaking, these modeling techniques fall into three categories: equation of state modeling,[12-14] statistical mechanical simulations,[15] and ab initio calculations.[16-19] Equation of state methods have not proved to be accurate enough to predict the phase behavior of polymer-CO_2 mixtures.[13] In principle, one could compute virtually all the thermodynamic properties of polymer-CO_2 mixtures through statistical mechanical simulations. However, this requires very accurate molecular interaction models, which are currently not available, especially for the CO_2-polymer cross-interactions. Another alternative is to bypass the use of potential models and directly use ab initio methods to generate the forces required for a simulation, such as is done in Quantum MD,[20-22] but this is impractical for polymer-CO_2 mixtures due to the large system sizes and weak interactions among the molecules. Weak interactions (such as dispersion or van der Waals forces) are difficult to compute from ab initio methods because high-level methods and large basis sets are needed to capture electron dispersion. Computationally efficient methods, such as density functional theory, are known to be generally inadequate for computing van der Waals interactions.[23-27] The Møller-Plesset (MP) perturbation method for including electron correlation has been used for weakly interacting systems, but is known to have convergence problems.[28-30] MP2 (second order Møller-Plesset perturbation theory) is the lowest order MP theory and it is not generally adequate for computing intermolecular interaction energies, except when a substantial electrostatic interaction is involved.[31,32] Methods that include triple excitations, e.g., MP4(SDTQ), coupled cluster with perturbational triples, CCSD(T) are required for many applications.[28,29,33] However, recent work indicates that failure of MP2 may in part be due to basis set superposition error.[30,34] In this work we perform MP2 calculations to compute the interaction energies of CO_2 with various polymer fragments. Our aim is to determine

the role of fluorine atoms in the backbone of the polymer on enhancing the solubility of the fluorinated copolymers in CO_2. We expect the MP2 method to be adequate for our purposes because we are interested in relative interaction energies for CO_2 on fluorinated and non-fluorinated polymer moieties; relative energies are expected to be more accurate than absolute energies. Further, the presence of fluorine atoms on the polymer should increase the relative importance of electrostatic interactions, making the problem more appropriate for the MP2 method. Our previous calculations indicate that MP2 energies are fairly close to CCSD(T) energies for similar systems.[35]

Experimental Section

Reagents. All chemicals were purchased from Aldrich (Ontario, Canada) and used as received unless otherwise specified. TFE was prepared by vacuum pyrolysis of PTFE[36] and stored at room temperature over d-limonene in a 300 mL stainless steel sample cylinder fitted with an 12.4 MPa safety rupture disk. [Caution: Tetrafluoroethylene is inherently dangerous and anyone contemplating handling TFE under high pressure should be very familiar with safe handling procedure.] TFE-co-VAc copolymers were synthesized as previously described,[5] with the only difference being the compositions synthesized. As previously described, polymers were synthesized without a surfactant and by radical copolymerization in supercritical fluid CO_2 using diethyl peroxydicarbonate initiation.[37] Copolymers of TFE-VAc were synthesized with a TFE molar composition from 7 to 63.3 %.

Characterization. Polymer molar mass was characterized by a GPC (Water U6K Injector, 510 pump) equipped with a refractive index detector (Water 2410) and a series of Ultrastyragel column (Waters 10^6, 10^4, and 500 Å). Using an ethyl acetate or tetrahydrofuran (THF) mobile phase at a flow rate of 1 mL/min, polymer molar masses were calculated relative to polystyrene standards. ^1H and ^{19}F NMR spectra (Varian Gemini spectrometer) were obtained in $CDCl_3$ at 300.75 and 282.33 MHz, respectively.

Elemental analysis was conducted by Guelph Analytical Laboratory Service (Ontario, Canada). Glass transition temperatures (T_g) were measured using a differential scanning calorimeter (DSC, Q1000), under an inert nitrogen atmosphere, with a heating rate of 10 °C/min and a scanning range of -20 to 100 °C.

The phase behavior of mixtures of CO_2 with copolymers of low TFE concentration (11.6-26.5 mol%) was studied using a variable volume view cell. Known amounts of the solid poly(TFE-co-VAc), ± 0.001 g, were introduced to the sample volume of a high pressure, windowed, variable-volume view cell (DB Robinson & Assoc. 3.18 cm ID, ~100 cm^3 working volume). After the sample volume was purged with CO_2 at 0.2 MPa, the volume of the cell was minimized. High pressure liquid CO_2 (22 K, 13.78 MPa) was then introduced to the sample volume as the silicone oil overburden fluid was withdrawn at the equivalent flow rate using a dual-proportioning positive displacement pump (DB Robinson & Associates). This technique facilitated the isothermal, isobaric addition of a known volume of CO_2 to within ± 0.01 cm^3 into the sample volume. The mass of CO_2 was determined from the displaced volume, temperature and pressure using an equation of state for carbon dioxide.[38] The initial concentration of each copolymer was 20 wt%. The copolymer-CO_2 mixture was then compressed to 67 MPa and mixed with a magnetically driven impeller (DR Robinson). During the compression and mixing, the poly(TFE-co-VAc) solubility in CO_2 was followed. If two-phase solid-liquid equilibrium was observed, then additional CO_2 was introduced to the sample volume until the copolymer concentration decreased by approximately one weight percent. If a single, transparent phase was attained, the two-phase boundary was determined by slowly expanding the sample volume until a second phase appeared, as evidenced by the sample volume becoming opaque due to the formation of dispersed liquid copolymer droplets throughout the sample volume. The mixed phases were then allowed to separate until two transparent phases were observed. It was also determined whether the second phase was composed of solid particles or droplets of a copolymer-rich liquid phase. The appearance of a copolymer-rich liquid phase would be indicative of copolymer melting point depression in the presence of dense CO_2, a phenomenon associated with highly CO_2-soluble polymers and compounds.[39] The pressure at which the second phase appeared

was considered to be a dew point if a small copolymer-rich phase settled to the bottom of the cell. Two-phase pressures were reproduced three times at each overall concentration to within approximately ± 0.5 MPa using a Heise pressure gauge (accurate to within ± 0.07 MPa for data to 67 MPa) and at each temperature (held to within ± 0.5 °C, using a type K thermocouple).

Copolymers with higher proportions of TFE (46.7 mol%) were expected to be more difficult to dissolve in CO_2. Therefore the phase behavior of these CO_2-copolymer mixtures was determined with equipment rated to significantly higher pressures. The apparatus and techniques used to obtain polymer-fluid phase behavior data are described elsewhere.[10,40] The main component of the experimental apparatus is a high-pressure, variable-volume cell (Nitronic 50, 7.0 cm OD x 1.6 cm ID, ~30 cm^3 working volume). The cell is first loaded with a measured amount of copolymer to within ±0.002 grams. To remove entrapped air the cell is degassed very slowly at pressures less than 0.028 MPa with the CO_2. CO_2 is then transferred into the cell gravimetrically to within ±0.02 grams using a high-pressure bomb. The mixture in the cell is viewed with a borescope (Olympus Corporation, model F100-024-000-55) placed against a sapphire window secured at one end of the cell. A stir bar activated by a magnet located below the cell mixes the contents of the cell. The solution temperature is held to within ± 0.3 °C, as measured with a type K thermocouple. A fixed copolymer concentration of approximately 5 wt% is used for each constant-concentration, phase boundary curve. The mixture in the cell is compressed to a single phase and the pressure is then slowly decreased until a second phase appears. The transition is a cloud-point if the solution becomes so opaque that it is no longer possible to see the stir bar in solution. These cloud points have been compared in our laboratories to those obtained using a laser light set-up where the phase transition is the condition of 90% reduction in light transmitted through the solution. Both methods gave identical results within the reproducibility of the data. The cloud-point transitions at this concentration are expected to be close to the maximum in the pressure-composition isotherms.[41-43] The system pressure is measured with Heise pressure gauges accurate to within ± 0.07 MPa for data to 69 MPa and to within ± 0.35

MPa for data from 69 to 276 MPa. Cloud points are reproduced two to three times to within approximately ± 0.42 MPa.

Molecular Modeling Theory

It is not possible to explicitly perform ab initio calculations on a polymer because of the large number of atoms. We therefore break the copolymer into small model segments. We then compute optimized geometries and binding energies for CO_2 interacting with these model segments. We performed geometry optimizations at the MP2/6-31+g(d) level of theory for a number of different polymer segment/CO_2 dimers. This relatively small basis set was used to make the optimizations feasible on the available computing resources. The optimized configurations were then used to calculate the more accurate single point binding energies at larger basis set, aug-cc-pVDZ, with standard counterpoise (CP) corrections[44] for the basis set superposition error (BSSE). The binding energy was computed from the supermolecule approach,

$$E_b = E(12) - E(1) - E(2) \quad (0.1)$$

where E_b is the binding energy, $E(12)$ is the total energy of the dimer (CO_2+polymer segment) and $E(i)$ is the energy of the isolated CO_2 or polymer segment molecule. Binding energies defined in this way are negative for energetically favorable dimers. We use the average of the raw and CP corrected interaction energies as an approximation to the complete basis set limit interaction energies. We do this to avoid the computationally expensive complete basis set extrapolation. This method has been tested by us previously[35] for similar systems and found to be in good agreement with the results of Feller and Jordan.[45] All binding energies reported in this paper are averages of the MP2/aug-cc-pVDZ corrected and uncorrected interaction energies. We have computed localized charge distributions for several of the model polymer segments using the NBO method. All calculations were performed with the Gaussian 98 package, revision A11.[46]

Experimental Results

A series of TFE-co-VAc copolymers was synthesized in supercritical CO_2 and characterized for yield, bulk composition, molar mass, and T_g, the results of which are summarized in Table 1. As shown, a series of copolymer compositions was prepared where monomer feed composition influenced polymer composition, from 11.6-to-63.3 mol% TFE. The yield (based on mass) was high for all compositions, between 78 and 86%. The T_g was similar for all samples, between 36°C and 38°C, which is similar to that of PVAc (38 °C). Since we were interested in comparing solubility in CO_2 as a function of composition, the samples were synthesized in such a manner to yield similar molecular weight characteristics, with M_w between 140 and 180 kg/mol and index of polydispersity (PDI) between 2.7 and 3.1. For 63.3 mol% TFE copolymer, however, M_w was higher and PDI lower than the other samples. It is important to note that this sample was measured by GPC in ethyl acetate whereas the other polymers were measured in THF. Ethyl acetate may have affected the hydrodynamic radius of the copolymer differently from THF, thereby accounting for the greater M_w and smaller PDI.

The phase behavior of poly(TFE-co-VAc) – CO_2 mixtures was strongly influenced by the copolymer composition. (The copolymer will hereafter be designated as TFE-co-VAc, with the value of the TFE subscript corresponding to the mol fraction of that monomer.) The three copolymers with the smallest proportion of TFE, $TFE_{11.6}$-co-VAc, $TFE_{19.3}$-co-VAc and $TFE_{26.5}$-co-VAc, melt-flowed in CO_2 when heated above their T_g's, as did the PVAc homopolymer (these are amorphous polymers). Like PVAc, these copolymers dissolved in the presence of liquid CO_2, and the general nature of the corresponding pressure-composition (P-x) diagram for such systems is illustrated in Figure 1.[39] The small box within Figure 1 illustrates the region where the CO_2-rich liquid – polymer-rich liquid data were measured. The results, shown in Figure 2, indicate that these three TFE-VAc copolymers with are more CO_2-soluble than PVAc as evidenced by the cloud-point curves of these copolymers being comparable to one another and 10 MPa lower than the PVAc cloud-point curve. Further, a single phase could not be achieved at a

PVAc concentration of 7 wt% at the pressure limit of 67 MPa. The greatest concentrations of the (TFE-co-VAc) polymers that could be attained in liquid CO_2 at the same pressure limit of 67 MPa were 7.5 wt%, 10 wt% and 8 wt% for the TFE11.6-co-VAc, TFE19.3-co-VAc and $TFE_{26.5}$-co-VAc polymers, respectively. These results indicate that $TFE_{19.3}$-co-VAc is close to the optimal composition for CO_2-solubility. These results also suggest that copolymers with a small proportion of TFE are unlikely to form large TFE blocks. The relatively low TFE content and copolymerization technique make it probable that lengthy block segments of TFE is low in these copolymers, and hence the propensity to crystallize and form CO_2-insoluble polymers is low.

The copolymers with higher concentrations of TFE, $TFE_{46.7}$-co-VAc and $TFE_{63.3}$-VAc, were markedly less CO_2-soluble. $TFE_{46.7}$-co-VAc was insoluble in CO_2 at temperatures below 75 °C, which is notably less CO_2 soluble than the three copolymers with lower TFE concentrations; however, the copolymer did dissolve at elevated temperature. At a copolymer concentration of 5 wt% in CO_2 -a representative mixture composition that typically yields a cloud point pressure at or near the maximum cloud point pressure of this portion of the phase diagram, as shown in Figure 3 - cloud point pressures were observed at higher temperatures. The cloud point pressure is 74 MPa at 75 °C and 91 MPa at 128 °C. $TFE_{63.3}$-co-VAc does not dissolve in CO_2 even at 144 °C and 210 MPa, however. This may be due in part to the increased crystallinity of the copolymer associated with TFE-rich regions or blocks.

Molecular Modeling Results

We have employed ab initio molecular modeling to identify reasons for the enhanced solubility of TFE-co-VAc relative to the PVAc homopolymer. Figure 4b illustrates that the fluorinated carbons in the copolymer backbone will be adjacent to either a methylene carbon or a methyne carbon from which the pendant -$OCOCH_3$ group extends. We take one representative portion of TFE-co-VAc with a relatively small concentration of TFE shown in Figure 4c and divide it into three small molecules, shown in Figure 4d, which are conducive to molecular modeling calculations. Firstly, we cut the molecule between

the two CF_2 functional groups, yielding two fluorous molecules, 3,3,3 tri-fluoro isopropyl acetate (TFIPA), and 4,4,4 tri-fluoro-sec-butyl acetate (TFSBA). The third small molecule is 2,2,3,3-tetrafluorobutane (FB), which is a model for the backbone of the polymer. The hydrocarbon analogs of these small molecules, shown in Figure 4e, are isopropyl acetate (IPA), sec-butyl acetate (SBA) and n-butane. These molecules are used for direct comparisons with the semi-fluorinated compounds.

We have identified four possible binding configurations for CO_2 interacting with TFIPA and TFSBA. We use the TFIPA molecule as an example to illustrate the possible binding configurations because TFSBA has similar CO_2 binding configurations. The specific binding configurations are illustrated in Figure 5 as: (A) ether oxygen, (B) carbonyl oxygen, tilted towards the methyl group, (C) carbonyl oxygen, tilted towards the ether group, and (D) backbone fluorine atoms. Geometry optimizations were started by placing the CO_2 molecule at various positions around the TFIPA and TFSBA molecules. From five to eight different starting geometries were used for each of the polymer fragments. The hydrocarbon analogues, IPA and SBA, were studied in the same way.

TFIPA/CO_2 and IPA/CO_2

Binding configuration (A) has an interaction energy of -15.9 kJ/mol. The optimized geometry for binding configuration (A) is shown in Figure 6. The dashed lines indicate interaction points between the two molecules. The atom-atom distances are also shown. The carbon atom of the CO_2 molecule binds both with the fluorine atom and the ether oxygen atom on TFIPA in this configuration. Each oxygen on CO_2 interacts with a hydrogen in what can be termed a weakly hydrogen bonding configuration.[18] We identify configuration (A) as quadradentate binding because the CO_2 molecule has four interaction points with the polymer moiety. In configurations (B) and (C), the CO_2 molecule mainly interacts with the carbonyl oxygen atom of the TFIPA. This gives interaction energies that are quite similar to those between IPA and CO_2. Figure 7 shows the interactions for configuration (D). This is also a quadradentate binding configuration. The carbon of the CO_2 interacts with two fluorine atoms while one oxygen of the CO_2 interacts with two hydrogens.

The binding energies for the four TFIPA/CO_2 binding configurations are listed in Table 2, along with the interaction energies for CO_2 with the hydrocarbon analogue, IPA. There is a difference of about 1.3 kJ/mol between the binding energies of TFIPA/CO_2 and IPA/CO_2 for configurations (A), (B) and (C). This energy value is within the uncertainty of the ab initio calculations. The uncertainty is due to lack of convergence in the theoretical method (MP2) and the choice of basis set. We conclude that the fluorine atoms on the polymer backbone do not substantially affect (positively or negatively) the binding energies of CO_2 with the acetate side chain.

We have not been able to find a configuration (D) for the IPA/CO_2 system, even though we started from several different initial configurations. In every case, the CO_2 molecule always migrates around the molecule to bind with the carbonyl or ether oxygen of the IPA molecule. This implies that there is no minimum corresponding to binding configuration (D) for the IPA/CO_2 system. However, the (D) geometry of TFIPA/CO_2 system shows a considerable binding energy of -9.6 kJ/mol. This additional binding site for the TFIAP/CO_2 system is probably one of the main reasons for the increase in solubility of the TFE-co-VAc molecule in CO_2.

TFSBA/CO_2 and SBA/CO_2

The TFSBA/CO_2 system was investigated using similar binding configurations to (A), (B), (C) and (D) of the TFIPA/CO_2 system. The SBA/CO_2 system was used for comparison. Table 3 lists the calculated binding energies for these systems. The calculations for TFIPA/CO_2 and IPA/CO_2 indicate that the binding energies for configurations (B) and (C) should be similar for the fluorinated and non-fluorinated segments. We therefore did not calculate binding energies for configurations (B) and (C) for the SBA/CO_2 system. We use the values of the binding energies for configurations (B) and (C) from the IPA/CO_2 system as an estimate for the binding energies for SBA/CO_2 for the same configurations. The binding energy of configuration (A) for TFSBA/CO_2 is -18.8 kJ/mol, which is much larger than the binding energies for any site

of any of the other systems. We have examined the NBO charge distributions of TFSBA and other molecules in order to determine the origin of the enhanced binding for configuration (A) of TFSBA/CO_2. The local charges on atoms of TFSBA are shown in Figure 8. Note that the charge on hydrogens H(1) and H(2) is about 0.26. This is significantly larger than on hydrogens in the same positions on SBA or on hydrocarbons, which is about 0.23. Thus, hydrogens H(1) and H(2) are more acidic than typical hydrocarbon hydrogens. This is due to the fact that they are on the carbon that is beta to the highly electronegative fluorines. Configuration (A) on TFSBA/CO_2 is a quadradentate binding site, with one CO_2 oxygen interacting with H(1). The acidic hydrogen acts as a better Lewis acid for the CO_2 oxygen Lewis base. This, we believe, is the reason for the enhanced binding of configuration (A) for TFSBA/CO_2.

The charges on the two oxygen atoms of TFSBA are very similar to those of SBA. This is why the binding energies of configurations (B) and (C) are very similar for all the system studied. Configuration (D) for the TFSBA/CO_2 system has a binding energy of -11.7 kJ/mol. This is larger than that for the same configuration on TFIPA/CO_2. We believe that the increase in binding energy is again due to the increased acidity of the hydrogens on the backbone. Note that our calculations could not locate a minimum for configuration (D) for SBA/CO_2, as was the case for IPA/CO_2.

FB/CO_2 and Butane/CO_2

In order to further investigate the interactions between the CO_2 molecule and the backbones of the polymers, FB and butane are used as models of the fluorinated and non-fluorinated backbones, respectively. Starting from several initial configurations, we identified a single geometry with the strongest interaction for each of the systems. Figure 9 shows the optimized binding geometries for the systems. The binding energies for butane/CO_2 and FB/CO_2 are -8.4 and -12.1 kJ/mol, respectively. The FB/CO_2 binding energy is 3.7 kJ/mol larger in magnitude than that for butane/CO_2. The FB/CO_2 binding energy is close to the configuration (D) binding energies for TFIPA/CO_2 and TFSBA/CO_2. This indicates that the backbone of the semi-fluorinated polymers act as effective simultaneous Lewis acids (H-O) and Lewis bases (F-C) toward CO_2. These

interactions are likely to significantly enhance the solubility of the polymer compared with non-fluorinated analogues. Note also that the acidic hydrogens are only available on semi-fluorinated backbones. This corroborates the experimental observation that high fractions of TFE in the co-polymer reduce the solubility.

Discussion

A CO_2 molecule can act simultaneously as both a Lewis acid and as a Lewis base if the molecule with which it is interacting has both Lewis base and acid groups. Our molecular modeling results show that this is precisely the case for semi-fluorinated polymers such as TFE-VAc. Perfluorinated polymers lack Lewis acid sites and also exhibit very high melting points. Furthermore, O-F interactions are only weakly attractive since both the oxygens in CO_2 and the fluorine in the polymer are electron-rich.[16]. This is one of the major reasons that partially fluorinated polymers are more CO_2-philic than perfluorinated ones. Raveendran et al. have also observed enhanced binding of CO_2 with partially fluorinated molecules. They performed ab initio calculations on CO_2-CF_nH_{4-n} for n=0 to 4. They concluded that there may be an optimal density of fluorine atoms in a molecule leading to maximum CO_2-phicility.[19] They attribute this optimal density to the competition among the individual electronegative fluorine atoms. In other words, fluorine atoms in highly fluorinated molecules are less effective electron donors. We believe this effect to be of minor importance compared with the requirement for a molecule to have both Lewis acid and base sites present in the correct geometry to interact simultaneously with CO_2. This is difficult to achieve in a small molecule like CF_nH_{4-n}.

Another important consideration is that fluorination of methane makes the hydrogen atoms become less acidic compared with hydrogen atoms in methane.[19] This is not the case for larger molecules. The hydrogen atoms on the carbon β to the fluorine atom are more acidic than the hydrogens on n-butane. NBO charges for hydrogens on FB and butane are about 0.26 and 0.23, respectively. The enhancement of H-atom acidity relative to the hydrocarbon cannot be observed by studying semi-fluorinated methane.

Binding of CO_2 to carbonyl functional groups is virtually unaffected by the fluorination, as shown in Table 2. In contrast, Raveendran et al. noted that fluorination decreases the carbonyl CO_2-phicility of partially fluorinated acetaldehyde.[17] Separation of the fluorine atoms from the carbonyl group by more than one carbon atom mitigates the effect of the fluorine on carbonyl-CO_2 binding, however. Note that the charges on the ether and carbonyl oxygens in both TFSBA and SBA are almost identical, as shown in Figure 8.

Summary

High molecular weight poly(TFE-co-VAc) with TFE content ranging between 11.6-26.5 mol% required lower pressure for dissolution in CO_2 at 25 °C and at low concentrations (<6 wt%) than PVAc homopolymer. Further, these poly(TFE-co-VAc) copolymers were soluble to higher concentrations in CO_2 (7.4-10 wt%) than PVAc (6 wt%). The copolymer composed of 46.7 mol% TFE was not soluble in CO_2 at 25 °C, but was CO_2-soluble at temperatures greater than 75 °C. The copolymer with 63.3 mol% TFE was insoluble in CO_2 at all conditions, possibly due to the presence of TFE blocks, which may be crystalline and thereby reduce solubility. Introduction of hexafluoropropylene units may disrupt this apparent crystallinity while maintaining the fluorocarbon content and enhancing CO_2-solubility.

Ab initio calculations have revealed the following reasons for the increased solubility of poly(TFE-co-VAc) relative to PVAc. (1) The specific geometry and functionality of the polymer gives rise to "quadradentate" binding of CO_2 to the polymer, having an interaction energy about 2.5 kJ/mol more favorable than the nonfluorinated analogue. (2) The interaction of CO_2 with the partially fluorinated backbone is 3.7 kJ/mol more favorable than with the hydrocarbon analogue. (3) The electron withdrawing effects of the F atoms on the backbone renders nearby H atoms slightly more acidic, promoting stronger hydrogen bonding with the O atoms in CO_2. Finally, we note that CO_2 acts simultaneously as both a Lewis acid and a Lewis base for many of the binding geometries identified through molecular modeling.

ACKNOWLEDGMENT

We are grateful to the following agencies for partial support of this research: Natural Sciences and Engineering Research Council of Canada (MSS); National Science Foundation (RE) and DOE National Energy Technology Laboratory and National Petroleum Technology Office (RE). Polymer syntheses were performed at the University of Toronto, extremely high pressure phase behavior measurements were taken at VCU, and computations were performed at the University of Pittsburgh Center for Molecular and Materials Simulations.

Supporting Information Available:

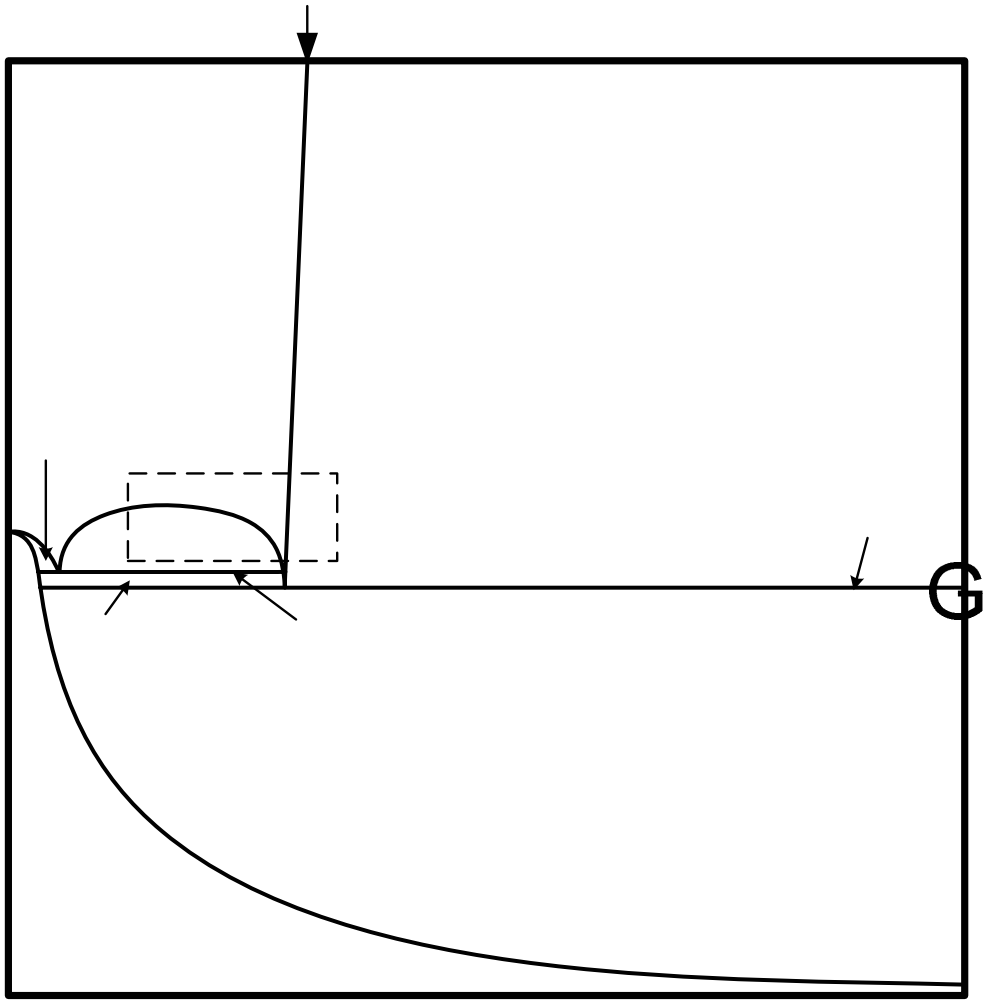

Figure 1.

L

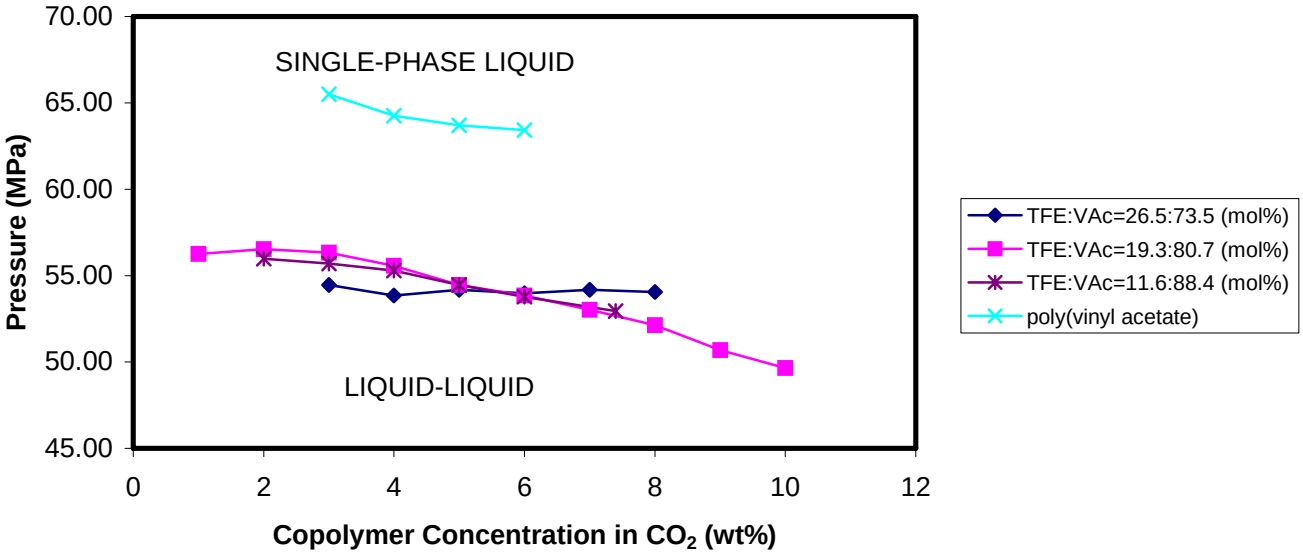
70.00
65.00
60.00
55.00
50.00
45.00
Pressure (MPa)
SINGLE-PHASE LIQUID
LIQUID-LIQUID
0
2
4
6
8
10
12
Copolymer Concentration in CO2 (wt%)
TFE:VAc=26.5:73.5 (mol%)
TFE:VAc=19.3:80.7 (mol%)
TFE:VAc=11.6:88.4 (mol%)
poly(vinyl acetate)

Figure 2

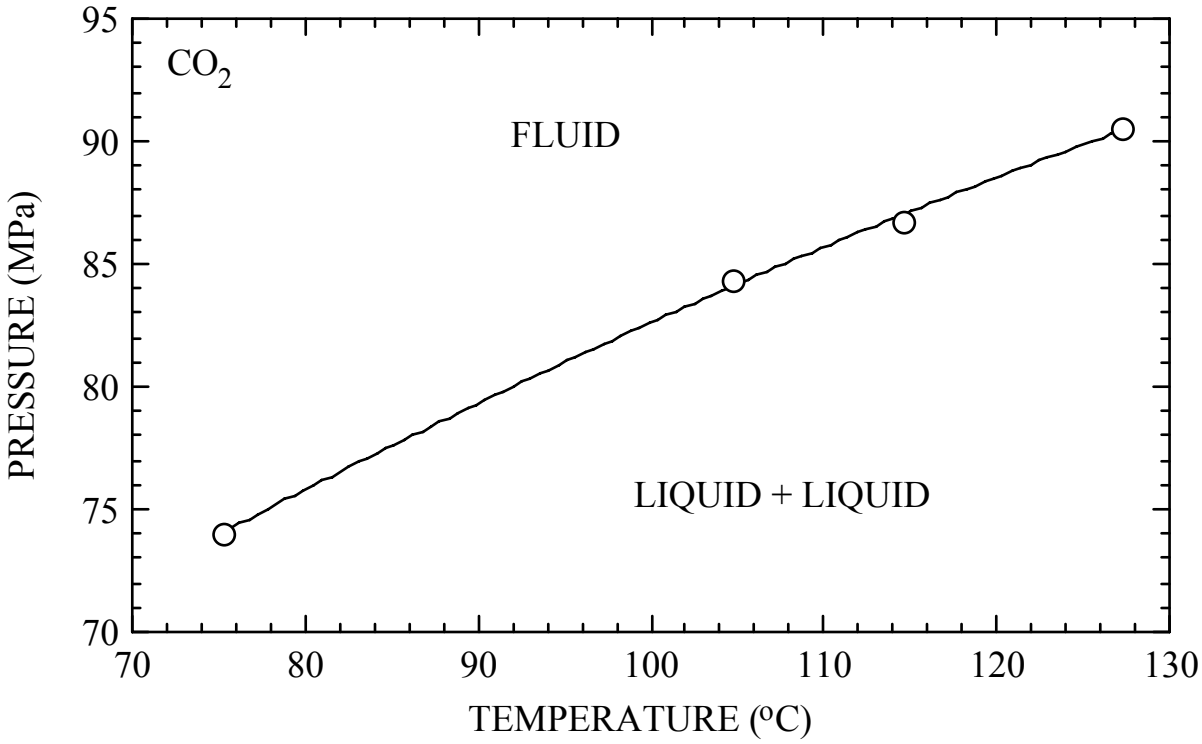
95
90
85
80
75
70
CO_2
FLUID
LIQUID + LIQUID
PRESSURE (MPa)
70
80
90
100
110
120
130
TEMPERATURE (ºC)

Figure 3.

a.

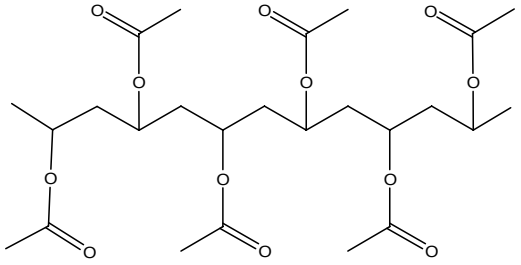

b.

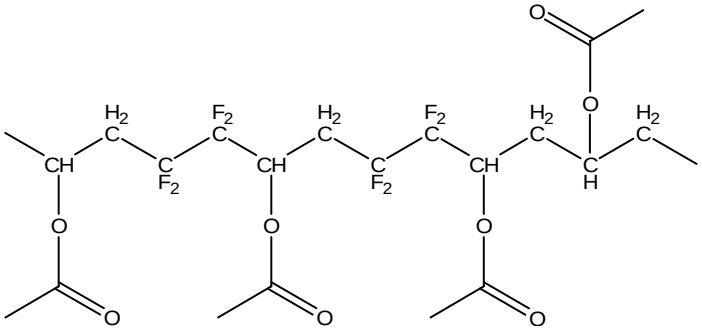

c.

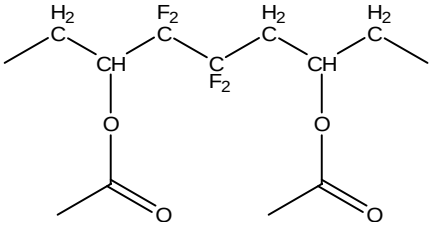

d.

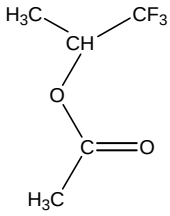

(TFIPA)

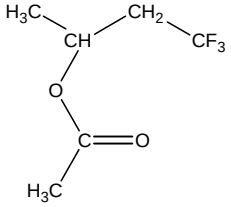

(TFSBA)

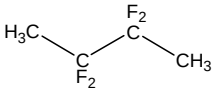

(FB)

e.

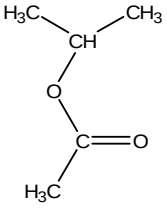

(IPA)

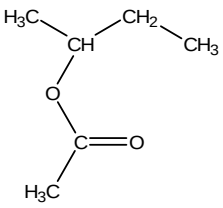

(SBA)

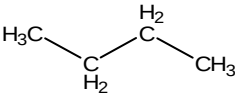

(butane)

Figure 4.

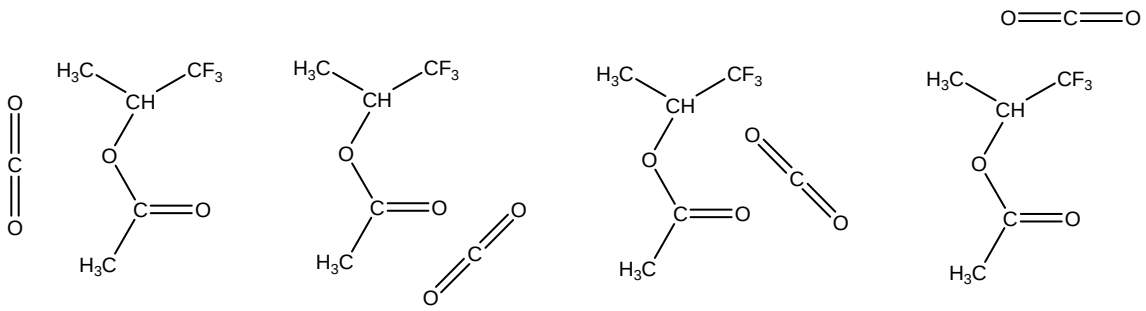

(A) (B) (C) (D)

Figure 5.

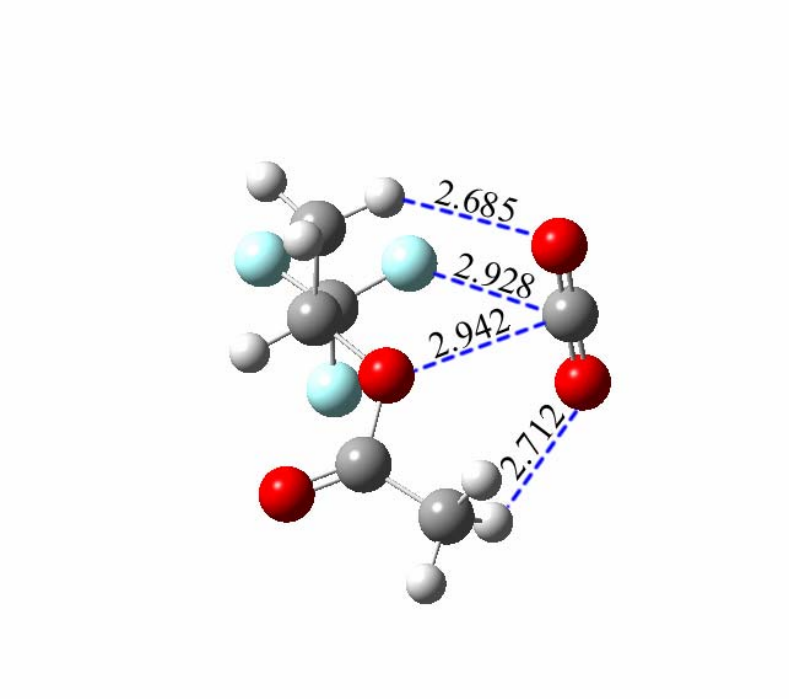

Figure 6.

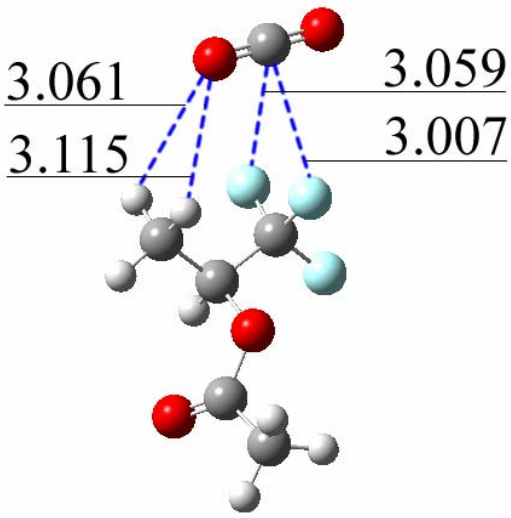

Figure 7.

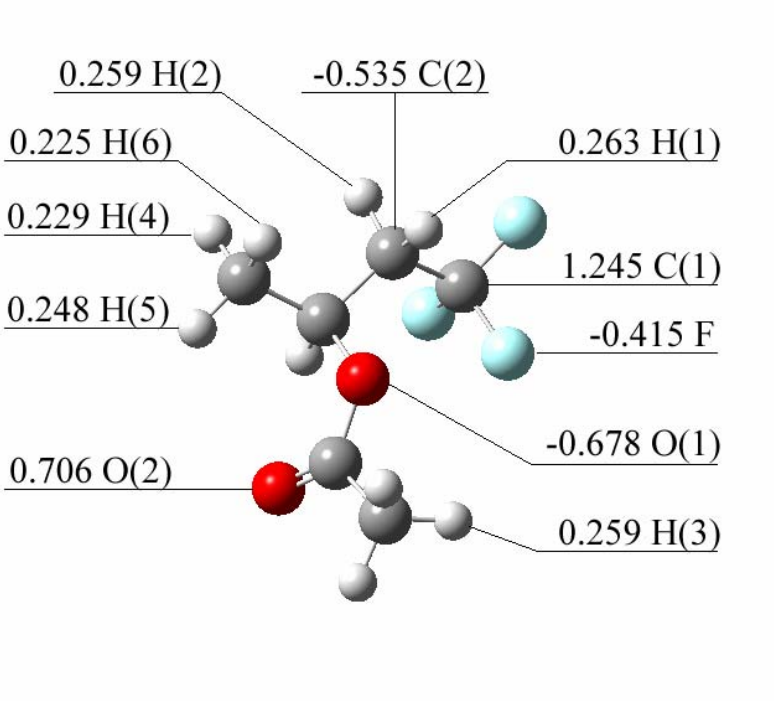
0.259 H(2)
-0.535 C(2)
0.225 H(6)
0.263 H(1)
0.229 H(4)
1.245 C(1)
0.248 H(5)
-0.415 F
-0.678 O(1)
0.706 O(2)
0.259 H(3)

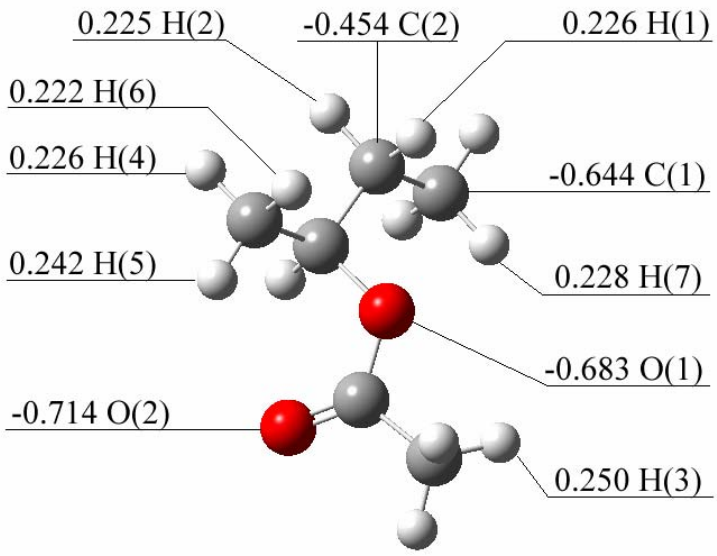
0.225 H(2)
-0.454 C(2)
0.226 H(1)
0.222 H(6)
0.226 H(4)
-0.644 C(1)
0.242 H(5)
0.228 H(7)
-0.683 O(1)
-0.714 O(2)
0.250 H(3)

Figure 8.

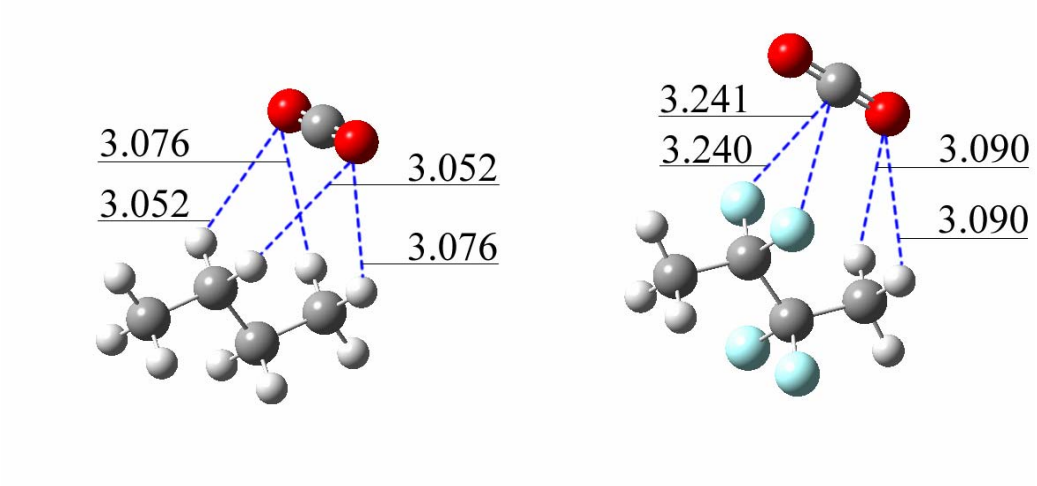

(A) butane/CO_2 (B) FB/CO_2

Figure 9.

FIGURE CAPTIONS:

Figure 1. General pressure-composition (P-x) phase diagram for CO_2 and solid CO_2-philic compounds or polymers.

Figure 2. Pressure-composition phase diagram for CO_2 + TFE-VAc copolymer system at 25 °C.

Figure 3. Cloud-point curve for ~5 wt% CO_2 + $TFE_{46.7}$ -co-VAc system.

Figure 4. (a) PVAc; (b) a portion of poly(TFE-co-VAc) that lacks TFE block segments; (c) a representative segment that of this copolymer; (d)the three small molecules used in molecular modeling that capture the features of the copolymer, tri-fluoro isopropyl acetate, tri-fluoro sec-butyl acetate, tetrafluoro-butane; (e) the hydrocarbon analogs of the small fluorous molecules isopropyl acetate, sec-butyl acetate, n-butane.

Figure 5. Four distinct binding configurations for TFIPA and a single CO_2 molecule. (A) Binding with the ether oxygen. (B) Binding with the carbonyl oxygen, tilting towards the methyl group. (C) Binding with the carbonyl oxygen, tilting towards the ether group side. (D) Binding with the fluorine atoms in the backbone.

Figure 6. Binding interactions of TFIPA/CO_2 for configuration (A). The distances are in Ångstroms.

Figure 7. Binding interactions of TFIPA/CO_2 for configuration (D). Distances are in Ångstroms.

Figure 8. Charge distribution on the TFSBA (top) and SBA (bottom) molecules.

Figure 9. Optimized binding geometries for the n-butane/CO_2 and FB/CO_2 systems. Distances are in Ångstroms.

TABLES.
Table 1. Bulk Analysis of TFE-VAc copolymers

TFE in feed (mol%)	Yield (wt%)	Elemental analysis[b]	Tg (°C)	Mw/Mn/PDI Kg ·mol^{-1}
17.6	80	11.6	37.2	140/42/3.2
23.6	80	19.3	36.8	156/49/3.1
35.6	86	26.5	36	166/61/2.7
53.7	78	46.7	37	180/55/3.1
67.7	79	63.3	37	290/157/1.84[c]

[b] Determined from %C analysis. [c] measured using ethyl acetate as mobile phase. Entries 1-4 THF is used as mobile phase for the measurement of molar masses.

Table 2. binding energies for TFIPA/CO_2 and IPA/CO_2 at each of the four binding configurations of Figure 3. Geometries optimized at the MP2/6-31+g(d) level of theory with binding energies computed at MP2/ aug-cc-pVDZ.

Binding energies / **Binding configurations**	**TFIPA/CO_2 (kJ/mol)**	**IPA/CO_2 (kJ/mol)**
(A)	-15.9	-14.7
(B)	-13.0	-14.2
(C)	-15.9	-15.9
(D)	-9.6	No minimum

Table 3. binding energies for TFSBA/CO_2 and SBA/CO_2 at each of the four binding configurations of Figure 3. Geometries optimized at the MP2/6-31+g(d) level of theory with binding energies computed at MP2/ aug-cc-pVDZ.

Binding energies / **Binding configurations**	**TFSBA/CO_2 (kJ/mol)**	**SBA/CO_2 (kJ/mol)**
(A)	-18.8	-16.3
(B)	-13.8	-14.2[a]
(C)	-15.5	-15.9[a]
(D)	-11.7	No minimum

[a]Estimated from IPA/CO_2 calculations.

REFERENCES

(1) Jones, C. W. *Unitied States Patent*, 5,723,556. 1998.

(2) Feiring, A. E.; Wonchoba, E. R. *Macromolecules* **1998**, *31*, 7103-7104.

(3) Kogel, H. C.; Vollmar, J. F. *Prosthetic Substitution of Blood Vessels*; Quintessenz: Munich, 1991.

(4) Lousenberg, R. D.; Shoichet, M. S. *Macromolecules* **2000**, *33*, 1682-1685.

(5) Baradie, B.; Shoichet, M. S. *Macromolecules* **2002**, *35*, 3569-3575.

(6) Rindfleisch, F.; DiNoia, T. P.; McHugh, M. A. *J. Phys. Chem.* **1996**, *100*, 15581-15587.

(7) Shen, Z.; McHugh, M. A.; Xu, J.; Belardi, J.; Kilic, S.; Mesiano, A.; Bane, S.; Karnikas, C.; Beckman, E. J.; Enick, R. M. *Polymer* **2003**, *44*, 1491-1498.

(8) Tuminello, W. H.; Brill, D. J.; Walsh, D. J.; Paulaitis, M. E. *Journal of Applied Polymer Science* **1995**, *56*, 495-499.

(9) Kirby, C. F.; McHugh, M. A. *Chemical Reviews* **1999**, *99*, 565-602.

(10) Mertdogan, C. A.; Byun, H. S.; McHugh, M. A.; Tuminello, W. H. *Macromolecules* **1996**, *29*, 6548-6555.

(11) Mertdogan, C. A.; DiNoia, T. P.; McHugh, M. A. *Macromolecules* **1997**, *30*, 7511-7515.

(12) Luna-Barcenas, G.; Mawson, S.; Takishima, S.; DeSimone, J. M.; Sanchez, I. C.; Johnston, K. P. *Fluid Phase Equilibria* **1998**, *146*, 325-337.

(13) Lora, M.; Rindfleisch, F.; McHugh, M. A. *Journal of Applied Polymer Science* **1999**, *73*, 1979-1991.

(14) Lora, M.; McHugh, M. A. *Fluid Phase Equilibria* **1999**, *157*, 285-297.

(15) Cui, S. T.; Cochran, H. D.; Cummings, P. T. *Journal of Physical Chemistry B* **1999**, *103*, 4485-4491.

(16) Diep, P.; Jordan, K. D.; Johnson, J. K.; Beekman, E. J. *Journal of Physical Chemistry A* **1998**, *102*, 2231-2236.

(17) Raveendran, P.; Wallen, S. L. *J. Am. Chem. Soc. Communications* **2002**, *124*, 7274-7275.

(18) Raveendran, P.; Wallen, S. L. *J. Am. Chem. Soc.* **2002**, *124*, 12590-12599.

(19) Raveendran, P.; Wallen, S. L. *Journal of Physical Chemistry B* **2003**, *107*, 1473-1477.

(20) Gross, A.; Scheffler, M. *Physical Review B* **1998**, *57*, 2493-2506.

(21) Remler, D. K.; Madden, P. A. *Moleular Physics* **1990**, *70*, 921-966.

(22) Car, R.; Parrinello, M. *Physical Review Letters* **1985**, *55*, 2471-2474.

(23) Wesolowski, T. A. *J. Chem. Phys.* **2000**, *115*, 1666-1667.

(24) Wu, X.; Vargas, M. C.; Nayak, S.; Lotrich, V.; Scoles, G. *Journal of Chemical Physics* **2001**, *115*, 8748-8757.

(25) Misquitta, A. J.; Szalewicz, K. *Chemical Physics Letters* **2002**, *357*, 301-306.

(26) Wesolowski, T. A.; Morgantini, P. Y.; Weber, J. *Journal of Chemical Physics* **2002**, *116*, 6411-6421.

(27) van Mourik, T.; Gdanitz, R. J. *Journal of Chemical Physics* **2002**, *116*, 9620-9623.

(28) Tsuzuki, S.; Uchimaru, T.; Matsumura, K.; Mikami, M.; Tanabe, K. *Chemical Physics Letters* **2000**, *319*, 547-554.

(29) Hobza, P.; Selzle, H. L.; Schlag, E. W. *Journal of Physical Chemistry* **1996**, *100*, 18790-18794.

(30) Rappe, A. K.; Bernstein, E. R. *Journal of Physical Chemistry A* **2000**, *104*, 6117-6128.

(31) Pedulla, J. M.; Vila, F.; Jordan, K. D. *Journal of Chemical Physics* **1996**, *105*, 11091-11099.

(32) Christie, R. A.; Jordan, K. D. *Journal of Physical Chemistry A* **2001**, *105*, 7551-7558.

(33) Woon, D. E.; Peterson, K. A.; Dunning, T. H. *Journal of Chemical Physics* **1998**, *109*, 2233-2241.

(34) Hobza, P.; Havlas, Z. *Theoretical Chemistry Accounts* **1998**, *99*, 372-377.

(35) Kilic, S.; Michalik, S.; Wang, Y.; Johnson, J. K.; Enick, R. M.; Beckman, E. J. *Industrial & Engineering Chemistry Research* **2003**, *42*, 6415-6424.

(36) Hunadi, R. J.; Baum, K. *Synthesis* **1982**, *39*, 454.

(37) Strain, F.; Bissinger, W. E.; Dial, W. R.; Rudoff, H.; DeWitt, B. J.; Stevens, H. C.; Langston, J. H. *J. Am. Chem. Soc.* **1950**, *72*, 1254-1263.

(38) Span, R.; Wagner, W. *J. Phys. Chem. Ref. Data* **1996**, *25*, 1509-1596.

(39) Hong, L.; Thies, M. C.; Enick, R. M. *Journal of Supercritical Fluids* **2004**.

(40) Meilchen, M. A.; Hasch, B. M.; MeHugh, M. A. *Macromolecules* **1991**, *24*, 4874-4882.

(41) Allen, G.; Baker, C. H. *Polymer* **1965**, *6*, 181-191.

(42) Irani, C. A.; Cozewith, C. *Journal of Applied Polymer Science* **1986**, *31*, 1879-1899.

(43) Lee, S. H.; Lostracco, M. A.; Hasch, B. M.; McHugh, M. A. *Journal of Physical Chemistry* **1994**, *98*, 4055-4060.

(44) Boys, S. F.; bernardi, F. *Moleular Physics* **1970**, *19*, 553-566.

(45) Feller, D.; Jordan, K. D. *Journal of Physical Chemistry A* **2000**, *104*, 9971-9975.

(46) Frisch, M. J.; Truck, G. W.; Schlegel, H. B.; Scuseria, G. E.; Robb, M. A.; Cheeseman, J. R.; Zakrzewski, V. G.; Montgomery Jr., J. A.; Stratmann, R. E.; Burant, J. C.; Dapprich, S.; Millam, J. M.; Daniels, A. D.; Kudin, K. N.; Strain, M. C.; Farkas, O.; Tomasi, J.; Barone, V.; Cossi, M.; Cammi, R.; Mennucci, B.; Pomelli, C.; Adamo, C.; Clifford, S.; Ochterski, J.; Petersson, G. A.; Ayala, P. Y.; Cui, Q.; Morokuma, K.; Salvador, P.; Dannenberg, J. J.; Malick, D. K.; Rabuck, A. D.; Raghavachari, K.; Foresman, J. B.; Cioslowski, J.; Ortiz, J. V.; Baboul, A. G.; Stefanov, B. B.; Liu, G.; Liashenko, A.; Piskorz, P.; Komaromi, I.; Gomperts, R.; Martin, R. L.; Fox, D. J.; Keith, T.; Al-Laham, M. A.; Peng, C. Y.; Nanayakkara, A.; Challacombe, M.; Gill, P. M. W.; Johnson, B.; Chen, W.; Wong, M. W.; Andres; Gonzalez, C.; Head-Gordon, M.; Replogle, E. S.; Pople, J. A. *Gaussian 98, Revision A.*, 2001, Gaussian, Inc. Pittsburgh, PA.

Section 6. CO_2 Solubility of Nitrogen-Containing Polymers

INTRODUCTION

Carbon dioxide has been perceived as the solvent of choice for many industrial applications because it is non-toxic, inexpensive and abundant material. CO_2 has a critical temperature near room temperature (31 ^oC), a modest critical temperature (73.8 bar) and a density higher than most critical fluids. Despite all these desired properties, CO_2 is, unfortunately, very feeble solvent. Therefore, it has been of interest for many researchers to understand the solvent character of CO_2. Based on thermodynamic solubility parameter calculations, Giddings et al. suggested that CO_2 has similar solvent characteristics with pyridine.[i] FT-IR spectroscopic studies suggested that CO_2 would behave like toluene.[ii] Based on hydrogen bond capability, CO_2 was likened to acetone.[iii] However, these perceptions have lost their validity over the years because many materials soluble in these solvents were found to be insoluble in CO_2. The weak solvent character of CO_2 has been mainly attributed its large quadrupole moment.[iv,v]

It is known that CO_2 is a solvent only one of its kind in terms of its solvent capability. Therefore, CO_2 solvent character needs to be investigated as separate. Thus far, perfluoroacrylates are found to be the most CO_2-philic polymers, and other fluorinated polymers, but not all, follow them in the list.[iv,vi,vii,viii] Upon high miscibility of fluorinated polymers with CO_2, researchers turned their focus on investigation of any possible specific interactions between CO_2 and fluorinated polymers. However, both the spectroscopic[ix,x,xi,xii] and the theoretical[xiii,xiv,xv] investigations revealed contradictory results regarding existence of any specific interactions in favor of miscibility. In a

number of experimental study, McHugh et al. evaluated the phase behavior of various fluorinated polymers and summarized the results in a review paper.[iv] The authors attributed the favorable miscibility of fluorinated polymers to polar-quadruopole interactions between polymers and CO_2, and suggested that fluorination imparts solubility to the polymer provided that some polarity is also introduced to the polymer via such fluorination. In addition, they also noted that a high level of fluorination shows an adverse effect on miscibility due to supremacy of dipole-dipole interactions between the polymer chains.[iv,xvi] Therefore, as of today, it is not lucid why fluorinated polymers exhibit high miscibility with CO_2.

A different hypothesis was put forward by O'Neill et al. They proposed that, since CO_2 is a feeble solvent, then a CO_2-philic material should possess weak self interactions.[xvii] The authors have tabulated that the compounds exhibiting CO_2-philic character (e.g.fluoroacrylates, siloxanes, polyethers) have indeed low surface tension, i.e. low cohesive energy density.

Investigations centering on understanding of the nature of CO_2 showed that CO_2 can act as both a Lewis acid and a Lewis base.[xviii,xix,xx,xxi,xxii] However, perception of CO_2 as a Lewis acid is more popular where the solubility of polymers in CO_2 is concerned. In mid 1990s, using FT-IR spectroscopy, Kazarian and coworkers reported the existence of specific interactions between the carbon atom of CO_2 and the lone pairs on the oxygen of a carbonyl group, and they stated that, in this interaction, CO_2 acts as a Lewis acid, and the carbonyl group as a Lewis base.[xxiii] Experimental efforts also showed that inclusion of

carbonyl groups imparts miscibility to the polymer otherwise known to be immiscible with CO_2.[xxiv,xxv] Subsequently, Xiao and colleagues showed that addition of carbonyl groups to triphenyl phosphine ligands allowed the creation of CO_2-soluble organometallic catalysts.[xxvi] Wallen and colleagues,[xxvii] as well as Hamilton et al.,[xxviii] showed that peracetylated monosaccharides and cyclodextrins are also miscible with CO_2, although miscibility pressures for the cyclodextrins are substantially higher than those of the simple sugars. In the interim, Meredith et al. reported that CO_2 can also interact with other Lewis base groups, such as tributyl phosphate and a tertiary alkyl amine.[xxix] In a recent study by Wallen et al., ab initio calculations results showed the presence of attractive specific interactions between CO_2 and the S=O group in dimethyl sulfoxide.[xxx] Our own ab initio calculations indicated that CO_2 can also interact with ether oxygen.[xxxi,xxxii] In the latter studies, it was also shown that low glass transition temperature of the polymer is also important to enhance the miscibility. Indeed, the polymers known to be CO_2-philic (i.e. perfluoroacrylates, siloxanes) exhibit also low glass transition temperature.

By reviewing these results closely, one can think of that presence of all these features in one polymer would result in highly CO_2-philic material, perhaps superior than any other polymer known to be CO_2-philic thus far. However, optimization of these features is necessary since they can inflate each other.[xxxi] The current work aimed to evaluate the phase behavior of a new potential class of polymers which are known to have low cohesive energy density and glass transition temperature[xxxiii] and as well as possess a functional group (i.e. trialkyl amine) that has the highest electron donating

capacity to promote favorable Lewis acid-Lewis base interactions with CO_2.[xxxiv] Phase behavior results were discussed in support of our ab initio calculations.

Experimental Procedure:

Materials: Linear Poly(ethyleneimine) hydrochloric salt (Mw≅2,000) was a gift from Polymer Chemistry Innovations, Inc. Poly(2-ethyl-2-oxazoline) with molecular weight of 5,000 (50 repeat units) was purchased from Scientific Polymer Products, Inc. N,N-dimethylacrylamide, 2,2,6,6-Tetramethyl-1-piperidinyloxy (TEMPO, 99%), anhydrous toluene, AIBN, anhydrous 1 M BH_3.THF complex and methyl acrylate were obtained from Aldrich. N,N-dimethylacrylamide was purified by distillation under reduced pressure, and AIBN was purified by crystallization from ethanol prior to use. Poly(4-vinyl pyridine) (Mn=3,000, PDI=1.50), Poly(2-vinyl pyridine) (Mn=3,000, PDI=1.12), and poly(N-vinyl imidazole) (Mn=9,500, PDI=3.00) were purchased from Polymer Source, Inc. All materials were used as received.

Polymerization of N,N-dimethylacrylamide: N,N-dimethyl acrylamide was polymerized following a procedure given by Li and Brittain.[xxxv] 0.50 g (3.04 mmol) AIBN and 0.47 g (3.01 mmol) TEMPO, such that [AIBN]/[TEMPO]=1, were charged into a 250 ml round-bottomed, three-neck flask equipped with a condenser and argon feed. 25.0 g (0.25 mol) N,N-dimethyl acrylamide and 100 ml anhydrous toluene were then added to the flask. The flask was then placed in an oil bath at 98 ^{o}C. Initially, the solution exhibited the orange color of TEMPO, but the color disappeared in less than 30 minutes. After 14 hours of polymerization, the product was precipitated into hexane. The

polymer was re-dissolved in toluene and re-precipitated into hexane twice, followed by vacuum drying overnight. White, hygroscopic, polymer powder was recovered at 99% yield. Molecular weight of poly(N,N-dimethylacrylamide) was determined via GPC using toluene as eluent (Mn=1,298, Mw=1,672, PI=1.29). ^{1}H NMR (300 MHz, C_6D_6): δ 2.7-2.9 (broad, 1H, -CH-CO-N-$(CH_3)_2$), δ 2.9-3.0 (broad, 6H, -N-$(CH_3)_2$), δ 1.5-1.9 (broad, 2H, -CH_2-CH-CO).

Synthesis of Poly(propylethyleneimine): Poly(propylethyleneimine) was synthesized via the reduction of poly(2-ethyl-2-oxazoline) by borane (Scheme 1). The glassware was oven-dried overnight and purged with ultra-high purity argon before use. 9.4 g of polymer was charged into a 500-ml three-neck, round-bottomed flask. The system was equipped with a magnetic stir-bar, a condenser, addition funnel and an argon feed. 25 ml of anhydrous tetrahydrofuran were added to completely dissolve the polymer. After dissolution, 430 ml 1 M BH_3·THF complex (4.2 equivalent) were added to the flask drop-wise over 180 min. The solution temperature was raised to reflux, and the solution was stirred for 4 days. After cooling, the excess borane was eliminated by dropwise addition of methanol until hydrogen gas ceased evolving. The THF/methanol mixture was evaporated under reduced pressure, and the sample was dissolved in 144 ml methanol. To the solution, HCl aqueous solution (6 N, 48 ml, 3 times excess) was added and the solution heated to 65 ^{o}C and stirred for 40 hours. Upon cooling the green solution, NaOH aqueous solution (6 N, 50 ml) was added to neutralize the mixture. Methanol was removed on rotary evaporator under reduced pressure, and water by azeotropic distillation with

toluene. The salt was removed by filtration after re-dissolving the polymer in methanol. In case some salt remained dissolved in the residual water after azeotropic distillation with toluene, methanol was removed, and polymer was dissolved in an non-aprotic solvent, chloroform. The solution was dried over $MgSO_4$. Upon removal of chloroform, a viscous, brown polymer was obtained (47% yield). Disappearance of the peak at 1647 cm^{-1} (corresponding to C=O stretching in poly(2-ethyl-2-oxazoline)) was a sign of complete reduction of the amide. ^1H NMR (300 MHz, $CDCl_3$) δ 0.90 (broad, 3H, (-N-CH_2-CH_2-CH_3), δ 1.5 (broad, 4H, -N-CH_2-CH_2-CH_3), δ 2.3-2.5 (broad, 4H, N-CH_2).

Preparation of Poly(propylmethylacrylate ethyleneimine):

Poly(propylmethylacrylate ethyleneimine) was prepared via Michael addition reaction.[xxxvi,xxxvii,xxxviii] Prior to that, poly(ethyleneimine) hydrochloric salt was neutralized with aqueous NaOH solution. 11.0 g poly(ethyleneimine) hydrochloric salt was allowed to dissolve in 60 ml water, then 5 g NaOH dissolved in 20 ml water was added slowly to the polymer solution until the pH of the solution was 8.0-8.5 by pH paper. The solution was stirred overnight. Upon precipitation of the polymer into acetone (twice), a yellowish viscous, oily polymer precipitated at the bottom of the flask. In case some salt remained dissolved in the residual water, polymer was dissolved in methanol and dried over K_2CO_3. Upon filtration, excess methanol was removed on rotary evaporator if necessary. The solution (~75 ml) was transferred to a 250-ml 3-neck, round bottom flask equipped with a condenser, and 18.5 g (0.22 mol) of methyl acrylate was then added. Initially, solution was opaque and yellow in appearance, but after 72 hours of stirring, the color turned to orange. After

filtration, the solution was concentrated under vacuum to remove unreacted methyl acrylate and methanol. A very viscous, red-brownish polymer was obtained (92% yield). ^{1}H NMR (300 MHz, $CDCl_3$) δ 1.5 (broad, 2H, -N-CH_2-CH_2), δ 2.3-2.5 (broad, 4H, -N-CH_2), δ 2.5-2.9 (broad, 2H, N-CH_2-CH_2-CO), δ 3.7 (s, 3H, CO-O-CH_3).

Synthesis of functional siloxane copolymers: Propyl acetate (PA) and propyl dimethyl amine (PDMA) functional siloxane copolymers were prepared according to the procedure described earlier.[xxxi]

Phase Behavior Measurements: Phase behavior measurements of the polymers were performed in the same way as described earlier.[xxxi] Typical variability in the cloud point measurements is less than ±0.7 MPa.

Results and Discussion:

Polyethyleneimines are new class of polymers that exhibit weak self-interactions and a relatively low glass transition temperature.[xxxiii] Polyethyleneimines' surface tension, and thus cohesive energy density (CED), is comparable to that of silicones, but moderately higher than that of fluorinated polymers (~10 mN/m). For example, poly(hexanoyliminoethylene) and polydimethylsiloxane have surface tension values of 23 and 21 mN/m at 20 ^{o}C, respectively.[xxxiii] While fluoroacrylates has glass transition temperature of 263 K, glass transition temperatures for these polymers are given as 283 K and 150 K, respectively. [xxxiii]

In the light of premise above, CO_2-philicity of a series of poly(ethyleneimines) (Table 1) were evaluated. Poly(ethyleneimines) are also of interest because, as explained in the Theory section, our ab inito calculations suggest that interactions between nitrogen in a trialkyl amine and CO_2 are much stronger than the interactions known to be very favorable between carbonyl oxygen and CO_2. In addition, the electron-donating capacity of nitrogen was earlier reported to be higher than that of carbonyl oxygen.[xxxiv]

Contrary to expectations, none of the side chain functional ethyleneimine-based polymers (PPEI, PEO, PPMAEI) was miscible with CO_2 down to 1 wt % and pressures up to 45 MPa. Our ab initio calculations also showed the presence of very strong self-interactions between trialkyl amine compounds. Besides, the ester group in PPMAEI and the carbonyl group in PEO did not even help overcome these self-interactions. Therefore, based on our calculations, we conclude that self-interactions between amine groups dominate over cross interactions by "pulling" the polymer out of solution. Self-interactions between CO_2 molecules due to qudrupole-quadrupole interactions may also accompany exclusion of the polymers from the solution.

In an attempt to understand if placing of nitrogen in the side chain as a Lewis base would make any difference to the CO_2-philicity of a material, poly(N,N-dimethylacrylamide) (PDMAA) was prepared and its phase behavior in CO_2 was tested. PDMAA was synthesized with a molecular weight of 1298 (13 repeat units). Unfortunately, PDMAA was not miscible with CO_2 at pressures of 45 MPa and concentrations of 0.7 wt %. The polymer was swollen to some degree by CO_2 possibly

due to carbonyl-CO_2 interactions. Increased temperature (80 ^oC) did not produce a single phase solution either. The immiscibility of PDMAA with CO_2 can be attributed to the very high cohesive energy density of the polymer (surface tension: ~52 mN/m at 20 ^oC) and very high Tg (362 K).[xxxiii] Here again, Lewis acid-base interactions of CO_2 with neither carbonyl nor nitrogen are effective in achieving miscibility. Besides, one can expect that the nitrogen atom as an electron donor strengthens the carbonyl group as a potential Lewis base and thereby increases carbonyl CO_2-philicity. However, it is also possible that the amine group can create steric barrier for a possible carbonyl oxygen/CO_2 complex formation.

The results above suggest that optimum number of side chain may be needed to be incorporated in the chain to balance all the factors and thus maximize miscibility. Indeed, incorporation of trialkyl amine groups on siloxane polymers (Figure 1) showed that there is a limit on the number of substitution for maximum miscibility, supporting our hypothesis. One and two (z=1 and z=2)-propyl-dimethylamine (PDMA) functional siloxane copolymers were found to be miscible with CO_2 at 295 K. The (z=5) and (z=11) PDMA-functional copolymers exhibit miscibility pressures beyond the limit of our instrument (~ 45 MPa) at 295 K, but only miscible with CO_2 at elevated temperatures (311 K) (Figure 2). This observed behavior suggests that, by the addition of trialkyl amine functionality, self-interactions between polymer segments become too strong so that even the favorable tri-alkyl amine/CO_2 interactions cannot overcome this force. Comparison of the phase behavior of PDMA-substituted with that of propyl acetate (PA)-substituted siloxane copolymer (Figure 1 for structures) at their optimum number of

substitution indicated that acetate functionality promotes the miscibility of the polymer at relatively low pressures as compared to tri-alkyl amine functionality (Figure 3). From these results, it is obvious that self-interactions between tri-alkyl amine groups are more decisive on determining the miscibility of the polymer with CO_2 than cross-interactions. These results are a good indication of existence of a balance between the forces working against and favoring the miscibility of the polymer with CO_2. It is likely that such an optimal degree of functionalization also exists for the ethyleneimine polymers. It is worthwhile to note that fully PA-functionalized siloxane polymer (z=25) was not miscible with CO_2 at pressures lower than 45 MPa, either.

A supportive situation emerges when one compares the phase behavior of the (z=5)-PDMA functional siloxane copolymer and (z=5) PA-functional siloxane copolymer at two different temperatures (Figure 3 and 4). Note that (z=5)-PDMA functional siloxane copolymer exhibits miscibility pressures beyond the limit of our instrument (~ 45 MPa) at 295 K while (z=5)-PA functional siloxane copolymer is miscible at moderate pressures (Figure 3). It is possible to achieve the single-phase solution of (z=5)-PDMA functional copolymer at 311 K, meaning that the phase behavior curve of PDMA functional copolymer shifts to lower pressures when the temperature is increased from 295 K to 311 K (UCST behavior). The miscibility of (z=5) PDMA-functional copolymer is enthalpically unfavorable at low temperature, indicating that the self-interactions are governing the system, and enthalpy of mixing (ΔH_m) is >0. At high temperatures, the $-T\Delta S_m$ term compensates for the positive ΔH_m to give the negative ΔG_m value required for miscibility. Unlike PDMA-functional polymer, the phase behavior of (z=5) PA-

functional copolymer moves to higher pressures with increasing temperature of the system due mainly to the decrease in solvent density (LCST behavior) (compare curves #2 in Figure 3 and 4). Miscibility process is exothermic ($\Delta H_m<0$) and ΔH_m always favors the miscibility. With increasing system temperature, CO_2 molecules tend to take more expanded gas-like configuration, resulting in a rapid drop in density. While CO_2 gains free volume, the interactions polymer segments increases, resulting in a large negative ΔS_m. This decrease in ΔS_m is compensated via condensing CO_2 molecules around the polymer chains by increasing the system pressure.[xxxix]

Given all these experimental and ab initio calculations results, we believe that unfavorable miscibility of the trialkyl amine functional polymers results from dominance of self-interaction between the amine groups over cross-interactions with CO_2. Meredith and coworkers, however, based on their ab initio calculation using density functional theory, earlier reported that interactions between CO_2 and trialkyl amine group is not favorable because the alkyl groups in tri-alkyl group form steric hindrance for attractive interactions with CO_2. However, they suggested that such barrier is not the case with pyridine and interactions with CO_2 are favorable.[xxix] In an attempt to inquire this conjecture, phase behavior of poly(2-vinyl pyridine) (P2VP), poly(4-vinyl pyridine) (P4VP) and poly(N-vinyl imidazole) (PVIZ) was also tested. None of the three samples was found to be miscible with CO_2 at pressures up to 55 MPa and at concentration down to 0.7 wt%. Elevated temperature (70 ^oC) did not result in a single phase solution either. Surface tensions of P2VP and P4VP were earlier reported as 45 and 71.5 mN/m at 20 ^oC, respectively.[xl] Therefore, both our own calculations and the literature data along with the

experimental results indicate the presence of very strong self-interactions between the tert-amine containing polymer chains and these interactions are more decisive in determination of miscibility of the polymers with CO_2.

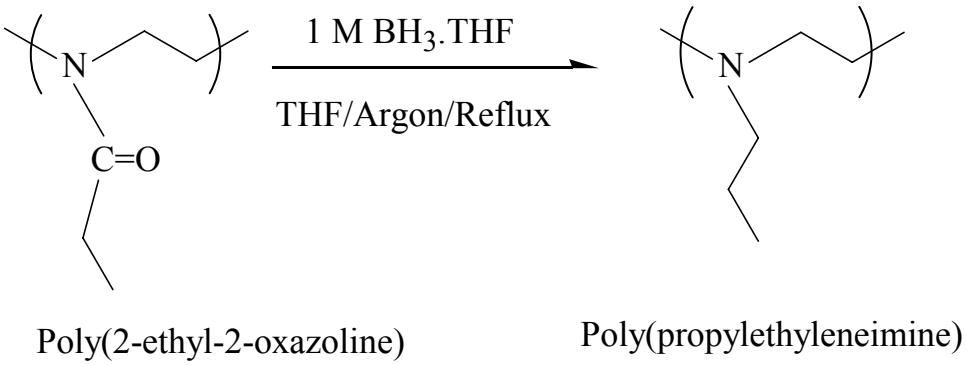

Poly(2-ethyl-2-oxazoline) Poly(propylethyleneimine)

Scheme 1. Synthetic route for preparation of poly(propylethylenimine)

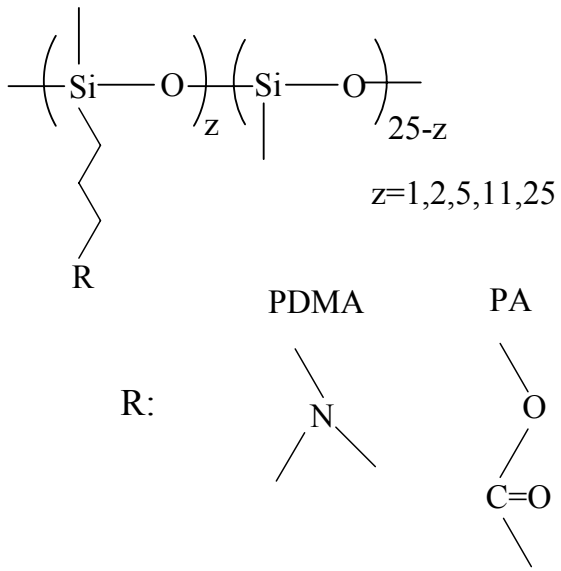

Figure 1. Structure of PDMA- and PA-functionalized siloxane copolymers.

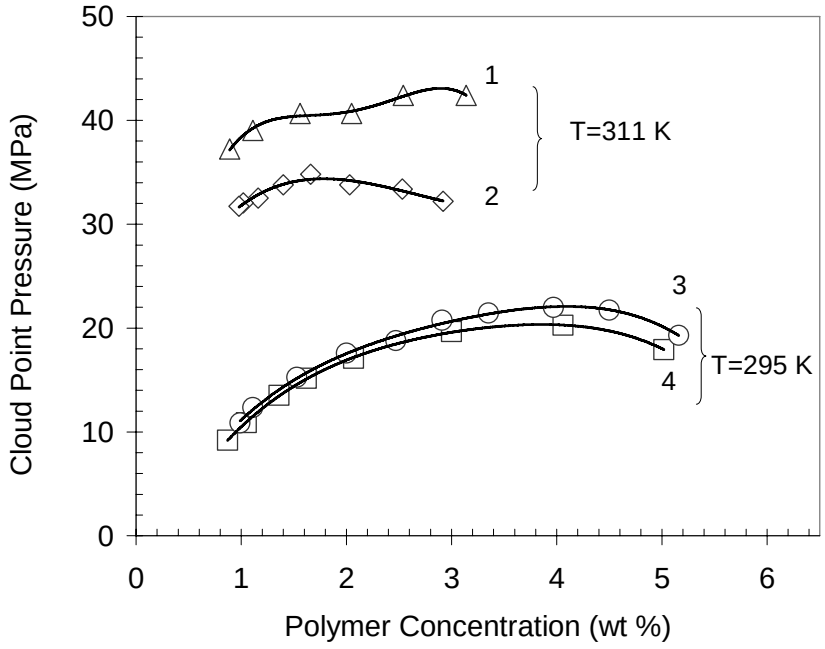

Figure 2. Phase behavior of propyl dimethyl amine (PDMA)-functional siloxane copolymers at different degrees of substitution. 1) z=11, T=311 K 2) z=5, T=311 K, 3) z=2, T=295 K, 4) z=1, T=295 K.

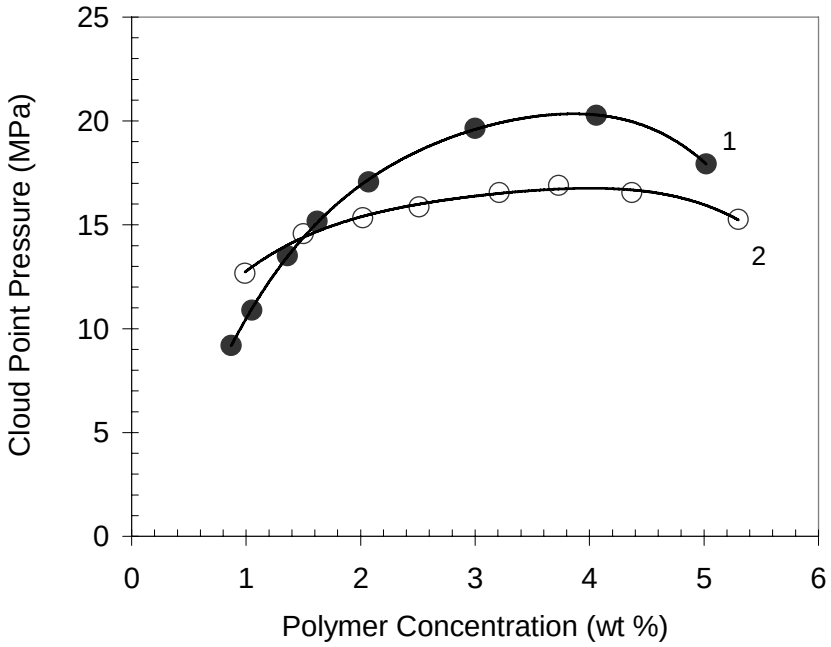

Figure 3. Comparison of phase behaviors of 1) (z=1) propyl dimethyl amine-functional (PDA), 2) (z=5) propyl acetate (PA)-functional siloxane copolymers at 295 K.

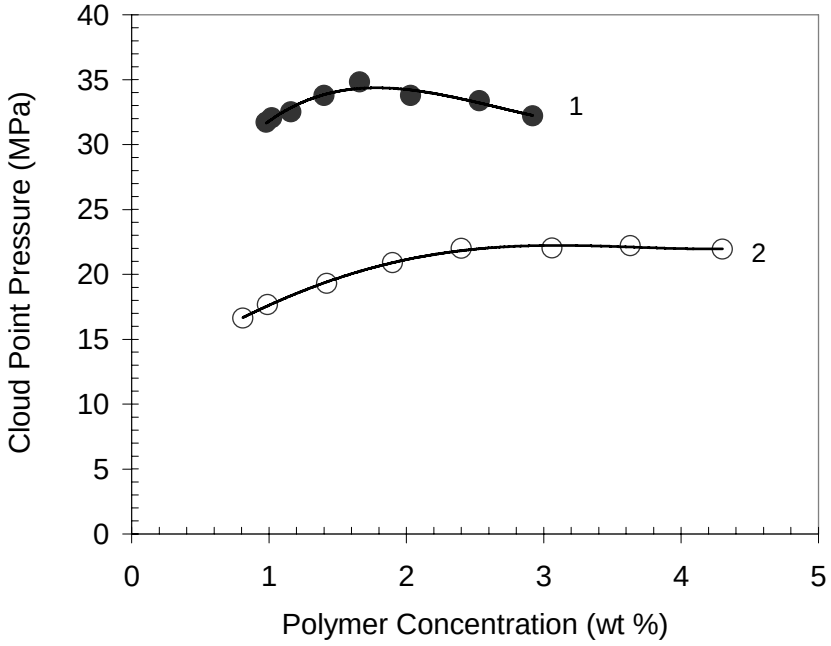

Figure 4. Comparison of phase behavior of (z=5)-functional siloxane copolymers at 311 K, 1) propyl dimethyl amine (PDMA) 2) propyl acetate (PA)

Table 1. Structure of Nitrogen-Containing Polymers

Name of the polymer	**Structure**
Poly(propylethyleneimine) (PPEI)	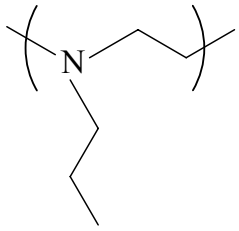
Poly(propylmethylacrylate-ethyleneimine) (PPMAEI)	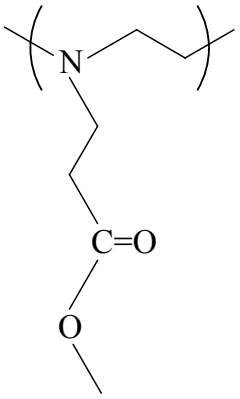
Poly(2-ethyl-2-oxazoline) (PEO)	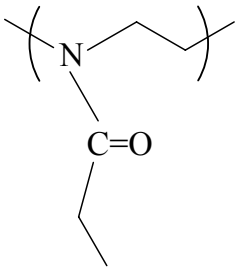
Poly(N,N-dimethylacrylamide) (PDMAA)	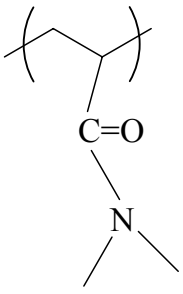

Poly(2-vinyl pyridine)
(P2VP)

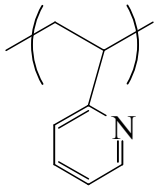

Poly(4-vinyl pyridine)
(P4VP)

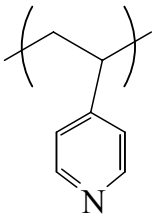

Poly(N-vinyl imidazole)
(PVIZ)

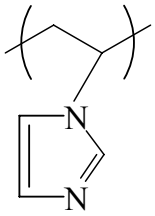

References:

[i] Giddings, J. C.; Myers, M. N.; McLaren, L.; Keller, R. A. High-pressure gas chromatography of nonvolatile species. Compressed gas is used to cause migration of intractable solutes. *Science* **1968**, 162, 67

[ii] Hyatt, J. A. Liquid and supercritical carbon dioxide as organic solvents. *J. Org. Chem*. **1984**, 49, 5097

[iii] Walsh, J. M; Ikonomou, G. D.; Donohue, M. D. Supercritical phase behavior: the entrainer effect. *Fluid Phase Eq.* **1987**, 33, 295

[iv] Kirby, C. F.; McHugh, M. A. Phase Behavior of Polymers in Supercritical Fluid Solvents. *Chem. Rev*. **1999**, 99, 565

[v] Kauffman, J. F. Quadrupolar Solvent Effects on Solvation and Reactivity of Solutes Dissolved in Supercritical CO_2. *J. Phys. Chem. A* **2001**, 105, 3433.

[vi] DeSimone, J. M.; Guan, Z.; Elsbernd, C. S. Synthesis of fluoropolymers in supercritical carbon dioxide. *Science* **1992**, 257, 945.

[vii] Hoefling, T.; Stofesky, D.; Reid, M.; Beckman, E. J.; Enick, R. M. The incorporation of a fluorinated ether functionality into a polymer or surfactant to enhance carbon dioxide solubility. *J. Supercrit. Fluids* **1992**, 5, 237.

[viii] Hoefling, T. A.; Newman, D. A.; Enick, R. M.; Beckman, E. J. Effect of structure on the cloud-point curves of silicone-based amphiphiles in supercritical carbon dioxide. *J. Supercrit. Fluids* **1993**, 6, 165.

[ix] Yee, G. G.; Fulton, J. L.; Smith, R. D. Fourier transform infrared spectroscopy of molecular interactions of heptafluoro-1-butanol or 1-butanol in supercritical carbon dioxide and supercritical ethane. *J. Phys. Chem*. **1992**, 96, 6172.

[x] Dardin, A.; DeSimone, J. M.; Samulski, E. T. Fluorocarbons Dissolved in Supercritical Carbon Dioxide. NMR Evidence for Specific Solute-Solvent Interactions. *J. Phys. Chem. B* **1998**, 102, 1775.

[xi] Bothner-By, A. A.; Glick, R. E. Specific medium effects in nuclear magnetic resonance spectra of liquids. *J. Am. Chem. Soc*. **1956**, 78, 1071.

[xii] Yonker, C. R.; Palmer, B. J. Investigation of CO_2/Fluorine Interactions through the Intermolecular Effects on the 1H and 19F Shielding of CH_3F and CHF_3 at Various Temperatures and Pressures. *J. Phys. Chem. A* **2001**, 105, 308.

[xiii] Cece, A; Jureller, S. H.; Kerscher, J. L.; Moschner, K. F. Molecular Modeling Approach for Contrasting the Interaction of Ethane and Hexafluoroethane with Carbon Dioxide. *J. Phys. Chem*. **1996**, 100, 7435.

[xiv] Diep, P; Jordan, K. D.; Johnson, J. K.; Beckman, E. J. CO_2-Fluorocarbon and CO_2-Hydrocarbon Interactions from First-Principles Calculations. *J. Phys. Chem. A* **1998**,102, 2231.

[xv] Raveendran, P; Wallen, S. L. Exploring CO_2-Philicity: Effects of Stepwise Fluorination. *J. Phys. Chem. B*. **2003**, 107, 1473.

[xvi] Rindfleisch, F., DiNoia, T. P., McHugh, M. A. Solubility of Polymers and Copolymers in Supercritical CO_2. *J. Phys. Chem.* **1996**, 100, 15581.

[xvii] O'Neill, M. L., Cao, Q., Fang, M., Johnston, K. P.; Wilkinson, S. P.; Smith, C. D.; Kerschner, J. L.; Jureller, S. H. Solubility of Homopolymers and Copolymers in Carbon Dioxide. *Ind. Eng. Chem., Res.* **1998**, 37, 3067.

[xviii] O'Shea, K. E.; Kirmse, K. M.; Fox, M. A.; Johnston, K. P. Polar and Hydrogen-bonding Interactions in Supercritical Fluids: Effects on the Tautomeric Equilibrium of 4-(phenylazo)-1-naphthol. *J. Phys. Chem.* **1991**, 95, 7863.

[xix] Hyatt, J. A. Liquid and Supercritical Carbon Dioxide as Organic Solvents. *J. Org. Chem*. **1984**, 49, 5097.

[xx] Sigman, M. E.; Lindley, S. M.; Leffler, J. E. Supercritical Carbon Dioxide: Behavior of π^* and β Solvatochromic Indicators in Media of Different Densities. *J. Am. Chem. Soc*. **1985**, 107, 1471.

[xxi] Phillips, J. H.; Robey, R. J. Solvent Strength and Selectivity Properties of Supercritical Carbon Dioxide Relative to Liquid Hexane. *J. Chromat*. **1989**, 465, 177.

[xxii] Dobrowolski, J. C.; Jamroz, M. H. Infrared evidence for carbon dioxide electron donor-acceptor complexes. *J. Mol. Struct*. **1992**, 275, 211.

[xxiii] Kazarian, S. G.; Vincent, M. F.; Bright, F. V.; Lioota, C. L.; Eckert, C. A. Specific Intermolecular Interaction of Carbon Dioxide with Polymers. *J. Am. Chem. Soc.* **1996**, 118, 1729.

[xxiv] Sarbu, T.; Styranec, T. J.; Beckman, E. J. Design and Synthesis of Low Cost, Sustainable CO_2-philes. *Ind. Eng. Chem. Res.* **2000**, 39, 4678.

[xxv] Sarbu, T.; Styranec, T. J.; Beckman, E. J. Non-fluorous polymers with very high solubility in supercritical CO_2 down to low pressures. *Nature* **2000**, 405, 165.

[xxvi] Hu, Y.; Chen, W.; Xu, L.; Xiao, J. Carbonylated Phosphines as Ligands for Catalysis in Supercritical CO_2. O*rganometallics* **2001**, 20, 3206.

[xxvii] Raveendran, P.; Wallen, S. L. Sugar Acetates as Novel, Renewable CO_2-philes. *J. Am. Chem. Soc.* **2002**, 124, 7274.

[xxviii] Potluri, V. K.; Xu, J.; Enick, R.; Beckman, E. J.; Hamilton, A. D. Peracetylated Sugar Derivatives Show High Solubility in Liquid and Supercritical Carbon Dioxide. *Org. Letters* **2002**, 4, 2333.

[xxix] Meredith, J. C.; Johnston K. P.; Seminario, Jorge M.; Kazarian, Sergei G.; Eckert, Charles A. Quantitative Equilibrium Constants between CO_2 and Lewis Bases from FTIR Spectroscopy. *J. Phys. Chem*. **1996**, 100, 10837.

[xxx] Raveendran, P.; Wallen, S. L. Cooperative C-H···O Hydrogen Bonding in CO_2-Lewis Base Complexes: Implications for Solvation in Supercritical CO_2. *J. Am. Chem. Soc.* **2002**, 124, 12590.

[xxxi] Kilic, S.; Michalik, S.; Wang, Y.; Johnson, K. J.; Enick, R. M., Beckman, E. J. Effect of Grafted Lewis Base Groups on the Phase Behavior of Model Poly(dimethyl siloxanes) in CO_2. *Ind. Eng. Chem. Res.* **2003**, 42, 6415.

[xxxii] Kilic, S.; Michalik, S.; Wang, Y.; Johnson, K. J.; Enick, R. M., Beckman, E. J.; Phase Behavior of Oxygen-Containing Polymers in CO_2. *Macromolecules*, Submitted.

[xxxiii] Brandup, J.; Immergut, E. H.; Grulke, E. A. *Polymer Handbook,* 4th Ed., New York : Wiley, **1999**.

[xxxiv] Gutmann, V. Solvent effects on the reactivities of organometallic compounds. *Coord Chem. Rev.* **1976**, 18, 225.

[xxxv] Li, D.; Brittain, W. J. Synthesis of Poly(N,N-dimethylacrylamide) via Nitroxide-Mediated Radical Polymerization. *Macromolecules* **1998**, 31, 3852.

[xxxvi] Smith, M. B.; March, J.; *March's Advanced Organic Chemistry: Reactions, Mechanisms, and Structure,* Wiley, John & Sons, **2000**.

[xxxvii] Kwiatkowski, S.; Jeganathan, A.; Tobin, T.; Watt, D. S. A synthesis of N-substituted β-alanines: Michael addition of amines to trimethylsilyl acrylate. *Synthesis* **1989**, 12, 946.

[xxxviii] Farahani, M.; Antonucci, J. M.; Karam, L. R. A GC-MS study of the addition reaction of aryl amines with acrylic monomers. *J. Appl. Polym. Sci.* **1998**, 67, 1545.

[xxxix] Patterson, D. Polymer compatibility with and without a solvent. *Polym. Eng. Sci.* **1982**, 22(2), 103.

[xl] Sauer, B. B.; Dee, G. T. Surface Tension and Melt Cohesive Energy Density of Polymer Melts Including High Melting and High Glass Transition Polymers. *Macromolecules* **2002**, 35, 7024.

Section 7. Novel Polymers Designed to Exhibit CO_2 Solubility

Poly(vinyl acetate), a commodity polymer, has been previously identified by our research group as the most CO_2-soluble oxygenated hydrocarbon polymer yet identified. Although this polymer can readily dissolve at high concentrations (e.g. 5wt%) even if its molecular weight is very high (e.g. 600,000), the pressure required to dissolve even dilute concentrations of PVAc in CO_2 lies well above the range of MMP values. Therefore PVAc is not sufficiently soluble to serve as the basis for a polymeric CO_2 thickener.

This summary listing details the structures of polymers that were designed to exhibit higher solubility than PVAc in dense carbon dioxide. Some of the polymers, poly(vinyl acetate), poly(vinyl methyl ether), poly(vinyl ethyl ether), poly(vinyl methyl ketone), poly(propylene) and poly(propylene oxide) were commercially available from Aldrich Chemical or Scientific Polymers or Polymer Source. The remainder were designed, synthesized, characterized and evaluated for CO_2 solubility in our laboratories.

In each case, a functional group that had the potential for favorable thermodynamic interactions with dense CO_2 was incorporated into the polymer structure. Specific groups that interact with CO_2 have previously been identified by our group or in the literature by those investigating the CO_2 solubility of small compounds. Examples used in this study included ether, carbonyl, acetate, amine, branched alkyl and sulfonyl.

After being synthesized and characterized, the CO2 solubility of each polymer was determined at 298 K at concentrations between 1-5 wt%. The pressure required to dissolve the polymer (if it was soluble at P<70 MPa) at a specific concentration was then compared to the pressure required to dissolve a PVAc polymer of the same number of repeat units at the same concentration in CO_2.

Unfortunately, all of these polymers were less CO_2 soluble than PVAc.

Table 1. Polymers Evaluated for CO_2 Solubility

Polymer Structure	Polymer name and CO_2 interaction site	CO_2 Solubility Result at 298 K and 70 MPa
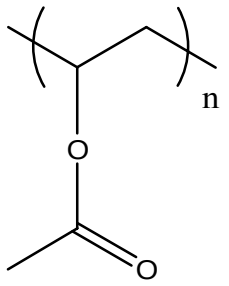	Poly(vinyl acetate) Lewis acid:Lewis base and complimentary weak hydrogen bond	Most CO_2-soluble non-fluorous polymer yet identified
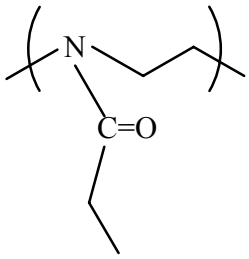	Poly(2-ethyl-2-oxazoline) Carbonyl and amine	Insoluble
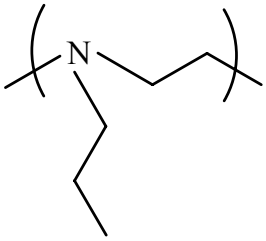	Poly(propylethylene imine) Amine	Insoluble

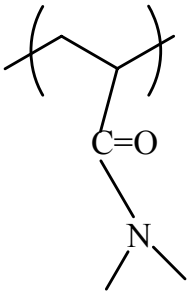	Poly(N,N-dimethylacrylamide) Carbonyl and amine	Insoluble
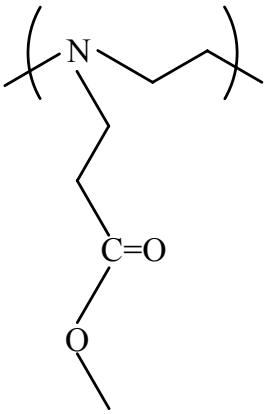	Poly(propylmethyl acrylate-ethyleneimine) Carbonyl, ether, and amine	Insoluble
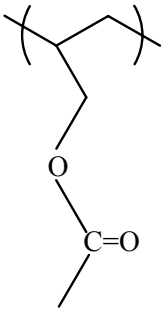	Poly(allyl acetate) Carbonyl and ether	Insoluble
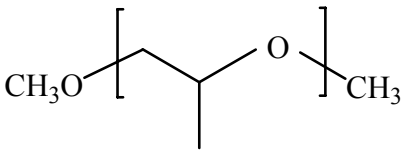	Poly(propylene oxide)	Low Mw oligomers are more soluble than PVAc at low T, Mw<2000 and conc. < 3wt%), but much less soluble at high Mw

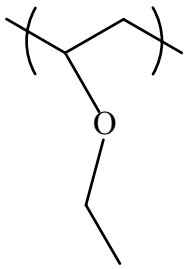	Poly(vinyl ethyl ether) Ether	(less soluble than PVAc)
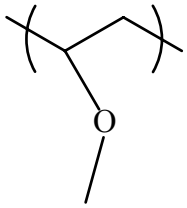	Poly(vinyl methyl ether) Ether	Less soluble than PVAc
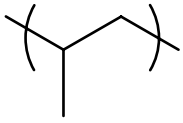	Poly(propylene) Branched hydrocarbon	Less soluble than PVAc
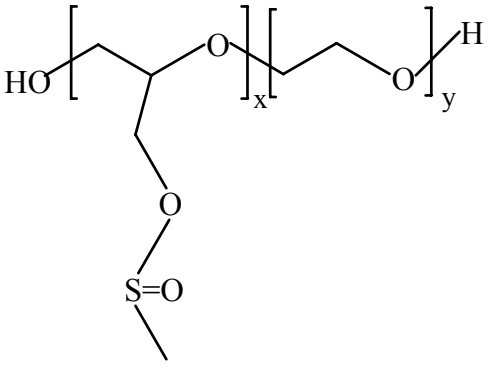	Partially sulfonate-functionalized poly(propylene glycol), x=0.44 Sulfonyl and ether	Insoluble

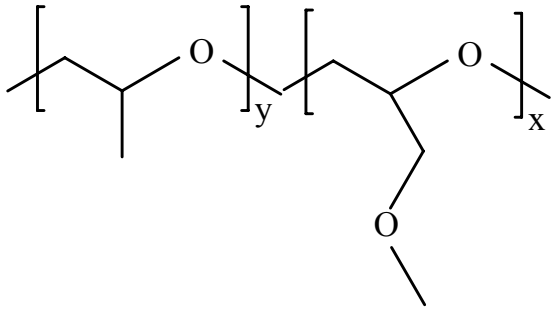	Partially methyl ether functionalized poly(propylene glycol), x=12, 22, 44 and 100	Insoluble
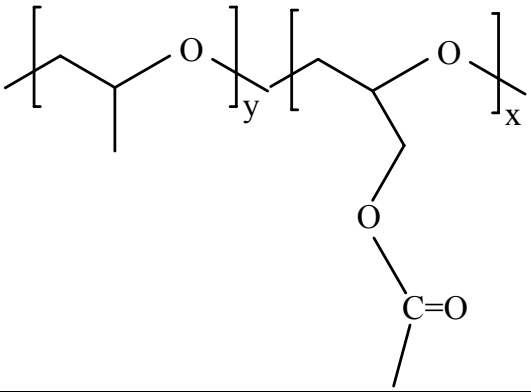	Partially acetate functionalized poly(propylene glycol), x=12, 22, 44, 69 and 100 (insoluble)	Less soluble than PVAc
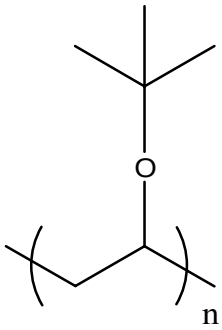	Poly(tert-butyl-vinyl ether)	Insoluble

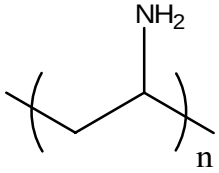	Polyvinyl amine Mw = 10,000 and 45,000	Insoluble
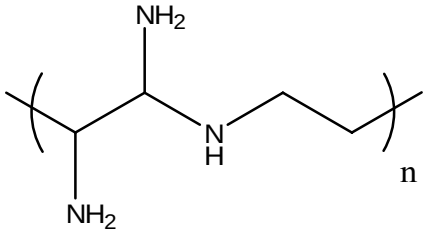	Poly(ethylenediamine-co-ethyleneimine	Insoluble

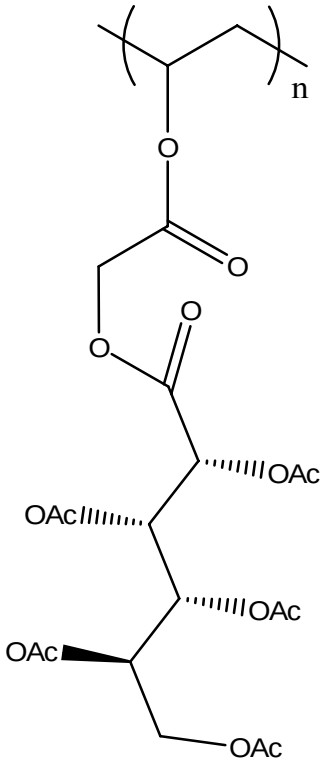	Poly(vinyloxycarbonyl methyl(penta-O-acetate) Ac=$COCH_3$	Insoluble

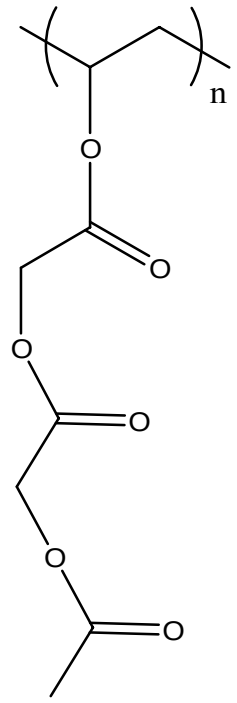	Poly (acetoxy acetoxy acetate) Carbonyl- and ether-rich polymer	Insoluble
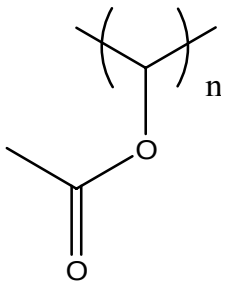	Poly(acetoxy methylene)	Insoluble

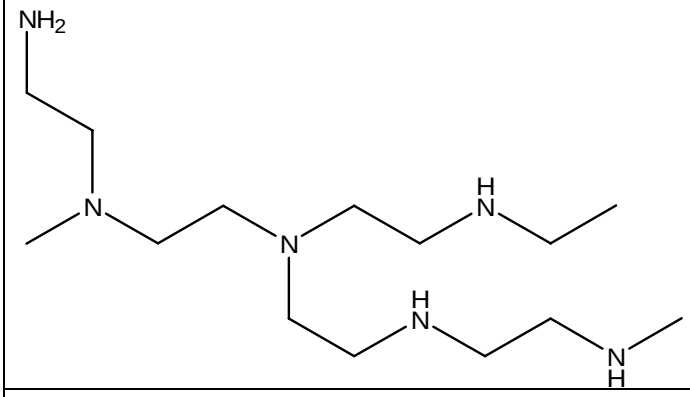	Poly(ethylene imine)	Insoluble Mw=800
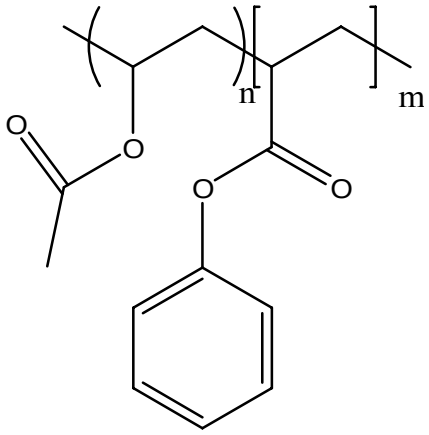	Poly(vinyl acetate-co-phenyl acrylate)	In progress
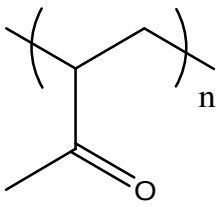	Poly(vinyl methyl ketone) Mw=500,000	Insoluble
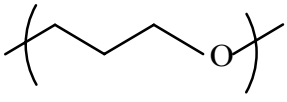	Poly(oxitane), Linear PPO	In progress

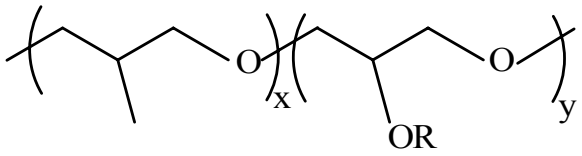 R: -O-CO-CH_3 -O-SO-CH_3		